

**Solar cooling technologies: Review, performance analysis
and application to case studies**

Laura Martín Méndez

Thesis to obtain the Master of Science Degree in
Energy Engineering and Management

Supervisors: Prof. Paulo José da Costa Branco

Dr. Raquel Simón Allué

Examination Committee

Chairperson: Prof. Edgar Caetano Fernandes

Supervisor: Prof. Paulo José da Costa Branco

Member of the Committee: Prof. João Filipe Pereira Fernandes

May 2019

I declare that this document is an original work of my own authorship and that it fulfils
all the requirements of the Code of Conduct and Good Practices of the
Universidade de Lisboa.

Acknowledgements

First of all, I would like to express my thankfulness to Raquel Simón, my supervisor from the company EndeF Engineering, who has supported and helped me in all this journey by not only providing her knowledge, books and scientific papers but also a lot of guidance and useful advice. It has not been easy during many months and a lot of changes in some of the approach had to be made but she has always been willing to help me progress. A special mention to Isabel Guedea as well, for supervising the work as head of R&D department in EndeF Engineering. I would also like to thank professor Paulo Branco from IST for making this possible, for being interested in the topic of this master thesis and trusting me from the beginning when I struggled to find a supervisor, even if he was very busy already and had many other students to supervise. Also thanks to Filipe Neves, who has provided me with all kind of help for installing the required software. Furthermore, I would like to thank professor Wojciech Nowak from AGH for his support as my third supervisor and his fast email replies and corrections.

Special thanks to professor Fátima Montemor as my CFAFE master's programme coordinator for all the advice and help during the last year of my master studies in Lisbon as well as for authorizing the realization of this master thesis and the required agreement with the company EndeF Engineering S.L. I would like to thank Joanne Laranjeiro as well, from IST, for all her help and nice willing attitude and fast management of administrative issues I had to face. Last but not least, I would like to thank professor Falcão de Campos for being a supportive MEGE coordinator.

I would also like to state my acknowledgements of gratitude to all my study colleagues who have been grown together as a family, to my best friends for being a supporting pillar during all these months and finally, to my family, who have supported my studies during several years. With a special mention to my favourite soul, who gave me life and I hope is watching and feeling me from up there.

Thank you all very much,

Laura Martín Méndez

Lisbon, 31st of January, 2019.

Abstract

The current master thesis intended to analyse the performance, economic and environmental feasibility of the most promising solar cooling technologies with hybrid panels to install on a 4-star hotel located in Madrid. These are solar electric cooling by means of a vapour compression cycle and absorption cooling, which is thermally driven. The study has been focused on the installation of 100 Ecomesh hybrid solar panels, patented by EndeF Engineering, on the rooftop of the hotel, and a comparative analysis of four case studies: initial case of the hotel, hotel with only the hybrid panels, installation of the hybrid panels coupled with a reversible heat pump and an absorption cooling system with the Ecomesh solar panels. After the analysis, the preferred option is the solar electric cooling system with Ecomesh solar panels and the heat pump. The achieved annual saving is 27,909€ and the CO₂ emissions cut is about 58 tons of CO₂/year. Since PV panels are much cheaper than hybrid ones, two alternative options have been suggested with PV panels. The first one consists on a solar installation with these PV panels and the other on the PV panels and a reversible heat pump for solar electric cooling. The second option with the reversible heat pump has been also recommended in case of deciding for Ecomesh PV panels instead of the hybrid ones. The total annual saving for this alternative case is of 21,043€ and the CO₂ emissions cut of almost 43 tons of CO₂/year.

Keywords

Absorption; F-Chart method; heat pump; hybrid panel; renewable energy; solar cooling

Resumo

A presente tese de mestrado pretende analisar o desempenho, a viabilidade económica e ambiental das tecnologias mais promissoras de refrigeração solar com painéis híbridos para instalação num hotel de 4 estrelas localizado em Madri. Estas são: arrefecimento elétrico solar por meio de um ciclo de compressão de vapor e arrefecimento por absorção, que é acionado termicamente. O estudo teve como foco a instalação de 100 painéis solares híbridos Ecomesh, patenteados pela EndeF Engineering, no telhado do hotel, e uma análise comparativa de quatro estudos de caso: caso inicial do hotel, hotel com apenas os painéis híbridos, instalação dos painéis híbridos acoplados a uma bomba de calor reversível e um sistema de refrigeração por absorção com os painéis solares Ecomesh. Após a análise, a opção preferida é o sistema de refrigeração elétrica solar com painéis solares Ecomesh e a bomba de calor. A economia anual alcançada é de 27909 € e o corte de emissões de CO₂ é de cerca de 58 toneladas de CO₂/ano. Como os painéis fotovoltaicos são muito mais baratos que os híbridos, duas opções alternativas foram sugeridas com painéis fotovoltaicos. O primeiro consiste numa instalação solar com esses painéis fotovoltaicos e o outro nos painéis fotovoltaicos e uma bomba de calor reversível para resfriamento elétrico solar. A segunda opção com a bomba de calor reversível também foi recomendada no caso de se decidir por painéis fotovoltaicos Ecomesh em vez dos híbridos. A economia anual total para este caso alternativo é de 21043 € e o corte de emissões de CO₂ de quase 43 toneladas de CO₂/ano.

Palavras-chave

Absorção; arrefecimento solar; bomba de calor; energias renováveis; método F-Chart; painel híbrido

Table of Contents

List of Figures	xiii
List of Tables	xv
List of Acronyms	xvii
List of Symbols	xxi
1. Introduction	1
1.1. Motivation	1
1.2. Aim.....	2
1.3. Scope of the thesis	2
1.4. Contents	3
2. State of the art	5
2.1. Solar panels.....	5
2.1.1. Photovoltaic solar panels	5
2.1.2. Thermal solar panels	8
2.1.3. Hybrid solar panels	12
2.2. Cooling technologies	15
2.2.1. Heat pumps and vapour compression cycle.....	16
2.2.2. Absorption cooling	21
2.2.3. Adsorption cooling	24
2.3. Solar cooling: State of the art	25
3. Technical analysis	37
3.1. Installation in a hotel. Description of the system	37
3.2. Analysis procedure for the hotel case studies.....	38
3.3. Performance indicators.....	40
3.3.1. Efficiency indicators	40
3.3.2. Economic indicators.....	44
3.3.3. Environmental indicators.....	45

3.4. Calculations and simulations in EES.....	46
3.4.1. The software: EES.....	46
3.4.2. Data and assumptions.....	46
3.4.3. Calculations and methods.....	47
4. Results.....	57
4.1. Hotel fully provided with gas and the common electrical grid.....	57
4.2. Hotel with Ecomesh hybrid solar panels.....	59
4.3. Hotel with Ecomesh hybrid solar panels and a reversible HP.....	61
4.4. Hotel with Ecomesh hybrid panels and absorption cooling.....	63
4.5. Comparison of the case studies.....	64
4.5.1. Economics.....	64
4.5.2. Environmental impact.....	69
4.6. Discussion.....	70
4.6.1. Additional consideration.....	72
5. Conclusion and outlook.....	77
Annex 1. EES codes.....	81
A.1. Calculations for the solar system.....	81
A.2. The vapour compression cycle.....	90
A.3. Absorption cooling cycle.....	93
Annex 2. Technical sheets.....	97
Annex 3. The company, EndeF Engineering S.L.....	101

List of Figures

Figure 1. Contents of the master thesis.	3
Figure 2. p- and n-doped semiconductors [17].....	5
Figure 3. The photovoltaic effect [16].	6
Figure 4. Economic evolution of solar PV panels [19].	8
Figure 5. Schematic of the energy flows in a flat plate collector [20].	10
Figure 6. Series (left) and parallel (right) connection of solar collectors [24].	11
Figure 7. Characteristic curves of different types of solar collectors [20].	11
Figure 8. Global solar thermal capacity and annual energy yields until 2017 [25].	12
Figure 9. Types of water-cooled PVT panels depending on the degree of insulation [24].	14
Figure 10. Schematic of a vapour compression heat pump system [37].	18
Figure 11. Ln(P)-h diagram of ideal (left) and realistic (right) vapour compression cycles [35].	20
Figure 12. Share of solar collector types for heat pump applications [26].	21
Figure 13. Schematic of an absorption air conditioner with economizer [33].	22
Figure 14. Energy use in the residential sector of OECD countries during 2011 [51].	26
Figure 15. Thermal collector used for cooling applications worldwide [67].	28
Figure 16. Solar electric air-conditioning [1].	29
Figure 17. Schematic of a typical solar absorption cooling system [33].	30
Figure 18. Worldwide share of large/small scale cooling installations [89].	33
Figure 19. Percentage use of the different solar thermal cooling technologies [89].	34
Figure 20. Extract of the technical sheet of the Ecomesh hybrid panel	37
Figure 21. Hybrid solar panels installation in the hotel to provide electricity and DHW.	38
Figure 22. Schematic of solar electric cooling system with PVT panels.	39
Figure 23. Schematic of absorption cooling system with PVT panels.	39
Figure 24. <i>f</i> -Chart method for heat transfer systems using liquids [22].	49
Figure 25. Generic pressure-enthalpy diagram of a vapour-compression cycle [33].	51
Figure 26. P-h diagram of R410A.....	53
Figure 27. LiBr-H ₂ O absorption cooling cycle.	54
Figure 28. Total energy consumption of electricity and heat in the hotel.	57
Figure 29. Electricity consumption [kWh] in the hotel along the year.....	58
Figure 30. Domestic hot water thermal demand [kWh] along the year.	58
Figure 31. Annual energy consumption [MWh] (left) and costs [€] (right) in the hotel.	59
Figure 32. Energy production [kWh] from the Ecomesh hybrid solar panels.	59
Figure 33. Monthly energy savings [€] from the installation of Ecomesh hybrid solar panels.	60
Figure 34. Monthly energy savings [%] from the installation of Ecomesh hybrid solar panels.	60
Figure 35. Comparison of the electrical and thermal annual energy savings [€].	66
Figure 36. Comparison of the electrical and thermal energy savings [€] during the summer.	66
Figure 37. Investment and operational costs of each of the case studies analysed.	67

Figure 38. Comparison of the Primary Energy Consumption [kWh] for the 4 case studies. 68
Figure 39. Comparison of the investment costs for PV and PVT panels. 73
Figure 40. Comparison of the annual energy savings for PV and PVT panels. 73
Figure 41. Comparison of the CO₂ emissions cut for PV and PVT panels. 74

List of Tables

Table 1. Performance of absorption cooling cycles [76].	31
Table 2. Data for the solar installation in Madrid.	37
Table 3. Relevant data for the solar cooling system dimensioning.	47
Table 4. Correction factors for the power of a hybrid solar panel based on a PV panel.	48
Table 5. EER and COP values of the real cycles subject to analysis.	56
Table 6. Annual energy production and energy savings from the Ecomesh hybrid panels.	60
Table 7. Carbon dioxide emissions cut achieved by the installation of Ecomesh hybrid panels.	61
Table 8. Energy yield and efficiency indicators for the installation of Ecomesh hybrid panels.	61
Table 9. Primary Energy Consumption and Primary Energy Ratio for the 2 nd case study.	61
Table 10. Efficiency indicators for the solar part of the cooling installation, 3 rd case study.	62
Table 11. Efficiency indicators related to the overall solar cooling system (HP) and the use of primary energy.	62
Table 12. Primary Energy Consumption and Primary Energy Ratio for the 3 rd case study.	62
Table 13. Efficiency indicators related to the solar part of the absorption cooling installation for the 4 th case study.	63
Table 14. Efficiency indicators related to the use of primary energy for the 4 th case study.	64
Table 15. Primary Energy Consumption and Primary Energy Ratio for the 4 th case study.	64
Table 16. Investment cost of each of the solar installations considered.	65
Table 17. Operational costs for each of the case studies.	65
Table 18. Simple Payback Period for each of the case studies.	67
Table 19. Total primary energy consumption in a year for each of the case studies.	68
Table 20. Cost of primary energy saved for each of the case studies.	69
Table 21. NPV (€) and IRR (%) results.	69
Table 22. CO ₂ emissions cut in tons of CO ₂ avoided for each of the case studies.	69
Table 23. Economic and environmental key indicators for a PV-based alternative system.	72
Table 24. NPV, IRR and SPP for a PV-based alternative system.	75

List of Acronyms

IEA	International Energy Agency
GHG	Greenhouse gases
CFC	Chlorofluorocarbon
HCFC	Hydrochlorofluorocarbon
EU	European Union
EC	European Commission
RES	Renewable energy sources
AC	Air conditioning
DHW	Domestic hot water
PVT	Photovoltaic-thermal
R&D	Research and Development
COP	Coefficient of Performance
SPF	Seasonal Performance Factor
EES	Engineering Equation Solver
PV	Photovoltaic
Si	Silicon
V_{oc}	Open-circuit voltage
mono-Si	Mono-crystalline silicon
p-Si	Polycrystalline silicon
a-Si	Amorphous silicon
GaAs	Gallium arsenide
CdTe	Cadmium telluride
InP	Indium phosphide
DSSC	Dye-Sensitized Solar Cell
FPPV	Flat-plate photovoltaic
CPV	Concentrator photovoltaic
PVB	Polyvinyl butyral
DC	Direct current
AC	Alternating current
MPPT	Maximum Power Point Tracker
ETC	Evacuated tube collector
CPC	Cylindrical parabolic collector
FPC	Flat plate collector
PVC	Polyvinyl chloride
PP	Polypropylene
PE	Polyethylene

CO ₂	Carbon dioxide
BIPVT	Building-integrated photovoltaic-thermal (system)
CPVT	Concentrator photovoltaic-thermal
TIC	Transparent insulating cover
TIM	Transparent insulating material
NG	Neutral gas
VIG	Vacuum insulated glass
CTE	Código Técnico de la Edificación
ODP	Ozone Depletion Potential
GWP	Global Warming Potential
SHP	Solar heat pump (system)
H ₂ O	Water
LiBr	Lithium bromide
NH ₃	Ammonia
ASHRAE	American Society of Heating, Refrigerating and Air-Conditioning Engineers
CSU	Colorado State University
SACE	Solar Air Conditioning in Europe
CESAR	Cost-effective Solar Air Conditioning
CGD	Caixa Geral de Depósitos
OECD	Organisation for Economic Co-operation and Development
DEC	Desiccant Evaporative Cooling
LiCl	Lithium chloride
PVAC	Photovoltaic air-conditioning (system)
HFC	Hydrofluorocarbon
R134a	Tetrafluoromethane
R410A	Near-azeotropic mixture of difluoromethane and pentafluoroethane
R32	Difluoromethane
TRNSYS	Transient System Simulation (tool)
SAC	Solar Assisted Cooling
SHC	Solar Heating and Cooling
EEC	European Economic Community
EPBD	Energy Performance of Buildings Directive
ETS	Emissions Trading Scheme
EPB	Energy performance in buildings
EER	Energy Efficiency Ratio
OSE	Overall System Efficiency
PEC	Primary Energy Consumption
PER	Primary Energy Ratio
SPP	Simple Payback Period
CPE	Cost of Primary Energy

NPV	Net Present Value
IRR	Internal Rate of Return
CMSAF	Satellite Application Facility on Climate Monitoring
PVGIS	Photovoltaic Geographical Information System
IDAE	Instituto para la Diversificación y Ahorro de la Energía
HP	Heat pump
HFC-152a	1,1-Difluoroethane
R290	Propane
HVAC	Heating, ventilation and air conditioning
HFO	Hydrofluoroolefin
HFO-1234yf	2,3,3,3-Tetrafluoropropene
HFO-1234ze	1,3,3,3-Tetrafluoropropene
KIC	Knowledge and Innovation Community
LCA	Life Cycle Assessment

List of Symbols

k	Heat loss coefficient (k-value)
A_c	Active area of collector
P_{DC}	Total power produced in a year
G	Total irradiance in a year
A	Total surface of the panels exposed to the sun
Q_u	Useful heat obtained from the solar collectors
E	Total irradiation on a tilted surface in a year
a_1	Heat losses coefficient of the solar collector,1
a_2	Heat losses coefficient of the solar collector,2
T_m	Mean operation temperature of the PVT panel
T_{amb}	Actual ambient temperature
SF_e	Solar fraction of electric cooling systems
P_s	Solar electric power gain from the PVT panels
P_{aux}	Auxiliary electrical power from the public grid
SF_t	Solar fraction of thermal cooling systems
\dot{Q}_u	Solar thermal power gain from the collectors
\dot{Q}_{aux}	Heat power required from an auxiliary source
f	Monthly solar fraction
F_{DHW}	Annual thermal solar fraction for a system that produces DHW
Q_{DHW}	Thermal energy demand for the domestic hot water consumption
F_{abs}	Solar fraction for the absorption cycle, during the summer
Q_g	Heat required at the generator of refrigerant
\dot{Q}_r	Cooling or refrigeration power demand
P_c	Power of the compressor
\dot{Q}_g	Heat power supplied to the generator of refrigerant
\dot{Q}_h	Heating power demand
FP	Coefficient related to the climatic conditions and the type of heat pump
FC	Coefficient that measures the difference between the distribution and the testing temperatures
G_{summer}	Total irradiance during the summer
G_{winter}	Total irradiance during the winter

W_{aux}	Auxiliary electrical energy from the common grid
$W_{parasitic}$	Electrical energy consumption of parasitic equipment (valves, pumps, etc)
Q_{aux}	Heat provided by the auxiliary (gas) heater
Q_{out}	Total energy output, usable energy
ΔC_{inv}	Extra costs over a conventional system
ΔC_{op}	Annual reduction of energy costs
$\Delta C_{a,s}$	Annual extra costs for solar technology
CF_i	Cash flow of year i
r	Interest rate
n	Lifetime of the installation
I_0	Initial investment cost
P	Electrical power produced by photovoltaic solar panels (or hybrid ones)
N_p	Number of solar panels
P_n	Nominal power
G_{STC}	Irradiance at Standard Test Conditions (STC)
T_{cell}	Temperature of the solar cell
T_{NOCT}	Normal operation cell temperature
D_1	Non-dimensional coefficient that relates the absorbed energy to the thermal demand
D_2	Non-dimensional coefficient that relates the energetic losses in the collector to the thermal demand
F'_R	Heat transfer efficiency coefficient of the collector
N_{month}	Number of days of the month
$F_R \cdot (\tau\alpha)_n$	Correction factor that corresponds to the optical efficiency of the collector
F'_R/F_R	Correction factor for the thermal losses collector-heat exchanger
ΔT	Total number of seconds of the month
$F_R \cdot U_L$	Global thermal losses coefficient
K_1	Correction coefficient for the storage capacity
K_2	Correction coefficient for the DHW
F	Annual solar fraction
\dot{m}_r	Mass flow rate of refrigerant
\dot{W}_c	Work of compression
\dot{Q}_c	Latent heat removed at the condenser (rejected to the environment)
T_e	Evaporator temperature
P_c'	Condensing pressure

P_e	Evaporator pressure
h	Specific enthalpy
h_{ve}	Vapour specific enthalpy in the evaporator
h_{le}	Liquid specific enthalpy in the evaporator
h_{lc}	Liquid specific enthalpy in the condenser
h_{vd}	Specific enthalpy of superheated vapour
T_d	Temperature of the superheated vapour
x_s	Mass fraction of LiBr in the refrigerant-absorbent solution
x_{ab}	Mass fraction of LiBr in the absorbent solution

Greek symbols

φ	Latitude
β	Tilt angle
θ	Orientation
η_{PV}	Photovoltaic annual performance
$\eta_{G,PV}$	Global efficiency of a photovoltaic system
η_{INV}	Inverter efficiency
η_t	Thermal annual performance
η_o	Optical efficiency of the solar collector
ε_{el}	Energy efficiency for primary energy electricity conversion
ε_g	Energy efficiency for primary energy (gas) thermal energy conversion
γ	Temperature coefficient for the power
$\tau\alpha$	Transmittance-absorptance product
$\tau\alpha/(\tau\alpha)_n$	Correction factor that represents the modification of the incidence angle

Chapter 1. Introduction

This chapter gives a brief overview of the relevance of research on solar cooling technologies and presents the scope of this master thesis, the main aim and contents. The current situation in the energy sector and the need of alternatives on cooling powered by renewable energy sources are described. This gives the justification of the topic investigated. At the end of the chapter, the structure of the work to be conducted in this research is also summarised.

1.1. Motivation

The global energy demand is increasing due to the population growth and the industrialization process. The indoor comfort demand is also increasing, which results in higher electricity demand. This can be critical during peak loads [1]. From 2003 to 2030, global energy consumption is estimated to increase in about 71% [2]. According to the International Energy Agency (IEA) [3], the energy demand could increase by 35% from 2010 to 2035. An interesting alternative to reduce the peak electricity consumption is the use of waste heat or renewable energy [1].

Fossil fuels are primary sources of energy and we are still heavily relying on them in the present days [4]. They actually account for 78.3% of the global energy consumption in 2014 [5]. It is estimated that more than 80% of the energy consumption will be obtained from fossil fuels in some developed countries in 2035 [6]. These traditional sources lead to higher gas emissions, which contribute to heavier air pollution and also accelerate global warming, as it is the case of Green House Gases (GHG) [4]. Global warming occurs when carbon dioxide, released mostly from fossil fuels (oil, natural gas, and coal) burning, and other gases, such as ozone, methane, nitrous oxide, chlorofluorocarbons (CFCs), hydrochlorofluorocarbons (HCFCs) and water vapour, accumulate in the lower part of the atmosphere [7]. Alternative energy sources like renewables are required to address the problem.

The dependence on energy imports in the European Union (EU), which was 50% in 2000, is expected to increase by approximately 70% by 2030 [8]. The Vienna Convention for the Protection of the Ozone Layer (1985), the Kyoto Protocol on Global Warming (1998) and the five amendments of the Montreal Protocol (1987) all discussed the reduction of CFCs in the atmosphere. In 2015, the European Commission (EC) prohibited all the HCFCs [9]. The European strategy to reduce energy dependence involves two objectives: policies to control the energy consumption and diversification of the supply sources. The key to diversification is the use of renewable energy sources (RES), as they contribute to sustainable development [10].

Moreover, the use of air-conditioning (AC) systems has experienced a noticeable growth in the last decades all over the world, mainly in residential and commercial buildings [11]. The energy consumption for these systems is estimated at 45% of the whole households and commercial buildings [12]. Thus, solar cooling technologies represent a unique opportunity, especially in sunny countries, due to the huge amount of solar radiation and the increasing cooling demand [4].

The solar radiation availability and the cooling requirements are always in seasonal and geographical concordance [13]. Therefore, the load matches the overall solar availability. Moreover, the heat obtained from the solar panels can be used for cooling purposes in a refrigeration cycle during the summer, when the consumption of domestic hot water (DHW) is not as high as in winter. This allows a better utilization of the solar collectors and improves its economic performance and profitability. The idea is not only providing heating and DHW but also cooling or AC systems [11].

Apart from the increasing demand issue, there is a problem of scarce electricity and storage in developing countries to adopt high energy consumptive systems such as conventional air-conditioning devices [7].

1.2. Aim

The present work aims to study the existing solar cooling technologies, specially focused on those driven by hybrid solar panels. The goal is not only to study the available technologies but to explore the best options for the real implementation of this kind of systems since they are still not usual or abundant in cooling installations in buildings and have several limitations.

The most promising solar cooling technologies are analysed for the case of a 4-star hotel, used as reference system.

A technical study including the description of the systems, yields and thermodynamic cycle's simulations is conducted. Then, a comparison of four different case studies for the hotel is undertaken, based on performance parameters and a simplified economic analysis. With this, the suitability of the different solar cooling technologies regarding the performance, energy yields and economic savings is studied for commercial buildings such as hotels or nursing homes.

The thesis is developed in collaboration with EndeF Engineering SL, a Spanish company specialised in solar energy technologies.

1.3. Scope of the thesis

First of all, a study of the existing technologies that combine solar panels with cooling systems is conducted. This revision is done at different levels: commercial solutions currently available at the market, solutions being currently tested at research environments (universities, R&D projects, research institutes) and other promising solutions for the future. Special attention will be paid to cases with PVT solar contribution since it is the main product developed and manufactured in EndeF Engineering S.L.

Based on the information collected in the state-of-the-art section, several technologies will be selected to be analysed more in-depth. Initially, a combination of hybrid solar panels with two different technologies to generate cooling is analysed. A technical description of each system is performed. The selected technologies are applied to the case of a 4-star hotel with 100 guests and suited to its energy demand. Some codes are developed in order to run simplified simulations of the systems.

With this, several parameters will be evaluated, such as the solar fraction, the annual energy production, the efficiency of the systems or the Coefficient of Performance (COP). The software to be used for the simulations is Equation Engineering Solver (EES).

In the end, a comparison of the different options of solar cooling systems for the hotel is performed regarding the economics and the environmental impact. For the case studies, apart from the energy production and the efficiencies, cost savings and emissions cut will be evaluated. The goal is to determine the most suitable solar cooling installation for this kind of application.

1.4. Contents

This thesis is structured in three main sections: state of the art, simulation of the systems and economic and environmental analysis by application to case studies for a 4-star hotel, as illustrated in Figure 1.

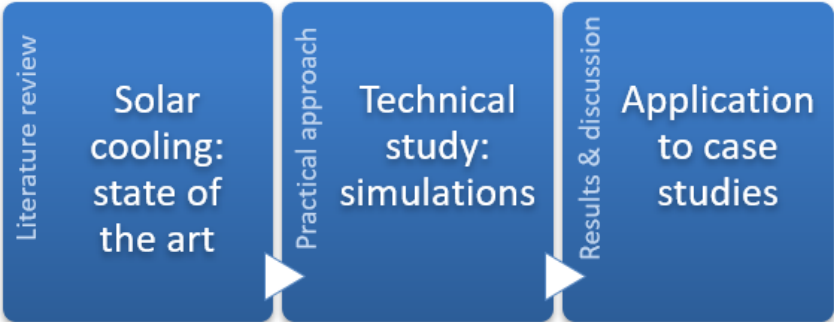


Figure 1. Contents of the master thesis.

Chapter 2. State of the art

This chapter provides a technical description of the solar panels and cooling systems available in the market. It also gives an overview of the state of the art of solar cooling technologies, their market status and barriers as well as the policy framework in the European Union.

2.1. Solar panels

2.1.1. Photovoltaic solar panels

Photovoltaic (PV) solar panels directly convert the sunlight into electrical energy. The photovoltaic effect was first observed by Edmond Becquerel in 1839 [14]. Solar photovoltaic technology started to gain importance as an alternative energy source with the oil crisis of the 1970s [15]. A variety of materials can be used for PV energy conversion but most of the systems use semiconductor materials in the form of a positive-negative (p-n) junction [16]. The silicon (Si) crystalline solar cell is the most commonly used.

In a typical solar cell, the Si atoms form a stable crystal lattice. Each Si atom has four valence electrons in its outer shell. In order to achieve its stable noble gas configuration (eight outer electrons), each of these atoms forms electron pair bonds with other four neighbouring atoms. In order to generate electricity, impurities need to be introduced into the lattice in a process called doping, illustrated in Figure 2. Doping atoms such as phosphorus (n-doped) or boron (p-doped) provide a surplus electron or a hole, respectively, to the lattice. This means that these atoms have one electron more or one electron less than Si atom in their outermost shell. The surplus electron can freely move in the crystal transporting electric charge. When a hole appears due to p-doping, neighbour electrons can fill the hole while creating a new one [17].

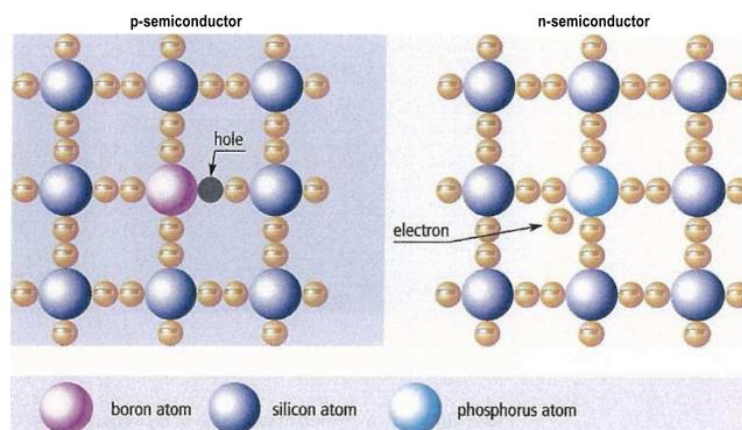


Figure 2. p- and n-doped semiconductors [17].

A p-n junction is formed when n- and p-doped semiconductor layers are joined. Since there is a concentration difference of electrons and holes between the two types of semiconductors, donor impurities from the n-type diffuse into the p-type layer [18]. This creates a transition region between the two types of semiconductors with few free charge carriers known as the space-charge region.

Positively charged atoms stay in the n-region and negatively charged ones remain in the p-region of the transition [17]. Diffusion is hindered by the electrical field created in the space-charge region from the separation of positive and negative charge densities [18].

Recombination occurs when a free electron bonds to an atom that lacks an outer electron (hole). The probability of recombination is higher outside of the space-charge region and it increases with the distance from this region.

The photovoltaic effect:

The production of current and voltage to generate electric power in a solar cell occurs when a photon is absorbed by an electron, raising it to a higher energy state. Then this electron moves from the solar cell into an external circuit, where it dissipates its energy and returns to the solar cell [16]. This is the photovoltaic effect, as described in Figure 3.

The basic steps in a solar cell operation are: generation of light-generated carriers, collection of the light-generated carriers to generate a current, generation of a large voltage (V_{oc}) across the solar cell and dissipation of power in the load and in parasitic resistances [16].

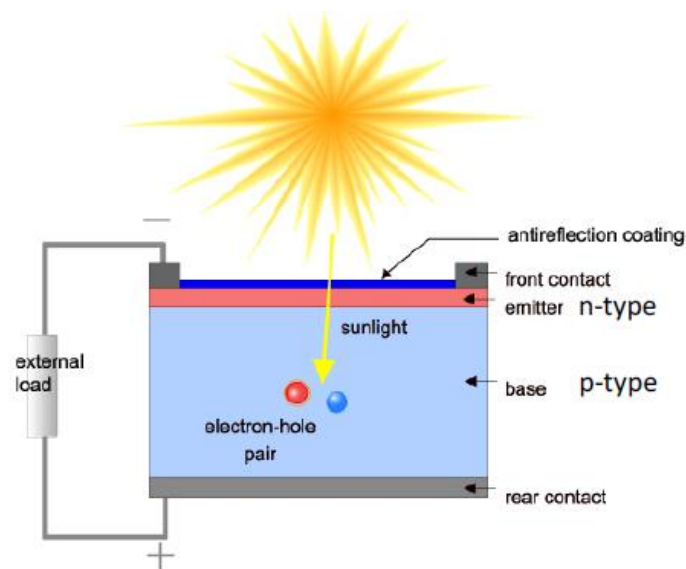


Figure 3. The photovoltaic effect [16].

The current generation in a solar cell involves two key processes: absorption of photons to create electron-hole pairs and collection of these carriers by the p-n junction. When the p-n-semiconductor (solar cell) is exposed to light, the electrons absorb photons. If the incident photons energy is greater than that of the band gap, the electron bonds are broken [16]. The released electrons are pulled into the n-region through the electrical field. The holes formed migrate in the opposite direction, into the p-region [17]. This prevents recombination, by which no current or power would be generated (the generated electron-hole pair is lost) [18].

When there is no load connected to the solar cell, a voltage is created by the diffusion of charge carriers to the electrical contacts (open circuit voltage, V_{oc}) [17].

A photovoltaic system is formed by solar cells connected electrically to form a photovoltaic module and several modules can form an array. Photovoltaic arrays can be connected in series or parallel.

A classification of the most important types of PV modules is presented below [15], [17]:

Types of PV modules:

Based on the photovoltaic cell materials:

- Silicon cell PV modules:
 - Single or mono-crystalline silicon (mono-Si) modules: these are the most widely used.
 - Polycrystalline silicon (p-Si) modules: they are less efficient than mono-Si modules.
 - Amorphous silicon (a-Si) modules: these have lower material and manufacturing costs than crystalline Si ones.
- Group III-V material cell PV modules, such as gallium arsenide (GaAs), cadmium telluride (CdTe) or indium phosphide (InP) crystalline solar cells, which is one of the most efficient cells developed so far, with an efficiency of 22%.
- Thin film cell PV modules: they have high radiation absorptivity and low cost, therefore they present a high potential. Dye-sensitized solar cell (DSSC) modules are a special type of this technology.
- Organic/polymer material cells modules.

Based on the module geometry:

- Flat plate photovoltaic modules (FPPV): most of the conventional systems in cities use them.
- Concentrator photovoltaic modules (CPV): they have higher power density than FPPV modules.

These are the main criteria of classification but there are some others such as the encapsulation material (Teflon modules, PVB modules and resin modules) or the structure (framed and frameless modules).

Photovoltaic panels' capital costs have experienced a dramatic decrease in the last decades due to the continuous research, development and improvement of PV technologies, which has also led to an abrupt increase of the global solar PV installations, as it can be observed in Figure 4.

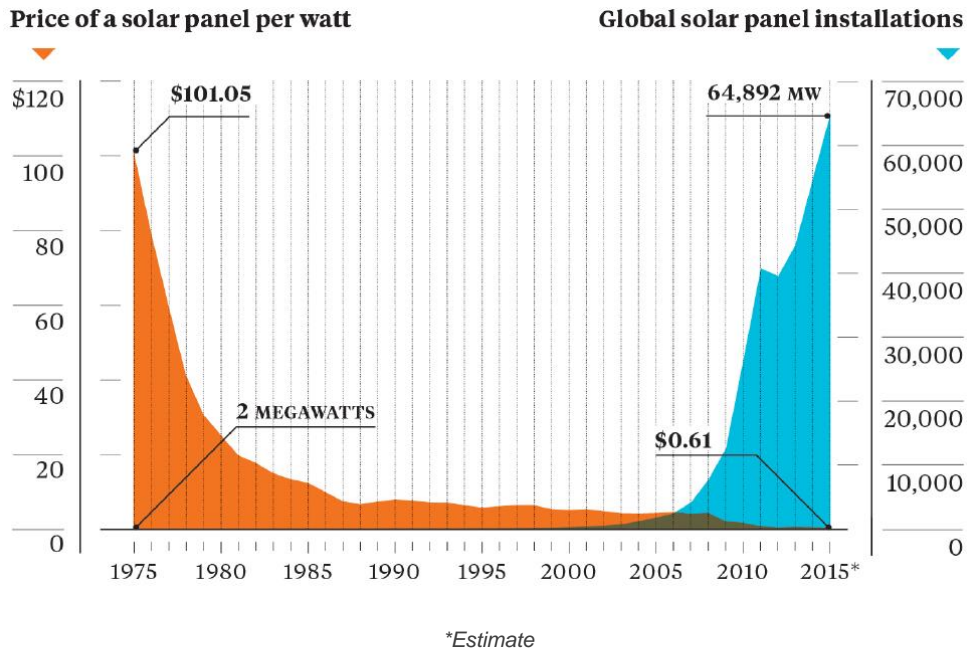


Figure 4. Economic evolution of solar PV panels [19].

2.1.2. Thermal solar panels

Solar collectors convert the short-wave radiation from the sun into heat. This thermal energy is used to heat up the fluid that flows along the collector tubes, which is normally water.

In the city centres, the main applications are the production of DHW for residential buildings and the heating of water in the swimming pools, as well as space heating.

The heat is produced when the absorber plate (usually a metal) collects the energy coming from the solar rays through its dark-coated surface [20]. In the absorber, a system of parallel pipes filled with a heat transfer fluid (usually water or water-glycol antifreeze solution) takes up the generated heat.

Types of solar collectors:

Most of the solar collectors used nowadays in urban areas are non-concentrating, liquid cooled thermal collectors. But there are many criteria to classify solar thermal collectors, with regard to the variation of the main features.

Based on the working temperature [21]:

- High-temperature solar collectors: high concentration index and sun-tracking system.
 - Heliostats: mirrors that concentrate solar radiation to a receiver on the top of a solar tower where it is converted to heat, reaching temperatures above 1000°C.
 - Parabolic discs: parabolic reflecting surfaces that concentrate solar rays to a gas receiver (air or helium) increasing its temperature up to 900°C.
- Medium-temperature solar collectors:
 - Evacuated tube collectors (ETC): they are formed of 10 to 20 vacuum tubes that allow convection losses reduction. They are expensive but highly efficient, can stand temperatures up to 100°C and do not need thermal insulation.

- Cylindrical parabolic collectors (CPC) or parabolic trough collectors: a cylindrical reflecting surface concentrates the radiation to a pipe where the fluid to be heated (oil) flows. They have a low concentration index and a solar tracking system. The working temperature range is 100-400°C.
- Low-temperature solar collectors: these are mainly flat plate collectors (FPC), which is the most common type nowadays in the urban areas and the main focus of this thesis. The working temperature is in the range 50-70°C. A wider description of these systems is given below.

Flat plate collectors are suitable for applications that require moderate temperatures, up to 70 to 90°C [22]. Unlike concentrating collectors, they use both beam and diffuse solar radiation and do not need sun-tracking systems. They are mechanically simpler and require less maintenance. They are mainly used for water heating, building heating systems and air conditioning [22].

Flat plate collectors are further classified according to several criteria into the following types [21]:

Based on the heat transfer fluid:

- Water collectors: they are more efficient. They can reach higher temperatures but are more expensive and difficult to maintain in case of leakage events.
- Air collectors: they allow low working pressures. However, they have poor thermal conductivity (air) and require a larger infrastructure.

Based on the presence of a cover:

- Glazed collectors: they have an external glass cover that reduces heat losses by convection on the frontal side. They allow higher supply and stagnation temperatures but are more expensive.
- Unglazed collectors: they do not include a frontal cover but a rear insulation. They have lower thermal efficiency at high ambient temperatures due to the convective effect with the surrounding air.
- Totally unglazed collectors: they neither include a frontal cover nor a rear insulation. They reach low working temperatures, around 25°C and are typically used for swimming pool heating.

Based on the material of the absorber:

- Copper collectors: highly conductive and resistant to corrosion. They have extended use despite their high price.
- Aluminium collectors: they have low density; they are a cheaper solution but have lower conductivity.
- Plastic collectors (PVC, PP, PE.): they are usually not covered (unglazed) neither insulated since they do not stand high temperatures. Their working temperature range is 25-35°C. They are made of a lighter material and are resistant to corrosion, but they also have lower conductivity. This type is especially recommended for outdoor swimming pools heating.

Working principle of a flat plate collector:

Figure 5 shows the energy flows in a FPC. First of all, the solar irradiance (G_0) hits the glass cover; before entering the collector, part of the energy (G_1) is reflected at the outer and inner surfaces of the glass. This cover is placed on the front to reduce heat losses by radiation and convection (Q_1) from the absorber surface. Therefore, the only heat losses by convection and radiation are those from the internally heated glass to the surroundings. The absorber surface also reflects a small part of the solar radiation (G_2) and converts the rest into heat. The thermal insulation on the rear part of the collector and on the sides reduces the losses via conduction (Q_2) as much as possible, by using suitable insulating materials. Q_A represents the finally usable heat [20].

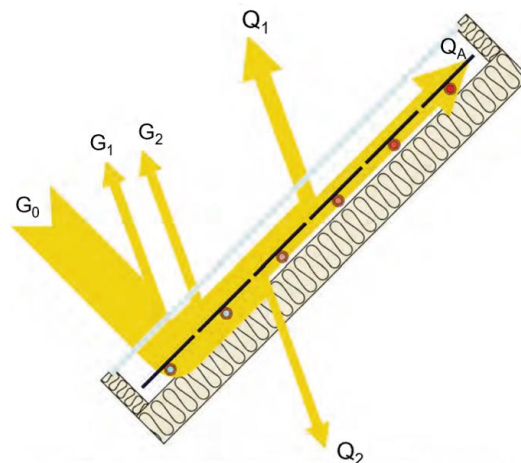


Figure 5. Schematic of the energy flows in a flat plate collector [20].

The efficiency is influenced by the design of the collector, by the particular optical and thermal losses. The optical losses represent the part of the solar radiation that cannot be absorbed by the collector, through the absorber surface. These losses depend on the transparency of the glass cover (transmission, τ) and the absorption capacity of the absorber surface (absorption, α). The thermal losses depend on the insulation, on the difference of temperature between the absorber and the outside air, and on the construction of the collector. The influence of the construction is described by the heat loss coefficient, k (k -value), measured in W/m^2K . The heat losses increase when the temperature difference between the outside air and the absorber increases for a constant irradiance. The average annual yield of a solar system with glazed flat plate collectors is 35–40% [20].

Common layouts of solar thermal collectors:

Solar thermal collectors can be connected in series or in parallel, as represented in Figure 6.

- » Series connection: the temperature increases from one collector to another. Thus, the yield of the system decreases. It may be an interesting solution for high-temperature applications. No more than 4 collectors should be connected in series [23].
- » Parallel connection: in this case, a bigger flow rate is obtained at lower temperature than the one in series. The pressure drop along the installation is also lower. This layout is more commonly used and provides a higher yield [23].

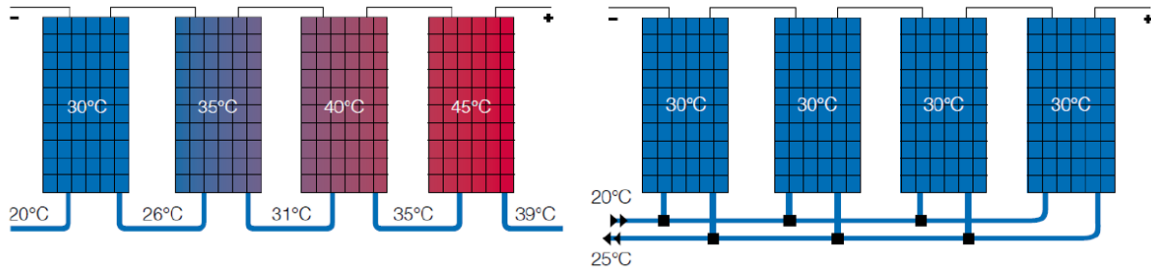


Figure 6. Series (left) and parallel (right) connection of solar collectors [24].

Stagnation temperature:

This temperature is achieved when the fluid and the absorber plate temperatures are the same and there is no liquid flow through the collector tubes [22]. This can happen when the solar irradiance is too strong and the circulation pump fails or if hot water is not used and the storage tank is hot (60–90°C) so that the system switches off and the collector stops providing heat. It is the maximum temperature possible inside the system. The greater the insulation, the higher the stagnation temperature. Well-insulated FPCs can reach stagnation temperatures of maximum 160–200°C. In case of ETCs the value may be around 200–300°C [20].

Collector characteristic curves and applications:

At the maximum temperature (stagnation temperature), the optical efficiency (η_0) of the collector equals zero, whereas at the minimum, when it is equal to the ambient temperature, this value, η_0 , is the highest. Figure 7 presents the efficiency curves (optical efficiency) and areas of application for different collector types with the same global solar irradiance [20].

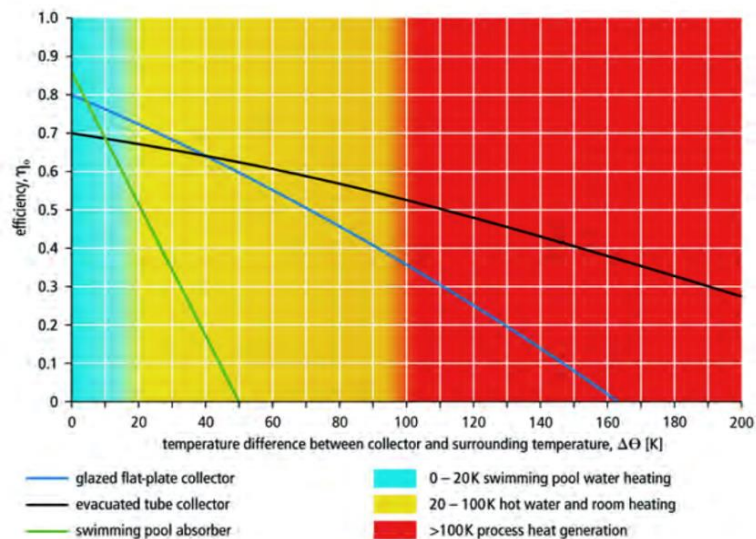


Figure 7. Characteristic curves of different types of solar collectors [20].

Global solar thermal capacity in operation grew from 62 GW to 472 GW between 2000 and 2017, as it can be observed in Figure 8. The corresponding energy yields in 2017 saved 41.7 million tons of oil and 134.7 million tons of CO₂ [25].

Moreover, Figure 8 also shows that the installation capacity increased considerably between 2007 and 2013; but since then, although there are still solar thermal systems being installed, the growth rate has been reduced.

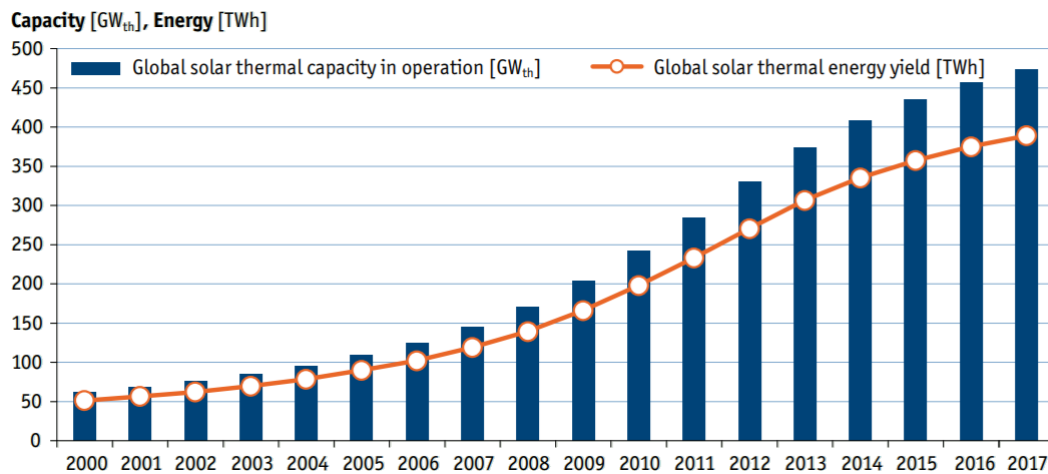


Figure 8. Global solar thermal capacity and annual energy yields until 2017 [25].

2.1.3. Hybrid solar panels

Photovoltaic-thermal collectors (PVT) are hybrid systems that produce both electricity and heat from the solar radiation. They include the PV cells and the thermal absorber. It is an emerging technology with a high potential in the market of solar panels, especially in combination with heat pumps [26].

The technology was globally developed after the significant increase of oil prices in the 1970s, motivated by three concepts: a better exploitation of the solar radiation, the PV laminate cooling to improve its efficiency and the optimisation of space on the rooftop.

In a conventional PV module, 5% of the incident solar radiation is reflected, 10-20% is converted to electricity and the remaining 75% is dissipated to the environment as heat. Hybrid panels make use of this excess heat, thus increasing the efficiency of the system [27].

With the incident solar radiation, some excess heat is generated in the PV cells that negatively affects the electrical performance, decreasing the yield. In PVT modules this heat is removed and converted into useful thermal energy. Thus, these panels generate more solar energy per unit surface area (40% more per m²) than a combination of PV panels and solar thermal collectors individually, which makes this technology a very interesting solution in buildings with limited space on the roof as it may be the case of urban areas [28].

Their thermal performance is normally lower than that of a standard thermal collector since part of the energy coming from the sun is used to produce electricity by the PV cells.

Nevertheless, the electrical performance is usually higher than that of conventional solar photovoltaic panels. This is because the thermal absorber material extracts heat from the PV cells while heating the water or working fluid that passes through the collector tubes [26]. This reduction of temperature in the cells increases the photovoltaic yield and the power production.

Thus, the thermal part of these systems can be also seen as a cooling effect of a conventional PV panel; in fact, hybrid solar panels were developed from this idea, in order to improve the performance of photovoltaic solar panels under high-temperature conditions. However, the mentioned cooling effect also depends on the design of the system.

Among the most common applications of PVT collectors, one can find swimming pool heating and radiant underfloor heating (low-temperature applications, up to 50°C), DHW provision (medium temperature, up to 80°C) and residential solar cooling in the so-called trigeneration systems (high-temperature applications, above 80°C) [24].

Types of PVT collectors:

Hybrid panels can be classified into several types according to different criteria [24]:

Based on the panel type: flat plate collectors (FPPVT), building-integrated collectors (BIPVT) and concentrator collectors (CPVT).

Based on the heat transfer fluid:

- PVT/w collectors: these hybrid panels are water-cooled. Most of the times together with glycol in an anti-freezing glycol-water solution. They have higher thermal and electrical efficiency but are also more expensive. They are used in natural or forced circulation systems.
- PVT/a collectors: the air is the heat-transfer fluid. They have a simpler design, less leaking and freezing problems but also lower efficiency. They are lighter, uninsulated and also cheaper.
- PVT/m collectors: both air and water act as heat transfer fluids, in different channels.
- PVT/c collectors: in these systems, the fluid is a coolant, a refrigerant usually coupled with a heat pump unit. They have no insulation since the liquid flows at a lower temperature than the ambient.

Water-cooled PVT collectors can be further classified into three different types depending on the panel insulating layers (frontal and rear):

- Unglazed PVT-0 collectors: similar to PV modules but with the addition of a heat recovery system with no rear insulation. This design was developed to cool down the photovoltaic cells increasing the electrical efficiency. The stagnation temperature is around 70°C.
- Unglazed PVT-1 collectors: in this case, there is a heat recovery system with thermal rear insulation. The recovered heat is used for low-temperature applications. They are common in warm climates and the stagnation temperature is about 85°C.
- Glazed PVT-2 collectors: similar to PVT-1 type but a thermally insulating cover is added at the front with two main goals. First, avoid the thermal losses from the frontal part to the environment, and second, avoid or reduce the losses by reflection with a transparent material. Therefore, the thermal yield is increased together with the energy produced per unit of area. The frontal cover is named Transparent Insulating Cover (TIC) and can be of four types: TIC-air, TIC-TIM (Transparent Insulating Material), TIC-vacuum and TIC-NG (neutral gas).

Since the heat losses are decreased in both the frontal and rear part of the panel, the stagnation temperature is much higher (150°C). The differences among these three types of water-cooled hybrid panels are summarised in Figure 9.

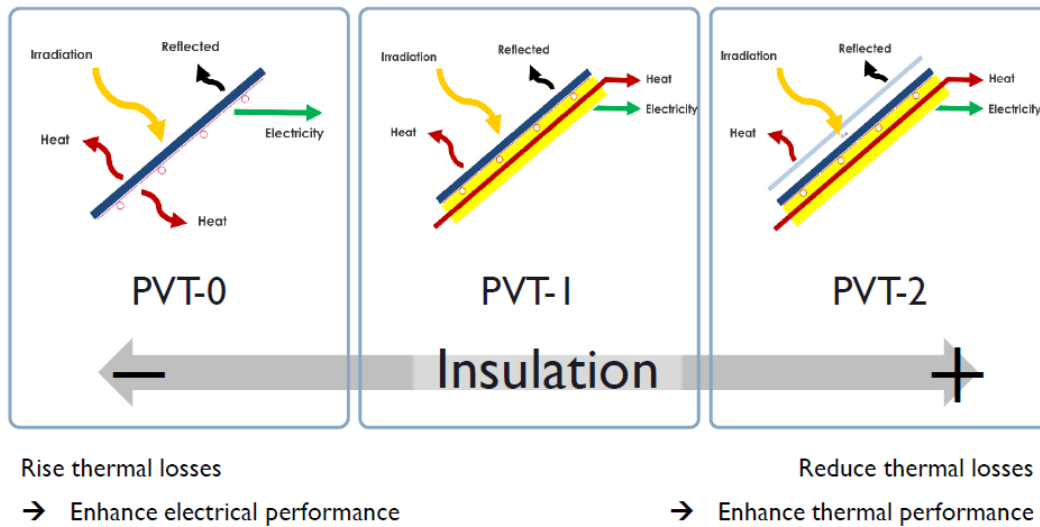


Figure 9. Types of water-cooled PVT panels depending on the degree of insulation [24].

Based on the absorber material:

- Copper-made PVT collectors: these are the most commonly used. They have high conductivity and resistance to corrosion, but are expensive.
- Aluminium-made PVT collectors: cheaper technology. They have low density and conductivity.
- Polymeric PVT collectors: they are relatively new. With a lighter material, they have low conductivity and limited working temperature.
- Steel-made PVT collectors: they have low conductivity and heavy material but also low price.

Based on the absorber geometry:

- Sheet-and-tube PVT type: one of the most commonly used. These collectors have high pressure bearing capacity and low contact surface. They are generally expensive.
- Flat-box structured PVT: these have high pressure losses. Their thermal efficiency can be improved by adding fins.

Other new approaches are flat plate tube absorbers, micro heat pipe absorbers, extruded or roll-bond heat exchanger absorbers.

Based on the PV cell type: monocrystalline silicon (mono-Si) PVT (best-known efficiency, 24.7%), polycrystalline silicon (poly-Si) PVT and thin film PVT (less common).

An especially thermal efficient PVT panel: Ecomesh

EndeF Engineering S.L. is an engineering company that has developed new products such as the Ecomesh hybrid solar panels. During a year, the company conducted experimental testing on a hybrid panel. From all the results obtained for the analysed model, it was concluded that when the average temperature of the panel was increased, the thermal efficiency of the panel was significantly reduced.

This occurred because the convection coefficient at the front of the panel was very high so there were large heat losses in this part of the panel [29]. Therefore, the possibility of placing a transparent insulating cover (TIC) to a hybrid panel was investigated. The aim was to achieve a heat loss reduction at the panel front part and to transfer the heat to the fluid, water, increasing the thermal yield. Three technologies were considered and further analysed for the insulating cover: a TIM (transparent insulation material), a VIG (vacuum insulated glass) and a neutral or inert gas (NG) glass. The three technologies were able to achieve important improvements regarding the yield. The thermal efficiency would increase by three times compared to a conventional hybrid panel without the cover exposed to high temperatures. This is because the transparent cover minimizes the thermal losses. However, the best solution, from both economic and technological points of view, was found to be the inert gas cover. The properties of different neutral gases were also thoroughly analysed and finally, a hybrid panel with improved energy efficiency was designed with an Argon transparent insulating cover [29].

Ecomesh solar panels produce both electricity and heat in a simultaneous way with a much lower collection area (reduced up to 40%) than the required for the corresponding photovoltaic and thermal panels of the same production capacity. In comparison with other hybrid panels present in the market, Ecomesh panels may need up to 15% less surface area to generate the same amount of energy, due to their innovative design (the TIC) that increases the efficiency [30]. This reduction of required collector area becomes crucial in cases of buildings in highly crowded cities where the free space is scarce. These panels are also intended to address the lack of space needed in many buildings for the integration of renewable energies, producing in a single system electricity and heat. Actually, the electricity production can be increased up to 15% because the heat is evacuated allowing the photovoltaic panels to operate in an optimal temperature range [30].

In fact, concerning the Argon transparent cover (the TIC), it has already been patented. It results in a more efficient product than the ones existing in the market and optimal for polygeneration and space scarcity problems. Nowadays, numerous installations are working with Ecomesh solar panels [31].

In Spain, the document “Código Técnico de la Edificación (CTE)”, which regulates the building sector in the country from 2006, states the obligation of installing solar collectors on residential buildings and photovoltaic panels in some other installations [32]. Ecomesh solar panels can contribute to these requirements.

More detailed information about the company EndeF Engineering S.L. and its involvement in European innovative projects and other interesting initiatives and features may be found in Annex 3.

2.2. Cooling technologies

The main methods of lowering air temperature for cooling are: refrigeration, by removing energy from the air, or evaporative cooling of the air. In refrigeration systems, the entering air can have any level of humidity, whereas for evaporative cooling the air must have a low relative humidity [33].

In humid climates, desiccant systems may be used for dehumidification since a large portion of the air conditioning is achieved by the removal of moisture from the air [33].

In this work, only refrigeration technologies are discussed. Later on, their application in solar cooling is analysed. The most widely used technology for air conditioning is the vapour compression refrigeration cycle. The energy input to the compressor may be provided as electricity or mechanical energy (from an engine), depending on the design and type of compressor [33]. The second most common cooling technology is based on the absorption cycle.

2.2.1. Heat pumps and vapour compression cycle

Heat pumps extract heat from the environment at a low temperature level (heat source) and “pump it” to a higher temperature level (heat sink). In order to drive this process of “pumping”, an energy source with higher exergy content is required. In electrically-driven compression heat pumps, this source is electricity that is used to drive the compressor of the refrigeration cycle [26]. These devices represent one of the most efficient and economical ways to produce heat with electricity since for each unit of energy consumed they are able to produce up to four units of thermal energy. They also have less environmental impact than other forms of heating, such as a gas boiler, as no fossil fuels are burned apart from the required amount to generate the electricity that powers them.

Around 1850, Swiss pioneers invented the first refrigeration machines, which can also be used as heat pumps for heating. However, it was the large demand for cooling that led to the fast development of this technology. Over 130 million heat pumps for heating and cooling purposes were already operating around the world by 2005 [34].

Heat pump systems have many different applications: space heating, air conditioning, integral AC systems that also produce DHW, indoor swimming pools water heating and industrial processes, among others [35].

Types of heat pumps:

Heat pumps may be classified according to different criteria, as shown below [36]:

Based on the medium for the heat exchange (the heat source and the heat sink nature):

- Air-to-air heat pumps: the heat is driven from the outside air to the inside air of the room or space that needs to be heated or conditioned. They are the most common ones due to their lower price and especially due to the higher availability of the heat source. They have the advantage of the higher specific heat of air, compared to the case of water.
- Water-to-air heat pumps: in this case, the heat source is the water and the heat sink the air of the room that must be heated. This type of heat pumps is not so common nowadays.
- Water-to-water heat pumps: they take the heat from an underground water stream to provide a hydraulic heating installation. These pumps have a higher Coefficient of Performance (COP) than the ones with air since the temperature of underground water streams remains nearly constant over the year.
- Air-to-water heat pumps: the heat is exchanged with a hydraulic circuit. One of the biggest advantages is the possibility to use them not only for space heating but also to produce DHW.

They are the most commercialised ones nowadays. Moreover, minimum maintenance is required.

- Ground-source heat pumps (ground-to-air or ground-to-water): these are very similar to the water-to-water heat pumps. But in this case, the heat exchange occurs with the underground surface by means of an auxiliary fluid. As already explained, the underground temperature remains nearly constant improving the efficiency. However, they are also more expensive.

For the residential sector, the outdoor air and the ground are the most common heat sources nowadays. In the case of outdoor air, evaporation usually takes place in an air-to-refrigerant heat exchanger located outside or integrated with the building architecture. In ground-source heat pumps, the heat is usually transported from the ground to the heat pump through a brine circuit [26].

Based on the configuration of the heat pump:

- Packaged heat pumps: all the components and controls are assembled in a single unit.
- Split-system heat pumps: they have an indoor unit and an outdoor unit, which normally includes the compressor. This avoids the noise from the compressor indoors.
- Multi split-system heat pumps: they have several indoor units to assist different rooms.

Based on the functionality:

- Reversible heat pumps: they allow both space heating and cooling applications by means of a 4-way valve that reverses the operation.
- Non-reversible heat pumps: these ones can only provide heat for space heating or DHW preparation or both.

There are also some special heat pumps such as those suitable for cold climates that include an electrical resistance in the outdoor unit or the so-called “inverter heat pumps”, which have an adaptable-power compressor. This means that the compressor is always working with a certain power that corresponds to the need for heating or cooling of the room, depending on its actual temperature. In this way, the power adapts to any change in the heating or cooling demand allowing a more efficient and stable operation and the subsequent electricity saving [36].

The vapour compression cycle:

The vapour compression cycle, also referred to as the reverse Rankine cycle, is the thermodynamic process used in most of the refrigeration systems [35]. A schematic diagram of the typical vapour compression cycle of a heat pump system is presented in Figure 10.

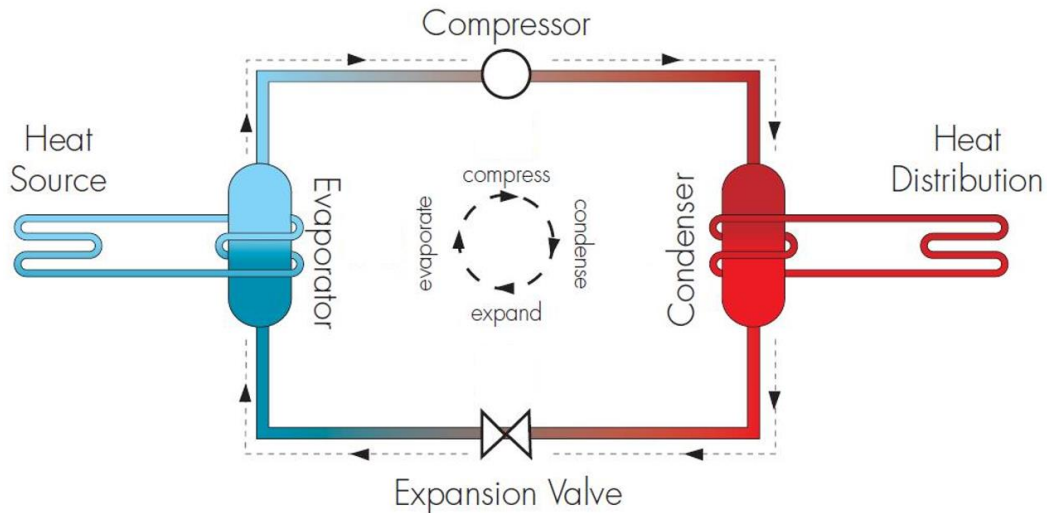


Figure 10. Schematic of a vapour compression heat pump system [37].

This thesis focuses on the reversible operation of heat pumps for cooling or air-conditioning applications. The cooling cycle in a vapour compression heat pump device is described as follows:

When the refrigerant reaches the compressor, its pressure and temperature are increased. Then the refrigerant vapour flows to the condenser, where it condenses at a temperature close to, but higher than, the ambient temperature, releasing heat to the environment [33]. Next, the liquid refrigerant pressure is reduced in the expansion valve, before reaching the evaporator. Then the low-temperature refrigerant is used to cool air or water by absorbing heat, as it evaporates, from the cooled medium. After the evaporator, the vapour of refrigerant returns to the compressor and the cycle starts again [33].

It is important to note that the standard mechanical refrigeration cycle is not considered to be a heat pump. A heat pump has a special compressor, it has to operate up to three times longer and over a much broader range of temperatures than a cooling-only compressor. It must operate also under severe conditions such as defrost cycles. In a cooling-only system, the condenser coil is larger than the evaporator coil. Typically, these evaporators do not work well as condensers and vice versa.

However, in a heat pump, each coil must be able to work as either condenser or evaporator, depending on the purpose (heating or cooling) or even both if the pump is reversible. The outdoor coil design must ease the defrost cycle [38].

Ideal and real vapour compression cycles:

In an ideal vapour compression cycle, the pressure drop is neglected in the heat exchangers (evaporator and condenser) and connecting piping. It is also assumed that the stream leaving the evaporator is saturated vapour and the one leaving the condenser is saturated liquid. The expansion process is considered isenthalpic and the compression process is isentropic.

Therefore, the state points for this type of cycle can be easily located on a $\ln(P)$ - h diagram, as the one shown in Figure 11 (left), with only two specified variables: the saturation pressures or temperatures for the evaporator and the condenser.

The specific heat capacity of a refrigerant has an important influence on the system performance, regarding both the compression work and the cooling capacity. The compressor work is turned into the internal energy of the gas, which can be increased in several ways: energy stored within the molecules (rotational or oscillatory motion) or kinetic energy (translational energy), which increase leads to a temperature increase. If a refrigerant gas has high specific heat capacity, a large amount of the increase in internal energy is stored within the molecules and only a small fraction leads to an increase in kinetic energy and therefore, its temperature. The compression work required increases with the temperature increase. When the gas stays relatively cool during the compression process, the work input is not as high as if the specific heat capacity were low and the temperature of the gas increased more quickly. Regarding the effect on the cooling capacity, when a high specific heat capacity refrigerant is expanded, a large amount of it is evaporated in order to cool the remaining liquid to the evaporator saturation temperature. Thus, less liquid is left to provide cooling [35].

In real vapour compression cycles, the pressure drop in both the evaporator and the condenser as well as in the connecting piping should be considered. Furthermore, the refrigerant leaving the evaporator is not saturated vapour as in the ideal cycle, but superheated, which presents two advantages [35]:

- All the refrigerant evaporates where it can contribute to the cooling capacity.
- Superheating within the evaporator (3-3a in Figure 11, right) ensures that the compressor does not receive any liquid entrained that could damage it.

In comparison with the ideal vapour compression cycle, there is a double penalty for the compressor due to the pressure drop in the evaporator and the superheating at its outlet. A higher-pressure difference should be overcome and also larger work is needed due to the higher temperature of the suction vapour. The compressor must also overcome the pressure drop of the refrigerant in the discharge line and the condenser, which also increases the required work input [35].

Before the condensation process, desuperheating of the vapour discharged by the compressor takes place in the condenser. Later on, after the vapour is condensed, the resulting liquid stream is subcooled (1a-1 in Figure 11, right) in the condenser as well. This step is important in many applications since it ensures that only liquid and no vapour bubbles enter the expansion valve, allowing for better flow control. Moreover, the presence of vapour in this stream could decrease the cooling capacity in the evaporator since there would be less amount of liquid to evaporate. It may lead to a loss of capacity and efficiency of the cycle. However, too much subcooling is also negative since if a high portion of the condenser is filled with liquid, there is less available area for heat rejection from the condensing fluid, which increases the saturation temperature along with the saturation pressure, increasing the required work input at the compressor [35].

A comparison of both ideal and real vapour compression cycles may be observed in Figure 11.

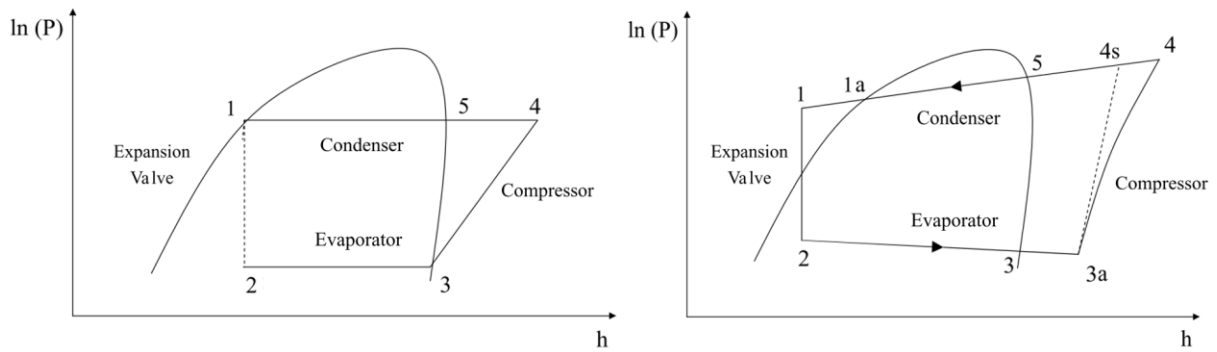


Figure 11. $\ln(P)$ - h diagram of ideal (left) and realistic (right) vapour compression cycles [35].

Performance of a heat pump:

Since there can be a big seasonal variation, in order to compare different heat pumps, an average value of efficiency over a year must be considered. The Seasonal Performance Factor (SPF) is a parameter used to define this overall efficiency of the system including all the auxiliary equipment. For air-source heat pumps in Central Europe, the average annual performance is about $SPF=2.9$. For borehole heat sources an average $SPF=3.9$ has been measured and for horizontal ground heat exchangers, $SPF=3.7$ [39], [40]. The values are different due to the higher temperatures of the ground heat source when the heat demand is maximum. Another reason for the lower SPF of the air-source heat pumps is the losses from the defrosting of the air-to-refrigerant heat exchanger [26].

The deviation of the performance of each heat pump from the average tested measurements may be high and it can be due to the difference in the temperatures of the heat source and of the useful heat to be delivered. It is important to note that under typical operating conditions, a decrease of 1K of the temperature difference between the evaporator and the condenser leads to an increase of about 2–3% in the COP [26].

As it has been explained when describing the ideal and real vapour compression cycles, the refrigerant properties influence the performance of the heat pump systems to a high extent. The main properties that a refrigerant must have for this application are: lack of corrosion (chemically inert), lack of toxicity, nonflammability, being environmentally safe, and other thermodynamic properties that allow achieving high energy conversion efficiency and sufficient capacity [35].

Some recent developments in heat pump technology are: the use of an economiser to overcome larger temperature differences between the source and the sink, the removal of refrigerants with large ozone depletion potential (ODP) and the development of other alternatives with lower global warming potential (GWP), the development of low temperature lift compressors with high COPs, such as turbocompressors [41].

Solar Heat Pump (SHP) systems:

Regarding the systems integrated with solar energy (Solar Heat Pump systems, SHP), heat pumps are usually provided with heat from the solar collectors at the evaporator, so that it runs on higher source temperature levels, improving the COP.

However, sometimes in this application the performance of the heat pump is overestimated. Some heat pumps are based on the assumption that the temperature increase for the superheating after the refrigerant evaporation is a constant value. However, this amount may increase with increasing source temperatures, especially for heat pumps that have thermostatic valves. Thus, in this case, the result would be the opposite, the COP achieved under these conditions would be reduced [26].

Regarding the use of solar collectors for heat pump applications, the type of collector plays an important role compared to other characteristics of the systems. Among the activities for task 44 from the IEA, these systems were surveyed by collector type for the use in solar heat pump applications [26].

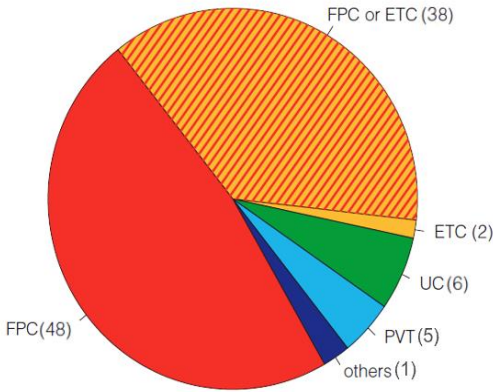


Figure 12. Share of solar collector types for heat pump applications [26].

In Figure 12 it can be observed that FPCs are utilized in nearly half of the systems (48%), whereas the use of ETCs is required only in some cases (2%). The choice between these two types (38%) is normally affected by the conditions of each particular installation and the preferences of the client. Uncovered or unglazed collectors (6%) are found only in certain applications such as series-only systems [26]. Hybrid solar panels (PVT collectors) have been recently developed; only a few SHP systems available in the market include this technology (5%) [26].

2.2.2. Absorption cooling

Absorption cooling is based on the physical or chemical affinity of two substances in different states. The solution process depends on the pressure and temperature conditions. At a low level of both variables, absorption of refrigerant vapour takes place, while at a high level the liquid absorbent releases the previously absorbed refrigerant.

The first example of an absorption refrigeration system was already found in the eighteenth century. As it was observed, ice can be made by evaporating pure H₂O within an evacuated container in the presence of sulphuric acid. In 1859, the French engineer Ferdinand Carré patented the first absorption machine, which used an ammonia-water working pair. In 1950, a new system was introduced with H₂O-LiBr as working fluid pair for commercial purposes [42].

In absorption refrigeration or air-conditioning systems, the refrigerant is dissolved in a liquid (the absorbent) in the absorption unit via an exothermic reaction.

Then the solution is pumped to a high pressure level. In the generator, heat is provided so that the refrigerant is evaporated (or distilled) and desorbed from the solution (endothermic reaction). The vapour of refrigerant is condensed in a water-or- air-cooled condenser and the liquid passes through a pressure reducing valve until the evaporator [33]. There it chills the water or the ambient air as it evaporates and the desired cooling effect takes place. The refrigerant vapour flows back into the absorber vessel, where it will be reabsorbed by a less volatile liquid absorbent. The heat required for desorption in the generator can be supplied directly from solar energy [33]. Figure 13 shows a typical absorption cooling cycle with an economizer (solution heat exchanger), which can be optional and recovers the internal heat to improve the performance of the system up to 60% [33].

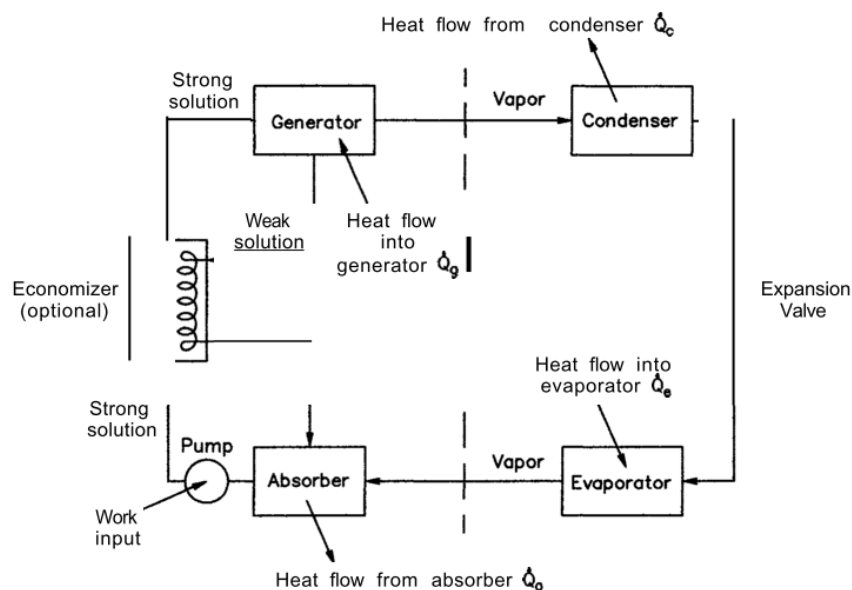


Figure 13. Schematic of an absorption air conditioner with economizer [33].

The performance of an absorption cycle depends on the refrigerant-absorbent pair. A list of desired properties for this pair is presented below [33]:

- A refrigerant more volatile than the absorbent in order to ease the separation in the generator.
- Low fluid viscosity, for a better heat and mass transfer and reduced pumping power.
- The absorbent must have a strong affinity for the refrigerant under absorption conditions.
- Highly stable system for long-term operations.
- Nontoxic and non-flammable fluids (especially for residential applications). The fluids must not cause long-term environmental effects.

The main absorption working pairs that meet most of the requirements are ammonia-water ($\text{NH}_3\text{-H}_2\text{O}$) and lithium bromide-water ($\text{LiBr-H}_2\text{O}$).

In the $\text{LiBr-H}_2\text{O}$ system, LiBr is the absorbent and water is the refrigerant, whereas, in the ammonia-water system, NH_3 is the refrigerant and water is the absorbent. LiBr is a non-volatile absorbent whereas H_2O is a volatile absorbent and the system needs an extra rectifier to obtain the pure refrigerant (ammonia) back after the absorption process. The $\text{LiBr-H}_2\text{O}$ system can operate at lower pressures since it has high volatility ratio.

It means that in the case of a solar installation, the system can be provided with thermal energy from flat plate collectors, which can achieve lower generator temperatures [33]. However, the system has to be operated above the freezing point of water and LiBr tends to crystallize when air cooled. Thus, the LiBr-H₂O system is usually operated at temperatures of 5°C or higher in the evaporator. In order to overcome the crystallization problem, a mixture of LiBr with some other salt can be used as absorbent [33].

Unlike the LiBr-H₂O, which can just be used for buildings cooling producing positive cold, the ammonia-water system can be operated at very low temperatures, producing negative cold [43]. For this reason, it is mainly used in the refrigeration field (industrial refrigeration). However, for temperatures below 0°C, water vapour must be completely removed from ammonia by means of a rectifying column to prevent the formation of ice crystals. Furthermore, ammonia is a safety Code Group B2 fluid (ASHRAE Standard 34-1992). It is toxic and its use indoors is restricted [44].

Ammonia's boiling point is much lower than that of water, so a much higher fraction of it is boiled off in the boiler, during the process of desorption, and only a small fraction of water also evaporates. In the rectifier, the vapour is cooled by the counter-current flow of the strong NH₃-H₂O solution from the absorber in order to separate this water (condensation) from the volatile ammonia [33]. The NH₃ that leaves the rectifier at high pressure and temperature is condensed releasing heat to the atmosphere. It may be further sub-cooled before reaching the expansion valve. In the evaporator, low-pressure ammonia provides the refrigeration effect by absorbing heat from the room or the surroundings during the vaporisation process. In the absorber, the water (or the weak solution, in a real system) absorbs the ammonia vapour coming from the evaporator. The weak NH₃-H₂O solution, after desorption, comes back to the absorber through a pressure reducing valve [33].

The main difference between the two main systems described above is that the NH₃-H₂O system has a rectifier after the boiler in order to condense as much steam out of the mixture vapour as possible [33].

Other refrigerant-absorbent pairs are: ammonia-salt, ammonia-organic solvent, ammonia-water-salt, alcohol-salt, methylamine-salt, etc [33]. An attractive feature of absorption technology is that the desorber can be driven by any type of heat source, including solar heat and waste heat [45].

The COP values range from 0.5 for a small unit (single stage) to 0.85 for a double-stage, steam-fired unit [33]. It is not recommended to compare directly the COP of an absorption installation like this with that of a vapour-compression cycle because in the second case, the value is usually quite higher than the unit, as it measures the efficiency of the conversion of electricity into heat or cool (thermal energy), but does not include the efficiency of electric power generation or transmission.

Based on the thermodynamic cycle and the solution regeneration, absorption systems can be classified into three categories: single-, half-, and multi-effect (double and triple) absorption cycles. The single-effect and half-effect chillers require relatively lower temperatures compared to multi-effect systems [46]. Single-effect absorption cooling system is the simplest arrangement [47] and consists on the basic absorption cycle, with a single absorber and a generator [7]. The half-effect cycle is named after its COP, which is almost half of that of the single-effect cycle [47].

A double-effect absorption cooling system is an effective combination of two single-effect systems, in which two generators connected in series work at different temperatures. The whole cycle has three different pressure levels: high, medium and low [7]. The COP almost duplicates the value of single effect systems [47]. It is usually around 1.1 and 1.2. These systems require higher driving temperatures in the range of 140–180°C.

Triple-effect absorption cooling systems can be classified into single-loop and dual-loop cycles. The single-loop type is basically double-effect cycles with an additional generator and an extra condenser. Since the H₂O/LiBr pair cannot work at relatively high temperatures, a different working pair must be used for the high-temperature cycle [7]. These cycles can achieve COPs of about 1.7 [48]. A dual-loop triple-effect cycle is composed of two cascaded single-effect cycles. These systems can obtain a theoretical overall COP of about 1.8 [48].

2.2.3. Adsorption cooling

Adsorption consists of bonding a gas or another substance on a solid surface [49]. This technology was first used in refrigeration in the early nineties [7]. In adsorption cooling, the adsorbent (solid) and the refrigerant (gas) experience a surface interaction, which can be physical or chemical depending on the forces that enable adsorption in each particular case. Physical adsorption takes place via Van der Waals type intermolecular forces (refrigerant molecules on the adsorbent surface) [50]. However, in chemical adsorption the refrigerant gas and the adsorbent (solid) share electrons (covalent bond) releasing energy.

Different working pairs are used for physical and chemical adsorption. Silica gel-water, activated carbon-ammonia, activated carbon-methanol and zeolite-water can be used for physical adsorption. Hydrogen-metal hydrides and ammonia salts with alkaline compounds can be used for chemical adsorption [43].

While absorption process is a volumetric phenomenon and the absorbent is a liquid, adsorption is a surface phenomenon and the sorbent is a solid [1], [7]. The adsorbent must be a solid porous surface with a large surface area and high adsorptive capacity.

Choudhury et al. (2010) [12] presented a review of solar powered air conditioning using adsorption process. Physical adsorbents such as silica gel, zeolites, activated carbon and alumina have highly porous and very selective structures and surface-volume ratios in the order of several hundred [12].

When the adsorbent and the refrigerant are in the same vessel, the former can maintain the pressure by adsorbing the refrigerant, once it evaporates. The process is intermittent because the adsorbent gets saturated. At this point, it must be regenerated by applying heat. Therefore, multiple adsorbent beds or sorption chambers are required for continuous operation [51].

The cycle consists of two sorption chambers, an evaporator and a condenser [7]. Adsorption cooling process occurs as described in the following steps:

1. In the evaporator, the refrigerant is vaporised at low pressure and temperature, producing the desired cooling effect.

2. The obtained vapour enters the sorption chamber where the solid adsorbent, such as activated carbon or silica gel, adsorbs the refrigerant. Since adsorption is an exothermic process, this compartment must be cooled to increase the efficiency of the process [1].
3. In the second sorption chamber, the refrigerant vapour is desorbed by applying heat. The solid adsorbent may be regenerated using hot water from an external heat source, such as solar collectors or waste heat [1].
4. In the last step, the condenser, the refrigerant vapour is condensed to liquid by heat removal using cooling water, normally supplied from a cooling tower [7]. The liquid is then sprayed in the evaporator [1].
5. After this, the functions of the two chambers are reversed by alternating the opening of the butterfly-type valves and the cooling and heating waters flow direction. This assures a continuous adsorption operation so that chilling water is constantly produced [7].

The driving heat temperatures of existing adsorption chillers are usually in the range of 60–95 °C [52] and the COP values typically between 0.5 and 0.6 [1].

The main advantages of adsorption chillers are: low driving temperature, starting from 60°C [53] [54], robust technology with no severe risk of crystallization, low electricity consumption due to the absence of solution pump and environmentally friendly materials are normally used (silica gel, zeolite). The main disadvantages are the lower COP as compared to absorption technology, the intrinsic intermittence of the system, the poor heat exchange between the adsorbent and the cooling or heating fluids and the high vacuum tightness as well as the careful design of external hydraulic circuits (due to the cyclic temperature variations) required [49].

2.3. Solar cooling: state of the art

The total global capacities for solar PV and solar thermal energy are reported to reach 227 GW and 435 GW at the end of 2015, respectively. Especially, the solar thermal capacity, widely used to provide heating and cooling, has greatly increased in the last decades [55]. Solar-driven cooling systems may be an interesting alternative to traditional air-conditioning installations powered by the electrical grid. These systems use electrical or thermal processes to convert solar radiation into cooling.

Conventional systems have several disadvantages: electrical energy is mainly obtained from the burning of fossil fuels, which leads to carbon dioxide emissions contributing to the greenhouse effect and therefore, to the global warming. The electrical grid undergoes peak loads during the summer months that cannot be covered by the power plants. Last but not least, the use of conventional air-conditioning units is unaffordable in many cases.

By contrast, solar cooling technologies offer a reliable and environmentally friendly solution, which major advantage is the seasonal coincidence between the high demand and the availability of solar radiation [56]. Efficient heat storage can cover the cooling demand during the night time [3]. Most of the suggested technologies are able to reduce or eliminate the harmful effects of traditional equipment as well as allow relevant energy savings [43]. Actually, Ullah et al. [46] reviewed different absorption and adsorption systems to conclude that solar cooling technologies can achieve primary energy savings of 40 to 50%.

First studies about solar cooling were published after the energy crisis of 1973. Some pilot plants were already constructed at that time, such as the famous Colorado State University (CSU) Solar Houses [57] [58]. At that time, solar cooling technologies with PV panels were considered too expensive, due to the high cost of PV modules until some years ago. They were only used for small applications like small fridges for transporting medicines. Nevertheless, gas-driven sorption systems were already available in the market [59].

Since the cooling demand increases during periods of time when the intensity of solar radiation is also higher, these technologies have been highly investigated throughout the years, and solar cooling has been an important issue since 1980 [60]. However, these technologies have not experienced large market penetration. They have several barriers such as the high cost of absorption chillers, the need of a cooling tower for the installation, the lack of standardisation and integration with building design [61]. There are several international projects and initiatives to address these limitations, such as SACE (Solar Air Conditioning in Europe), CLIMASOL CESAR (Cost-Effective Solar Air Conditioning) or SOLAIR [47]. Among the projects in the SACE database, the 70% is based on absorption cooling with the LiBr-H₂O working pair [62]. In fact, in many of the mentioned projects, the aim is to develop a small-scale efficient absorption unit [47].

In 2011, worldwide, around 750 solar cooling systems were installed, including small installations with a capacity lower than 20 kW [3]. Very large installations have already been completed or are under construction. One remarkable example is the system at the headquarters of the CGD bank in Lisbon, Portugal with 400 kW of cooling capacity and a collector field of 1560 m² [3].

According to the IEA, the worldwide solar energy production in 2011 was equal to 959 PJ. The 74% was solar thermal, 24% electrical (PV) and the remaining 2% corresponds to concentrating solar power [51]. The distribution of energy consumed in the OECD countries in the residential sector in 2011 is presented in Figure 14 (IEA, 2013). As it is observed, space heating represented almost 50% of the energy use whereas space cooling consumed around 6%. The utility buildings sector is not included, but it usually has a large heating and cooling energy consumption [51].

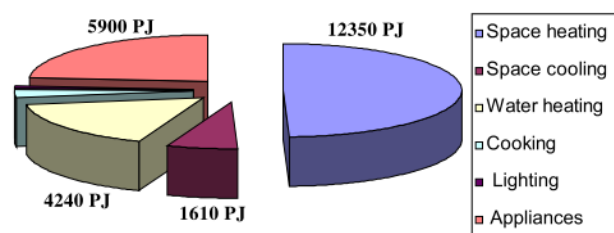


Figure 14. Energy use in the residential sector of OECD countries during 2011 [51].

Solar cooling systems can be classified into four different categories that also include subcategories:

- Solar electric cooling (solar photovoltaic cooling systems)
- Solar thermo-electrical cooling systems
- Solar thermo-mechanical cooling systems
- Solar thermal cooling systems

The first one is a PV-based system where solar energy converts to electrical energy and is used for cooling in a similar way as conventional methods. The second one produces cold (cooling) by thermoelectric processes. In the third category, thermal energy is converted to mechanical energy that is used to produce the cooling effect. The fourth group corresponds to heat-driven cooling technologies such as absorption powered by solar collectors. In some cases even the solar collectors directly heat the refrigerant that flows through the collector tubes [7].

Thermally-driven technologies can be also divided into two main groups or categories: open sorption systems, also called open cycles (direct treatment of air temperature and humidity), and closed sorption systems or closed cycles (chilled water systems) [1].

- Open cycle processes refer to Desiccant Evaporative Cooling (DEC) systems and use water as the refrigerant and a hygroscopic material as a desiccant (sorbent) to condition the air. They are further classified on solid sorption-based systems (desiccant wheels, coated heat exchanger, silica-gel or LiCl-matrix) and liquid sorption-based systems (packed bed, plate heat exchanger, and LiCl solution) [1].
- In closed cycles, the most common sorption machines are absorption and adsorption chillers. Liquid sorption or absorption systems can use water-lithium bromide (H_2O -LiBr) or ammonia-water (NH_3 - H_2O) as working fluid pair. Solid sorption or adsorption cycles mostly include the systems H_2O -silica gel or H_2O -zeolite. Another type of closed cooling cycle is the ejector system [1].

Adsorption cooling has some disadvantages like the poor heat exchange between the solid adsorbent and the refrigerant or the intrinsic intermittence. However, despite their low values of COP, these systems can work with low-temperature heat input, around 60 to 70°C [59]. Moreover, some multi-staged adsorption units can be driven by heat sources at even lower temperatures, of 40 to 50 °C [56]. This seems to be an advantage for solar-driven systems, especially if flat plate collectors (or, in general, non-concentrating ones) are used.

Nevertheless, adsorption systems are more expensive and bulkier than absorption ones. Among the thermal closed-cycle systems, the single-effect LiBr- H_2O absorber was found to be the cheapest option by Kim and Infante Ferreira [63].

Porumb et al. [64] evaluated the potential of solar cooling technologies for an office building in Romania. They studied two options: an absorption chiller connected to solar thermal collectors and an electrical chiller driven by photovoltaic panels. They tested the annual solar cooling fraction, which was about 24.5% for the thermal system and around 36.6% for the photovoltaic system. Another relevant comparison between thermal and electric cooling was performed by Hartmann et al. [65] for a small office building located in Freiburg and Madrid. One of the chillers is driven by photovoltaic modules whereas the other is an adsorption unit connected to advanced FPCs. Regarding both economical and primary energy savings, the photovoltaic system showed better performance. Otanicar et al. [66] studied the future prospects of solar cooling technologies in economic and environmental terms. Solar electric cooling systems were estimated to require the lowest capital investments by 2030 due to the high COPs of vapour compression cycles and the cost reduction forecast for PV technology.

Medium-temperature (around 200 °C) solar cooling plants with a field of concentrating collectors have recently gained importance among the European researchers. These systems can reach higher operating temperatures and work with more efficient absorption chillers, of double or triple effect type. They can reach a higher overall solar energy conversion ratio compared to low-temperature systems, which reduces the investment cost and the solar collector area [11].

Regarding liquid desiccant systems, only a few are available in the market. They are completely different from the closed cycle systems, they treat the air directly and it is difficult to install them in existing buildings. Some other alternative technologies are thermo-electric, ejection systems, thermoacoustic or magnetic refrigeration, but very few of them are commercially available [59].

Solar thermally-driven cooling or air-conditioning systems include solar thermal collectors to produce heat from the incident radiation, a buffer heat storage tank for the extended time of use, the cooling unit (sorption chiller), cooling towers (dry or wet) that release heat to the ambient, the auxiliary heating system used when there is no solar radiation, pumps to regulate the flow rate and the necessary automatic controllers [1].

In general, flat plate and evacuated tube collectors are the most commonly used for solar thermal cooling technologies. Figure 15 shows the global percentage of use of different types of collectors for solar cooling (2012).

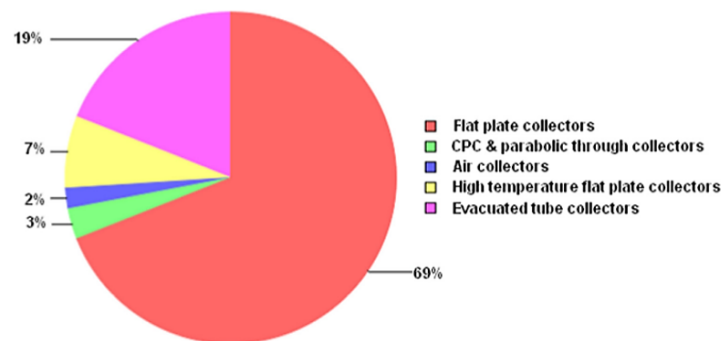


Figure 15. Thermal collector used for cooling applications worldwide [67].

Solar photovoltaic cooling systems:

In solar electric cooling systems, photovoltaic solar panels are coupled with a conventional vapour compression cycle. The panels produce electricity from the solar radiation that is used to run the compressor of the system. The excess is provided to the electrical grid acting as storage. In case of scarce solar radiation, the compression chiller is powered by the grid [1].

Solar photovoltaic panels have lower efficiencies (usually between 15 and 18%), but the solar cooling system as a whole is simpler and involves few components compared to solar thermal systems [1]. The basic schematic of this technology is shown in Figure 16.

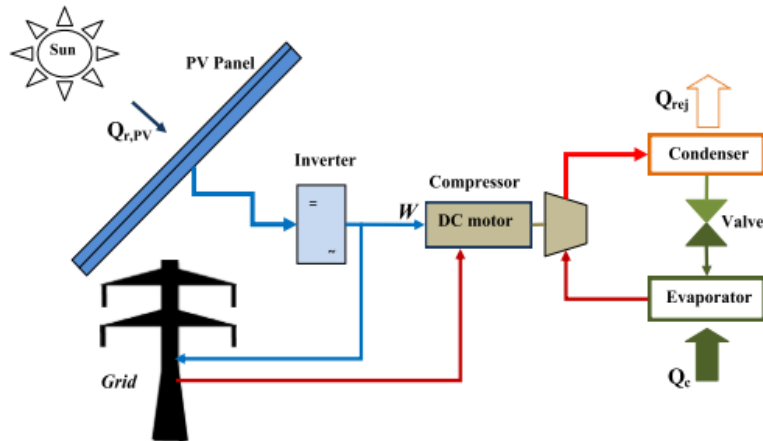


Figure 16. Solar electric air-conditioning [1].

The application of these systems was limited due to the high initial cost and the low efficiency of PV panels until recent years [51], [59], [66]. However, the PV modules price has recently undergone a large decrease and these systems have gained importance. In fact, PV air-conditioning (PVAC) systems are predicted to attract more attention in the future, taking into account the potential PV market and the massive cooling market [55].

Some researchers studied the operation characteristics of these systems for its application in residential or commercial buildings [68], [69]. The PVAC systems showed a stable and reliable operation.

The most common and promising PVAC systems are those connected to the electrical grid, the so called grid-connected PVAC systems, where the grid acts as a backup. When there is an excess of power from the PV system, it can be sent to the grid. Likewise, when the PV power is lower than what the compressor needs, power is supplied from the electrical grid [55].

According to the type of connection of the solar PV system to the vapour compression cycle, these systems can be also characterised as direct current (DC)-driven PVAC and alternating current (AC)-driven PVAC systems. The PV panels generate direct current electricity. AC systems can be easily connected to the conventional air conditioner by adding an inverter, the PV and control systems [69], whereas DC-driven PVAC use the electricity directly from the panels with no need for conversion from DC to AC. The energy efficiency may be improved in this second case since the losses from the inverter are avoided [55]. These systems have been recently commercialised by several Chinese companies. One example is a centrifugal chiller installed in an office building in Zhuhai (China) with a cooling load of 2790 kW. It is important to note that for large-scale commercial buildings, the price of electricity is much higher than in domestic ones. Thus, it is important to estimate the generation and the savings that these PV installations can bring for commercial buildings and decide for the better option before investment.

Several developments are also required for PVAC technology to spread. Efficient energy control strategies are necessary to improve energy efficiency, balancing the changing PV power generation and the variation of power flows from and into the grid. These strategies must also determine if the PV power is consumed only by the PVAC system or is sent to the grid depending on the electricity price.

Unlike PV power stations, most of the PV power is directly utilised by the PVAC and cannot be sold to the grid at a high price. Therefore, this should change. The subsidy policy for PVAC systems should guarantee that the PV system in these installations can obtain the same subsidy as the PV power stations [55].

For solar cooling applications, different refrigerants may be used in vapour compression cycles. Since chlorofluorocarbon (CFC) refrigerants such as R12 were prohibited due to their high Ozone Depletion Potential (ODP), hydrochlorofluorocarbons (HCFC) started to be used although they still have a relatively high ODP and were finally banned in 2010 [70]. Later on, hydrofluorocarbon (HFC) refrigerants such as R134a or R410A gained importance for refrigeration and cooling purposes. However, these ones contribute to the greenhouse effect and the global warming. They are greenhouse gases and have higher GWP than the former. Last generation low-GWP refrigerants include difluoromethane (R32), which is an HFC with zero ODP and a GWP of about one-third of that of R410A [71].

Solar absorption cooling systems:

Absorption air-conditioning systems are compatible with solar energy since the heat input is required at temperatures that available flat plate collectors can provide [33]. A schematic diagram of this type of systems is presented in Figure 17.

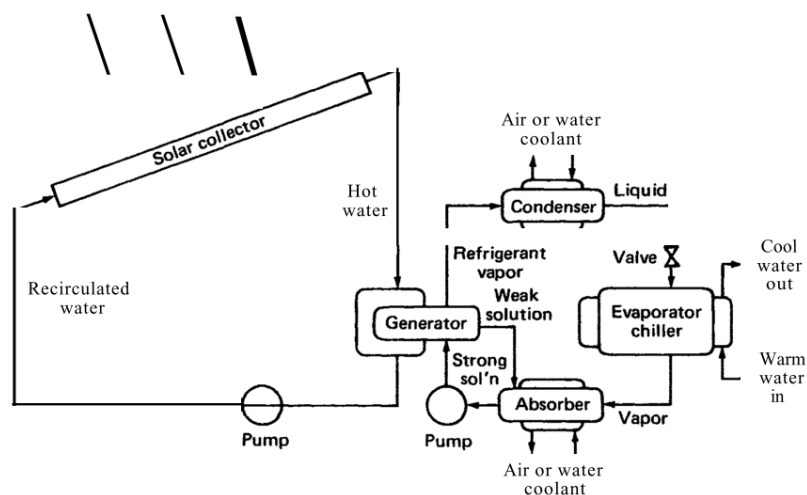


Figure 17. Schematic of a typical solar absorption cooling system [33].

Nowadays, the dominating technology in the market of solar thermally driven cooling systems is based on absorption [1]. It requires very low electric input and the physical dimensions of an absorption machine are smaller than those for adsorption machines of the same capacity, due to the high heat transfer coefficient of the absorbent [51].

Most solar cooling systems available in the market are based on the single-effect LiBr–H₂O absorption chillers provided by flat plate or evacuated tube collectors [72]. The driving temperatures are between 80 and 100 °C for water-cooled systems. For air-cooled systems, an increase of 30 K is needed [63]. The COP of these chillers ranges from 0.6 to 0.8.

Nakahara et al. [57] developed a single-effect absorption chiller run by H₂O/LiBr pair. The nominal cooling capacity of this system is 7 kW and the cycle is coupled with a 32.2 m² flat plate solar collectors array. During the summer period, the cooling capacity was 6.5 kW. The COP was in a range of 0.4–0.8 at the generator temperature of 70 °C to 100 °C. Syed et al. [73] also researched an H₂O/LiBr absorption system with 49.9 m² of FPCs in Madrid. With generator temperatures of 65–90°C, and 35 kW of cooling capacity, the average collector efficiency was approximately 50%.

Kim and Machielsen [74] carried out a comparative study in terms of performance and cost of different absorption systems and concluded that a half-effect LiBr–H₂O cycle represents the best alternative for air-cooled solar absorption air conditioning. However, this kind of system would require about 40% more heat exchange area and 10–60% bigger collector area compared to a single-effect system of the same cooling capacity.

Double-effect absorption chiller was launched in 1956 [7], superposing an extra stage cycle to the single effect system [47]. These systems are only available for large cooling capacities of 100 kW and above [63]. Tierney [75] compared four different systems with 230 m² area of collector and summarised that the double-effect chiller coupled with a trough collector had the maximum potential savings (86%) among the studied systems for a 50 kW cooling load.

Non-concentrating flat plate or evacuated tube solar collectors are able to achieve the required temperature for the generator. Nevertheless, the COP is lower in comparison with other technologies such as multi-effect absorption systems, often driven by steam produced from concentrating solar collectors, which are generally more expensive [7]. These cycles utilise an additional generator and heat exchanger to desorb the refrigerant with lesser heat input. The cooling capacity demand, the available solar intensity, the overall performance and cost determine the most suitable cycle configuration [7].

Grossman [76] carried out a comparison between the single-effect, double-effect and triple-effect chillers for solar cooling applications, concluding that the economics of the systems are dominated by the solar system cost. Flat plate solar collectors are suitable for the single-effect cycle, whereas the multi-effect absorption cycles require high temperatures (above 85 °C) that only evacuated tube or concentrating-type collectors can provide. They are able to reach higher COPs but those collectors are also more expensive. Typical cooling conditions for the different systems are shown in Table 1.

Table 1. Performance of absorption cooling cycles [76].

Absorption system	COP	Heat source temperature [°C]	Type of solar collectors matched
Single-effect	0.7	85	Flat plate
Double-effect	1.2	130	Flat plate/compound parabolic concentrator
Triple-effect	1.7	220	Evacuated tube/concentrating collector

Infante Ferreira et al. [51] investigated different absorption technologies with several working pairs and configurations as well as their combination with different types of solar thermal collectors. It may be concluded that as far as crystallisation limits are not reached, the system with concentrating parabolic trough collectors coupled with double-effect H₂O-LiBr chillers presents the lowest investment cost.

The next most suitable alternative, with acceptable investment levels, is represented by FPCs in combination with single-effect absorption units; H₂O-LiBr chillers are preferred but, when the operating conditions limit its use, the NH₃-H₂O working pair must be selected.

Balghouthi et al. [77] studied the feasibility of solar cooling systems in Tunisia, with simulations using the EES and TRNSYS programs. In Spain, Castro et al. [78] built a prototype of a 2 kW air-cooled absorption chiller for air-conditioning with LiBr-H₂O as working pair.

Lithium bromide-water systems have higher COPs than ammonia-water ones at the same temperature range because water has larger latent heat than ammonia. Moreover, the NH₃-H₂O cycle requires high temperature in the generator, in the range of 125 to 170 °C [47]. Thus it is not suitable for most of the solar applications. Only in case of using parabolic trough collectors, which are not convenient for the residential sector due to the high maintenance requirements [79].

Solar adsorption cooling systems:

Adsorption cooling power densities are much lower than those for absorption chillers. Therefore, adsorption technology is not competitive in small- or medium-size solar cooling systems. It is too bulky and expensive for these systems [51].

Adsorption systems may be a suitable alternative to the absorption chillers, which still dominate the refrigerant market in Europe [80], when the hot water coming from the solar collectors is below 90 °C [81]. Nevertheless, adsorption technology still presents a lower value of performance (COP) than that of absorption systems.

The performance of solar adsorption cooling systems has been reported in several research papers. Wang et al. [82] developed a prototype adsorption system with activated-carbon/water. The system had a solar collector of 2 m² and was able to produce 60 kg of hot water at 90 °C and 10 kg of ice per day. Henning and Glaser [83] designed a pilot adsorption cooling system with silica gel-water working pair. This system was powered by the solar heat produced in vacuum tube collectors with a surface area of 170 m². They reported a COP between 0.2 and 0.3.

Fasfous et al. [84] investigated the potential of a zeolite-water adsorption chiller powered by conventional FPCs in the University of Jordan in Amman. It was proved that a surface area of 40 m² of solar collectors could supply enough solar heat to power an air-conditioning system of 8 kW. Koronaki et al. [85] studied solar adsorption cooling systems for different types of collectors and Mediterranean climatic conditions. When FPCs were used, the maximum cooling capacity was 14.7 kW, achieved in Nicosia (Cyprus).

Santori et al. [86] developed an autonomous refrigerator to make ice for humanitarian aid. It was a solar adsorption system with the activated carbon-methanol pair. The prototype had 1.2 m² of solar collector area and was able to produce 5 kg of ice with a solar COP of 0.08. El Fadar et al. [87] developed a solar adsorption system with a thermal sensible storage and two adsorbers, in order to overcome the intermittency of adsorption cycle. The system was tested in Tetouan (Morocco); it achieved a cycle COP of 0.43 and a cooling effect of 2515 kJ for a collector area of 0.8 m².

Solar cooling with PVT systems:

Several types of solar cooling systems, most of them based on absorption technology with different types of cycles have been reviewed in the scientific papers, but there is not much work published about the use of photovoltaic thermal collectors (PVT) with absorption or adsorption chillers [88].

M. Alobaid et al. [4] analysed a solar driven absorption cooling system with photovoltaic thermal panels. They reported that 50% of primary energy was saved and the maximum electrical efficiency of PVT panels achieved was in the range of 10-35%. In this study, several systems with PVT panels were presented as possible options with different performances. The thermal efficiency of a combined system with PVT panels and a LiBr-H₂O single effect absorption chiller is in the range of 23-35% for a collector area of 30-70 m². The photovoltaic efficiency for this system is 10% and the COP in the range of 0.6-0.8. Another system with PVT panels and a heat pump was also presented, with a thermal efficiency of 15-21% for an area of 70 m² and a photovoltaic efficiency in the range of 15-17%. Moreover, PVT systems can produce 18% electrical efficiency at an outlet fluid temperature of 60 to 80°C [4].

It is important to note that glazed PVT collectors, such as the Ecomesh, have higher fluid and cell temperatures due to the front cover, providing a good thermal insulation and therefore a high thermal yield. This leads to additional optical interfaces and reflections providing a lower electrical yield [27].

Market status of solar cooling systems:

More than 1000 solar cooling plants have been installed so far all over the world ranging from small- to large- scale units. More than 254 installations are located in Europe [43]. Figure 18 shows the worldwide distribution (2009).

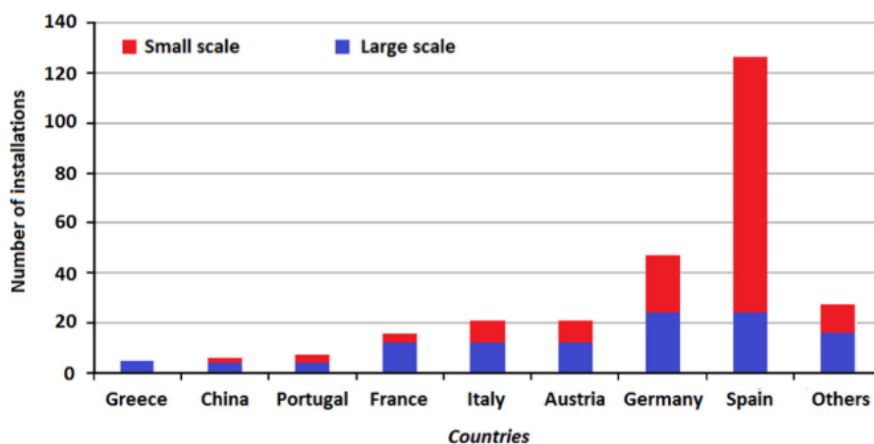


Figure 18. Worldwide share of large/small scale cooling installations [89].

In order to apply solar cooling technologies at large scale, the following factors must be considered:

- The major hindrance in the widespread of these systems is their high initial cost. These technologies should be produced on a mass scale and supplied to the developing countries at reduced prices [1].

- The governments must provide incentives or subsidies to show a “reward” or positive compensation to the reduced usage of fossil fuels and the environmental protection actions that lead to sustainability and renewable energy sources exploitation [1].

Nowadays, there is a noticeable growth in the solar cooling European market using sorption processes [43]. The distribution of these technologies in the global market is shown in Figure 19. Desiccant cooling is only used in large-scale applications.

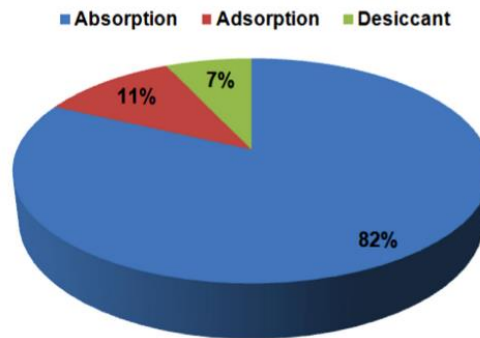


Figure 19. Percentage use of the different solar thermal cooling technologies [89].

In the last decades, thermal systems cost has decreased due to the lower prices of FPCs and ETCs as well as those of sorption chillers. The specific cost of a solar system based on FPCs is around 150 to 200 €/m² while that of ETCs is in the range of 250 to 300 €/m². The cost of the collector is 50 to 80% of the overall system cost and depends on the operating temperature of the chiller to a high extent. The implementation of solar thermal cooling systems is technically and economically limited to medium to large scale applications [1].

Market barriers:

Economic barriers:

- High initial cost and lower performance as compared to conventional cooling systems.
- Lack of subsidies in developing countries and commercial and industrial investors [43].
- Relatively high payback times that can even reach 20 years [43].

Technological barriers:

- Highly complex systems.
- Few demonstration and pilot plants to assess performance, lack of experience.

Moreover, the standardisation of these systems prototypes is difficult due to the worldwide variability of climatic conditions. Tax reductions and other financial incentives would help to increase the use of these new technologies [43].

Policy framework: European regulations for the energy sector

Nowadays, there is a general increase in the environmental concerns regarding carbon emissions and climate change caused by global warming. These big environmental problems in our planet have become more and more obvious throughout the years.

The increase on the sea level, the progressive melting of ice in the poles and the already tangible climate change characterised by weather instability make a noticeable impact on human life. In this context, the European authorities have become stricter regarding the shift of primary energy sources and the necessary changes in the energy sector, seeking sustainable and renewable solutions. The European Union (EU) has established several policies and objectives to be achieved by 2020 and others by 2030 for the energy sector. They are briefly described below:

Objectives for 2020:

- Greenhouse gas emissions cut of 20% (from the levels of 1990).
- 20% of the energy in the European Union supplied from renewable sources.
- Energy efficiency must be improved in 20% in the EU.

Objectives for 2030:

- Greenhouse gas emissions cut of 40% (from 1990 levels).
- 27% of the energy in the European Union supplied from renewable sources.
- Energy efficiency must be improved in 27% in the EU.
- Solar energy contribution: 50% of low-temperature heating and cooling demand.

Moreover, the International Energy Agency Solar Heating and Cooling Programme (IEA SHC) was founded in 1977 as one of the first multilateral technology initiatives. Organised in tasks (work packages), it gathers international collaborative efforts to reach the goal for solar energy to contribute to 50% of the low-temperature heating and cooling demand by 2030. Out of a total of 53 projects, 39 have been completed. SHC tasks 25, 38, 48 and 53 correspond to solar cooling research [26].

The European Parliament and the European Commission establish several regulations and directives in order to address the environmental problems and combat climate change. This master thesis is developed in the framework of the Solar Heating and Cooling programme, from the International Energy Agency. Some of these directives related to energy consumption, renewable energy sources and sustainability need to be highlighted:

- ✓ **Directive 2009/125/EC: “EcoDesign”**. Valid from 20/11/2009. Transposition into Member States: 20/11/2010.

It establishes the requirements for ecological design applicable to energy-related products.

All the stages of the product life cycle are considered: the raw materials, the manufacturing process, packaging and distribution, as well as the installation, maintenance, the usage and the end of its useful life. The products that meet the requirements are labelled with “EC” and can be sold anywhere of the European Union [90].

- ✓ **Directive 2010/30/EU: “EcoLabelling”**. Valid from 19/06/2010. Transposition into Member States: 20/06/2011. It derogates Directive 92/75/EEC.

Framework: indication and information to the consumers about the energy consumption of the energy-related products [91].

Key aspects:

- All these products should be labelled with the information concerning the electric energy consumption.
- The suppliers are obliged to give these labels to the distributors for free and the information about the product [91].

- ✓ **Directive 2010/31/EU: “Energy performance of buildings (EPBD)”**. Valid from 07/07/2010. Transposition into Member States: 09/07/2012. (Revised and updated in 2016). It promotes the improvement of energy efficiency in buildings in the European Union, establishing that all the new buildings built in the EU from 2020 must be nearly zero-energy buildings [92].

Key aspects:

- National authorities must have an energy efficiency certification system and establish a set of minimum requirements for energy efficiency revised, at least, every 5 years (heating, DHW and air-conditioning installations).
- New buildings owned by public authorities must become zero-energy buildings for December 2018 [92].

- ✓ **Directive 2013/114/EU: “Renewable Energy”**.

Calculation of the amount of renewable energy with respect to the Directive 2009/28/EC. Promotion of the use of energy from renewable sources to meet the requirements concerning the CO₂ emissions of Horizon 2020. By 2020, 20% of the global energy in the EU must be supplied by renewable energy sources [93].

Key aspects:

- Carbon cap-and-trade scheme in the EU is revised, according to the new European Union Emissions Trading Scheme (EU ETS).
- Emissions from sectors uncovered by the EU ETS (dwelling, agriculture, wastes and transport) are reduced depending on the individual country.
- Energy efficiency: according to the “2011 Energy efficiency plan” and the Directive 2012/27/EU [93].

- ✓ **Directive 2012/27/EU: “Energy Efficiency. EcoDesign and energy labelling”**.

An increase of 10% in the annual economic savings. New EcoDesign Working Plan for the 2016-2019 period [94].

Key aspects:

- The list of labelled products is extended and the circular economy is increasingly applied.
- Minimum efficiency requirements for air heating and cooling products.
- The regulations are simplified for corporate agreements.

- ✓ **Directive 2010/31/EU (revised): “Energy performance in buildings (EPB)”**.

Smart, Simple and Supportive (increasing incentives and certifications) buildings.

Key aspects:

- Long-term building renovation strategies.
- Automation techniques and improvements in the control systems of the installations [92].

Chapter 3. Technical analysis

In this chapter, the system subject to analysis is described as well as the different options of installations to be studied. The methodology and the main parameters on which the analysis is based are explained and the calculation methods in the software EES are also summarised.

3.1. Installation in a hotel. Description of the system

This study focuses on Ecomesh hybrid solar panels, patented by the company EndeF Engineering, in combination with the main cooling technologies: vapour compression cycle and absorption. In this chapter, different solar cooling configurations are analysed for the same application: a 4-star hotel with a capacity of 100 guests located in Madrid, Spain. Some relevant data for Madrid and the solar panels installation are presented in Table 2:

Table 2. Data for the solar installation in Madrid.

Latitude (ϕ)	40.4°
Longitude	3.7 W
Tilt angle (β)	40°
Orientation (θ)	0° (south)
Active area of collector (A_c)	1.56 m ²

The technical characteristics of the Ecomesh hybrid panels as well as the thermal and electrical data are shown in the technical sheet presented in Annex 2. Figure 20 shows the electrical and thermal specifications:

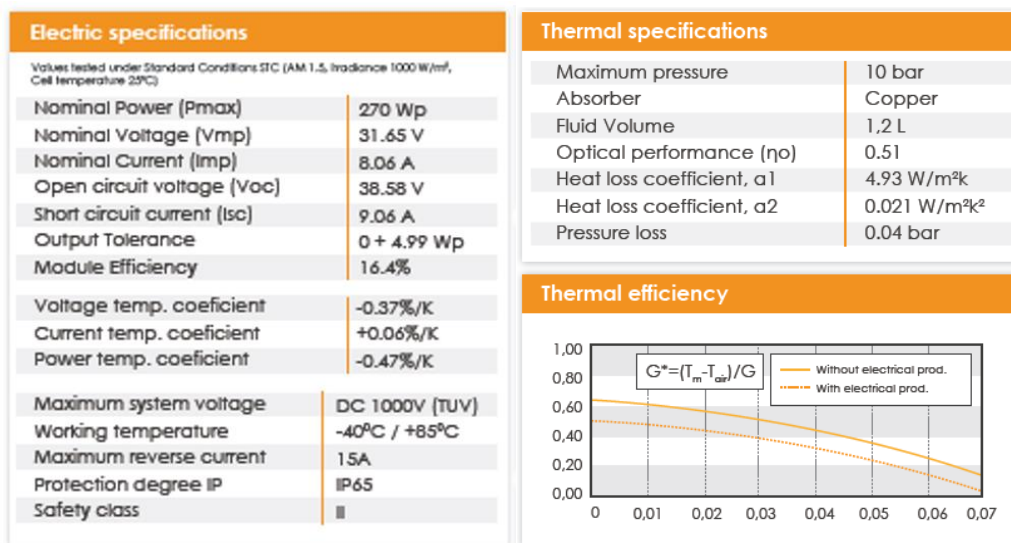


Figure 20. Extract of the technical sheet of the Ecomesh hybrid panel

The installation consists of 100 hybrid solar panels, Ecomesh, on the rooftop of the hotel building. Two different options for the cooling cycle are analysed: first, a reversible heat pump (vapour compression cycle), which will generate heat during the winter for the heating system in the hotel and cooling in the summer for air conditioning; second, a single-effect LiBr-H₂O absorption chiller. In both cases, the heating or cooling is achieved by means of an underfloor system, although the scope of the master thesis comprises only the upstream part of the whole installation (solar panels coupled with the corresponding cooling unit). As already explained in Chapter 2, adsorption cooling systems present much lower performance than absorption units. This is why only the latter is considered in this study as solar thermal cooling technology.

3.2. Analysis procedure for the hotel case studies

The present work is based on the analysis and comparison of four different case studies for the hotel installation. The different configurations are the following:

1. The hotel energy needs are fully covered by the common electrical grid and a gas boiler (there are no solar panels). This is the initial situation of the 4-star hotel considered.
2. The hotel is provided by a number of hybrid solar panels (Ecomesh). They supply heat to obtain DHW as well as electricity for the use in the hotel. The installation is described in Figure 21.

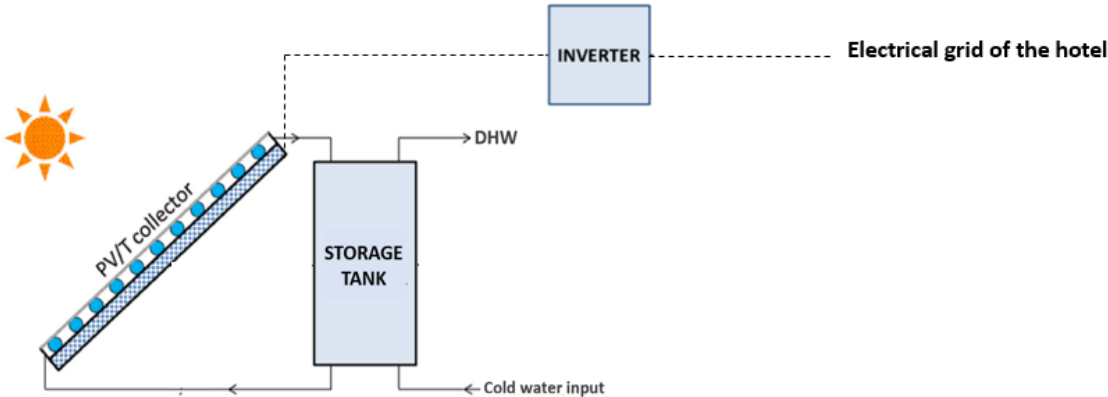


Figure 21. Hybrid solar panels installation in the hotel to provide electricity and DHW.

3. The hotel is provided by a number of hybrid solar panels and an air-water reversible heat pump that works on heating mode during the winter and cooling mode in the summer, providing the desired cooling. The panels are directly connected (on the electrical side) to the heat pump and provide the electricity needed to make it work. If there is excess of production, the electricity from the panels can feed the rest of the appliances and the internal grid in the hotel. The thermal part of the hybrid panels generates heat to provide DHW for the hotel. This system is illustrated in Figure 22.

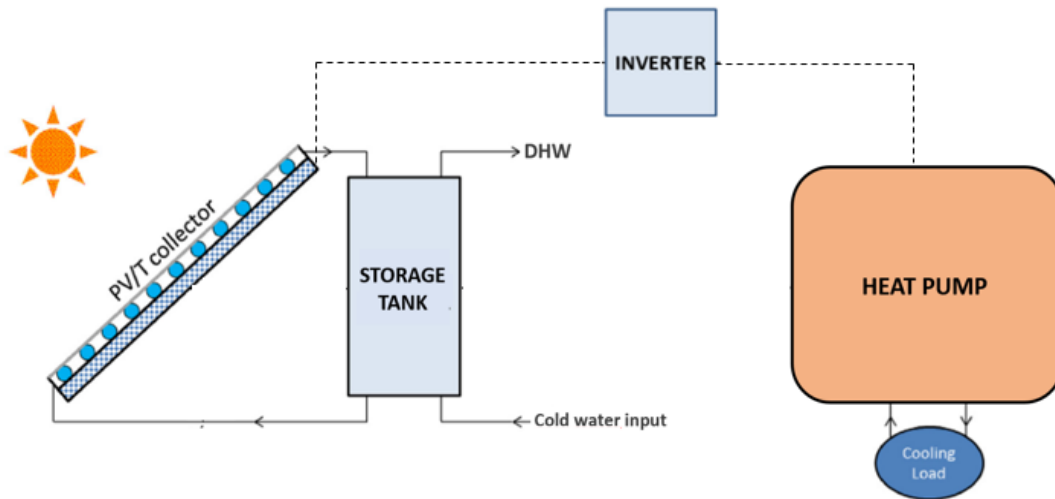


Figure 22. Schematic of solar electric cooling system with PVT panels.

- The hotel is provided by a number of hybrid solar panels and an absorption chiller that only works during the summer to provide air conditioning. The electricity from the panels is used in the internal grid of the hotel during the whole year. In the winter, the thermal energy from the panels is used to produce DHW whereas during the summer months, this energy feeds the absorption unit, providing heat to the generator of refrigerant. However, due to the high temperature required at the generator of the absorption unit, an additional boiler (used as back up in other cases) is required in order to assure that the hot water that runs the cycle is at 88°C. During the summer, a conventional boiler of the hotel provides the DHW. Figure 23 presents a schematic of the system.

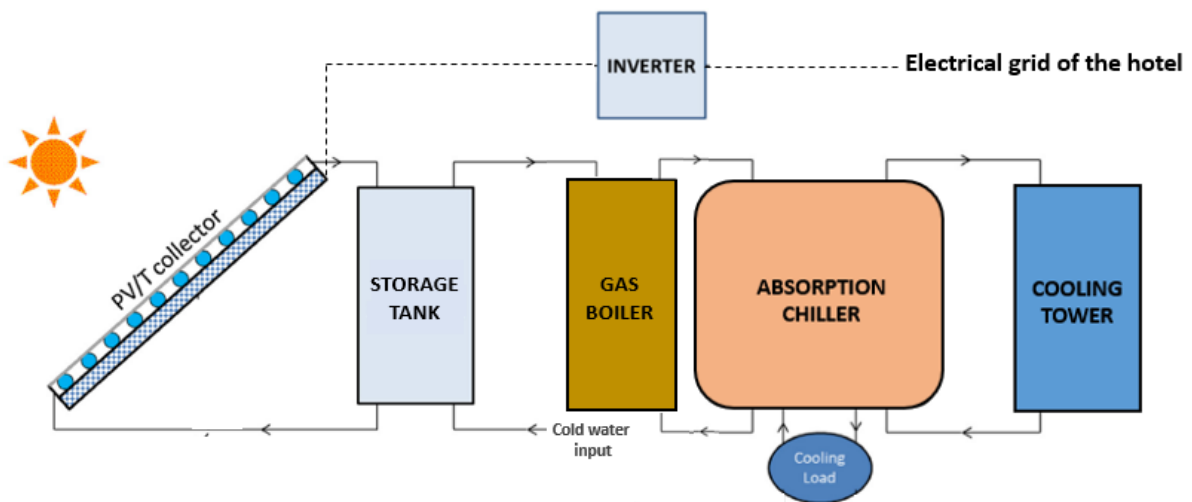


Figure 23. Schematic of absorption cooling system with PVT panels.

It is important to note that winter has been considered to last from October until March, both included, and summer from June until September, also included. This is eight months of winter and four months of summer. The spring months of April and May do not account for heating or cooling needs.

The comparison of these cases will be conducted in economic and environmental terms. It will be based on the energy savings (electricity and DHW), on the current prices of the electrical and the thermal kWh , as well as the CO_2 emissions cut.

At the end of the comparison in Chapter 4, the study is generalised for different situations or hotels, including the case of a hotel that already has PVT panels on the rooftop or the installation of photovoltaic solar panels from EndeF Engineering instead of the hybrid ones due to the high investment cost. This will help to determine the most suitable solar cooling technology depending on the situation of the hotel.

3.3. Performance indicators

The design and calculations on the solar system have been done taking into account the two contributions of a hybrid solar panel: electrical and thermal.

3.3.1. Efficiency indicators

Solar performance:

- *Photovoltaic part:*

The photovoltaic annual performance, η_{PV} , is defined as follows:

$$\eta_{PV} = \frac{P_{DC}}{G \cdot A} \quad (1)$$

Where,

P_{DC} = total power produced in a year [W].

G = total solar irradiance in a year [W/m^2].

A = total surface area of panels exposed to the sun [m^2].

The global efficiency of a photovoltaic system, $\eta_{G,PV}$, taking into account the losses from converting DC current to AC current is [56]:

$$\eta_{G,PV} = \eta_{PV} \cdot \eta_{INV} \quad (2)$$

Being η_{INV} the inverter efficiency.

- *Thermal part:*

The thermal annual performance, η_t , is defined by the following expression:

$$\eta_t = \frac{Q_u}{E \cdot A} \quad (3)$$

Where,

Q_u = useful heat obtained from the solar collectors [MJ].

E = total irradiation on a tilted surface in a year [MJ/m^2].

A = total active area of collectors [m^2].

The efficiency of a thermal solar collector is defined by the following expression:

$$\eta_t = \eta_o - a_1 \cdot \frac{T_m - T_{amb}}{G} - a_2 \cdot \frac{(T_m - T_{amb})^2}{G} \quad (4)$$

Where η_o (optical efficiency), a_1 and a_2 (thermal losses coefficients) are thermal parameters defined for the particular solar collector. In this case, these values can be found in the technical sheet of the Ecomesh hybrid panels. T_m is the mean operation temperature of the panel and T_{amb} the actual ambient temperature.

Solar fraction or solar savings fraction:

It defines the portion of solar energy contribution compared to the total energy required for the solar cooling system since an auxiliary energy source is usually needed.

It is normally used for thermal solar panels or thermal calculations of hybrid panels, when F-Chart method is applied, but it can be also defined for photovoltaic panels or PV contribution of hybrid panels.

- *Photovoltaic part:*

The solar fraction of solar electric cooling systems, SF_e , is defined as follows [95]:

$$SF_e = \frac{P_s}{P_s + P_{aux}} \quad (5)$$

Being P_s [kW] the solar electric power gain from the panels (corresponds to P_{AC} of a PV panel) and P_{aux} [kW] the auxiliary electrical power from the public grid.

- *Thermal part:*

This parameter measures the percentage of the energy demand covered by the solar collectors in a solar thermal installation or in this case, by the hybrid solar panels.

Generally, the solar fraction of solar thermal cooling systems, SF_t , is defined by this expression:

$$SF_t = \frac{\dot{Q}_u}{\dot{Q}_u + \dot{Q}_{aux}} \quad (6)$$

Being \dot{Q}_u [kW] the solar thermal power gain from the collectors and \dot{Q}_{aux} [kW] the heat power required from an auxiliary source [95].

It is important to note that the Spanish regulations found in "Código Técnico de la Edificación (CTE). Documento Básico HE4: Contribución solar mínima de agua caliente sanitaria" establish the minimum solar fraction required, in percentage, according to the climatic conditions of each particular location, since 2013. For the case of Madrid, the annual solar fraction must be at least 60%, for new buildings being constructed or renovated ones [32].

In the calculations for the case studies presented in section 3.2, the solar fraction (defined as F in EES) adopts different forms depending on the application, as shown below:

- Case of water heating:

With the F-Chart method (explained in section 3.4), the monthly solar fractions, f , can be easily obtained. The annual value of solar fraction, F_{DHW} , is calculated as follows:

$$F_{DHW} = Q_u/Q_{DHW} \quad (7)$$

Being Q_{DHW} the thermal energy demand for domestic hot water consumption.

- Case of heat input for sorption cooling:

In the case of absorption cycle, the solar fraction, F_{abs} , is calculated by means of the heat required at the generator of refrigerant, Q_g :

$$F_{abs} = Q_u/Q_g \quad (8)$$

Energy Efficiency Ratio (EER):

It is a measure of the efficiency of cooling/refrigeration technologies such as vapour compression cycles (or reversible heat pumps) and absorption chillers. This parameter is differently defined for each particular technology.

- Reversible heat pump (vapour compression cycle):

$$EER = \dot{Q}_r/P_c \quad (9)$$

Where,

\dot{Q}_r = cooling or refrigeration power demand [kW].

P_c = power of the compressor [kW].

- Absorption chiller:

$$EER = \dot{Q}_r/\dot{Q}_g \quad (10)$$

Where,

\dot{Q}_g = heat power supplied to the generator (from the solar panels) [kW].

Coefficient of Performance (COP):

It is similar to the EER but this parameter is normally used for heating systems. Therefore, in this master thesis it is calculated for the winter mode of the reversible heat pump cycle, as follows:

$$COP = \dot{Q}_h/P_c \quad (11)$$

Where,

\dot{Q}_h = heating power demand [kW].

Seasonal Performance Factor (SPF):

This parameter is a measure of the efficiency of heat pump systems over a year.

Since the COP can vary a lot throughout the year, the operating performance of an electrical heat pump is better defined by the SPF . It gives an average efficiency over a year including the parasitic consumption of all the auxiliary equipment. This value allows to compare different heat pumps, normally conventional ones.

$$SPF = \frac{\text{Total annual heat output}}{\text{Total annual input of electricity}} \quad (12)$$

In this case, the heat pump is reversible and the COP is calculated for the winter mode whereas the EER is obtained for the summer, both refer to its performance.

However, the SPF can be also calculated to know if the heat pump is considered as a renewable energy source according to the European Directive 2009/28/EC (art. 5, Annex VII).

For this purpose, there is another expression that depends on the nominal COP found in the technical sheet of the heat pump and two coefficients, FP and FC:

$$SPF = COP_{nominal} \cdot FP \cdot FC \quad (13)$$

The FP coefficient depends on the climatic conditions in the particular location of study as well as the type of heat pump and installation. The FC measures the difference between the distribution temperature and the testing temperature at which the nominal COP has been estimated. The heat pump is considered renewable when the SPF value is higher than 2.5 [96].

Overall System Efficiency:

It refers to the efficiency of converting the solar energy into cooling and is obtained from the following expression, in which G_{summer} refers to the total value of irradiance during the summer:

$$OSE_{summer} = \dot{Q}_r / (G_{summer} \cdot A) \quad (14)$$

Another way of expressing this parameter is $OSE = COP \cdot \eta$, where the COP of the cooling system (reversible heat pump or absorption) previously obtained may be substituted as well as the photovoltaic or thermal efficiency (η) of the hybrid panel, depending on the particular installation.

For the case of a heat pump in winter mode, the following formula applies, with the corresponding G :

$$OSE_{winter} = \dot{Q}_h / (G_{winter} \cdot A) \quad (15)$$

Primary Energy Consumption (PEC):

In order to calculate the primary energy consumption (non-renewable), two conventional energy sources are considered: electricity and gas. Their energy efficiencies are presented below [97]:

- Energy efficiency for primary energy-electricity conversion: $\varepsilon_{el} = 40\%$,
- Energy efficiency for primary energy (gas)-thermal energy conversion: $\varepsilon_g = 90\%$.

Therefore, for solar electric cooling systems [95]:

$$PEC_{elect} = (W_{aux} + W_{parasitic}) / \varepsilon_{el} \quad (16)$$

Where,

W_{aux} = auxiliary electrical energy from the common grid [kWh].

$W_{parasitic}$ = electrical energy consumption of parasitic equipment (valves, pumps, etc) [kWh].

For absorption cooling systems [95]:

$$PEC_{thermal} = Q_{aux}/\varepsilon_g + W_{parasitic}/\varepsilon_{el} \quad (17)$$

Where,

Q_{aux} = heat provided by the auxiliary (gas) heater [kWh].

Primary Energy Ratio (PER):

This parameter relates the energy output to the primary energy consumption as follows [98]:

$$PER = \frac{Usable\ energy}{Primary\ energy\ consumption} = \frac{Q_{out}}{PEC} \quad (18)$$

Where,

Q_{out} = total energy output, usable energy [kWh].

3.3.2. Economic indicators

Capital cost or investment cost:

It refers to the total initial cost of the solar cooling installation subject to study.

Operational costs:

These refer to the variable costs, the ones derived from the energy consumption from conventional energy sources (fossil fuels), which are the electrical common grid and the natural gas boiler previously installed in the hotel. These sources provide auxiliary energy to the solar cooling installation.

Simple Payback Period (SPP):

It measures the time needed to recover the extra costs over a conventional system. The *SPP* does not consider the interest rate for the investment neither the energy prices inflation [99]. It represents, as a first approximation, the time required to recover the initial investment, so it has been chosen in order to easily compare the investigated options of installations in the hotel. Since the costs of all the components and systems involved are not stable, the decision was to avoid further uncertainty in the economic analysis by the usage of this simple parameter, which is calculated as follows:

$$SPP = \Delta C_{inv}/\Delta C_{op} \quad (19)$$

Where,

ΔC_{inv} = extra costs over a conventional system [€].

ΔC_{op} = annual reduction of energy costs [€].

Cost of primary energy saved:

This parameter is defined by eq. 20 as follows [99]:

$$CPE, saved = \Delta C_{a,s} / PE_{saved} \quad (20)$$

Where,

$\Delta C_{a,s}$ = annual extra costs for solar technology [€].

PE_{saved} = primary energy saved [kWh_{PE}].

Net Present Value (NPV) and Internal Rate of Return (IRR):

These two parameters determine the economic viability of a project. Even though this is a preliminary study of solar cooling technologies, these values can be useful for the economic comparison of the case studies presented in Chapter 4. The NPV should be positive for the project to be profitable. It is calculated from the following formula:

$$NPV = \sum_{i=1}^n \frac{CF_i}{(1+r)^i} - I_0 \quad (21)$$

Where,

CF_i = cash flow of every year [€]. It is the net annual energy saving minus the maintenance cost (500€).

r = interest rate (%). For this kind of installations, it is 2%.

n = number of years in operation, life time of the installation.

I_0 = initial investment cost [€].

The Internal Rate of Return (IRR) corresponds to the interest rate when the NPV is zero. The return of investment must be higher than the investment cost. Therefore, the IRR should be higher than the interest rate used to obtain the NPV for the project to be economically feasible.

3.3.3. Environmental indicators

CO₂ emissions cut:

It is the amount of CO₂ avoided when renewable energy sources are used for cooling (or heating) instead of conventional systems based on fossil fuels combustion. However, the CO₂ emissions from the manufacturing process of the solar panels or any other component required for the installation are not taken into account here since this data cannot be easily estimated.

Global Warming Potential (GWP):

This is an indicator of the contribution of certain greenhouse gases to the global warming effect. It is mainly measured for several refrigerants employed in vapour compression cycles [43]. For the solar electric cooling system simulated with EES and explained in section 3.4, several options of refrigerants with different GWP values have been considered.

Ozone Depletion Potential (ODP):

This indicator measures the impact of the degradation that a chemical compound can cause to the ozone layer [43]. This is done by comparing the destructive effects of the substance with those of trichlorofluoromethane (CFC-11), which is the reference (ODP=1), for the same mass. The refrigerants used nowadays have low ODP values since previously used CFC and HCFC refrigerants have been banned in the EU for more than eight years due to the big damage of the ozone layer.

3.4. Calculations and simulations in EES

3.4.1. The software: EES

Engineering Equation Solver (EES) is a general equation-solving program that can be used to solve non-linear, differential and integral equations, perform linear and non-linear regression, optimization, convert units, and generate good quality plots [100]. One of the biggest advantages of EES is the highly accurate thermodynamic and transport property database provided for hundreds of substances. This makes it a preferable option compared to other equation-based software such as Matlab when there are thermodynamic cycles or specific properties in the calculations.

For this master thesis, several options were considered when selecting the software for the simulations, but EES would ease the work to a high extent since many of the calculations and simulations are about thermodynamic processes and cycles, and this program has properties of a high amount of substances and refrigerants.

Some basic features of the software are listed below [100]:

- Equations can be entered in any order
- Single and multi-variable optimization capability
- Uncertainty analysis and regression capability
- Heat transfer library functions for conduction, convection, and radiation
- Link to Fortran, C/C++, Python, Excel, and MATLAB

3.4.2. Data and assumptions

Some assumptions have been made in order to estimate the energy production for a hotel with 100 guests and the coverage of its cooling needs:

- The number of Ecomesh hybrid panels has been assumed as 100, regarding the capacity of the hotel and its standard.
- The cooling capacity or cooling power demand of the hotel is considered as $\dot{Q}_r = 64 \text{ kW}$. The heating demand of the hotel during the winter, which is considered in the 3rd case study (winter mode of the heat pump) is $\dot{Q}_h = 72 \text{ kW}$. These data have been provided by the company EndeF Engineering.
- The thermal demand of DHW has been calculated from the consumption of water per person in a 4-star hotel, given in L. This is specified in the Spanish regulations, in the document called "Código Técnico de la Edificación (CTE). Documento Básico HE4: Contribución solar mínima de agua caliente sanitaria".

All of these data are summarised in Table 3:

Table 3. Relevant data for the solar cooling system dimensioning.

N° of Ecomesh hybrid panels	100
Cooling power demand (kW)	64
Heating power demand (kW)	72
DHW consumption (L)	5500

3.4.3. Calculations and methods

- **The solar system:**

Photovoltaic part:

The calculations for the photovoltaic part of the hybrid solar panels have been made in an hourly basis since the photovoltaic dimensioning requires the global hourly radiation on a tilted surface.

This means that the results would not be reliable if monthly or daily values were used instead. For this purpose, the global irradiance on a tilted (40.4°) surface, G , and the ambient temperature for Madrid in 2016 have been obtained from the solar radiation database called CMSAF, from the Photovoltaic Geographical Information System (PVGIS), an interactive tool provided by the European Commission. The most recent data that may be found in PVGIS-CMSAF is from 2016.

In order to calculate the photovoltaic yield, the maximum electrical power provided by the hybrid panels must be obtained by applying correction factors to the values obtained for a conventional photovoltaic solar panel. The electrical power produced by N_p photovoltaic solar panels, P , depends on the temperature of the panel (or cell temperature) according to this formula:

$$P = N_p \cdot P_n \cdot \left(\frac{G}{G_{STC}} \right) \cdot (1 + \gamma \cdot (T - T_{amb})) \quad (22)$$

Where γ is the temperature coefficient for the power. It defines the variation of the power with the cell temperature; as mentioned before, when the temperature of the cells increases the power decreases and so does the electrical efficiency. P_n is the nominal power, the peak power of the panel (in STC).

In the case of a PV panel T can be estimated from this formula as T_{cell} :

$$T_{cell} = T_{amb} + \left(\frac{T_{NOCT} - 20}{0.8} \right) \cdot G \quad (23)$$

However, as explained in section 2.3 of hybrid solar panels, the main advantage is that the temperature of the panel (or the cells) is reduced by releasing the heat that could accumulate in the photovoltaic cell and using it to cover thermal loads such as DHW.

Therefore, the already mentioned correction factors for the increased power (and energy) obtained with a hybrid solar panel in comparison with a photovoltaic one are presented in Table 4.

They have been obtained from the values of production provided by the company EndeF Engineering for both photovoltaic and hybrid solar panels in Madrid, for every month of the year.

Table 4. Correction factors for the power of a hybrid solar panel based on a PV panel.

Correction factors for the power of Ecomesh hybrid solar panels	
January	1.004
February	1.007
March	1.010
April	1.020
May	1.032
June	1.058
July	1.088
August	1.087
September	1.054
October	1.016
November	1.010
December	1.0081

Thermal part:

The thermal calculations for the 4-star hotel have been carried out in a monthly basis regarding daily average irradiance and sunny hours. This allows to apply the F-Chart method, which is recommended for long time periods as considered here (yearly production and yield). Moreover, the Spanish building legislation and regulatory documents such as the CTE (Código Técnico de la Edificación) and the specification for solar installations from IDAE (Instituto para la Diversificación y Ahorro de la Energía) recommend the use of average monthly values for solar thermal installations [23], [32].

The same database has been used as in the photovoltaic calculations, the PVGIS-CMSAF, providing the values of irradiance (G) and ambient temperature from 2016. The temperature of the cold water in Madrid is obtained from the document *Guía Asit de la Energía Solar Térmica (May, 2010)*.

F-Chart method

Among the different calculation methods, the most suitable one according to the characteristics of the solar installation should be chosen [23]. In this case, among the different possibilities, a simplified method called “F-Chart method” or “ f -curves method” has been used for the thermal calculations.

F-Chart method allows to obtain the coverage of a solar system, which is the percentage of the total thermal demand that is covered by solar energy, and the average yield in a long time period. This method is highly accepted as an accurate calculation process for long-term estimations. It must not be applied for weekly or daily calculations.

The method uses monthly average meteorological data and it can determine the yield and the solar fraction in solar thermal installations with flat plate collectors. It can be applied in a systematic way, identifying the non-dimensional variables of the solar system and using the software to size the correlations among these variables and the average yield of the system for a given period of time [23].

The calculation process follows this sequence:

1. Evaluation of the thermal loads for water heating to obtain DHW or for space heating.
2. Estimation of the incident solar radiation on the tilted surface of solar collector(s).
3. Calculation of D_1 non-dimensional parameter.
4. Calculation of D_2 non-dimensional parameter.
5. Determination of f parameter for the monthly solar fraction or coverage.
6. Determination of the annual solar fraction F .

The main equation used in this method is:

$$f = 1.029D_1 - 0.065D_2 - 0.245D_1^2 + 0.0018D_2^2 + 0.0215D_1^3 \quad (24)$$

The f parameter is the monthly fraction of the thermal load that is supplied by the energy delivered from the solar collectors. The previous equation is only valid for those systems that work with liquids as heat transfer medium. Coefficients D_1 and D_2 in the equation correspond to Y and X in Figure 24, respectively. In order to use this correlation, they must be in the range defined below [22].

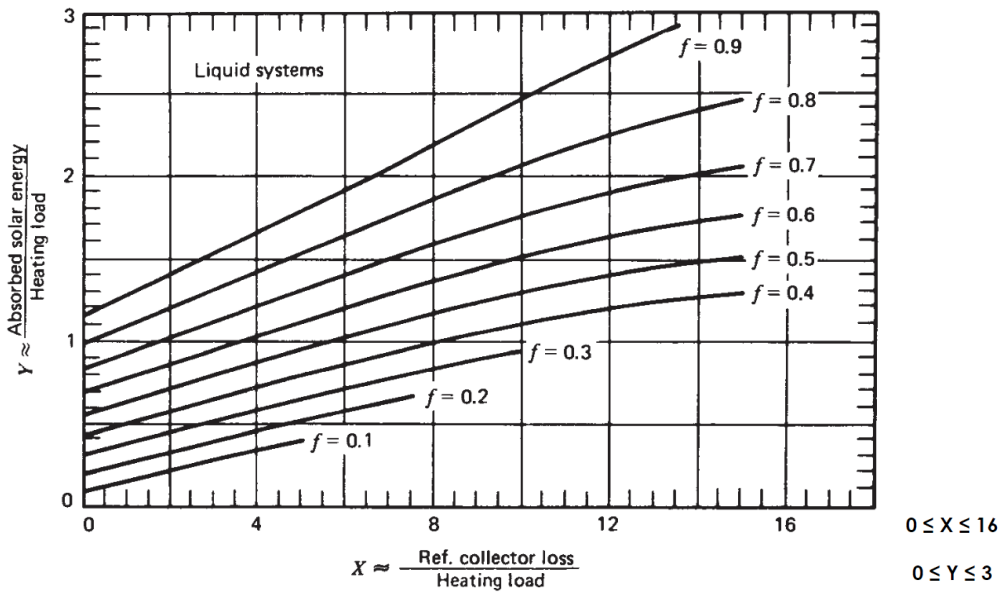


Figure 24. f -Chart method for heat transfer systems using liquids [22].

Coefficient D_1 represents the relationship between the absorbed energy by the collector and the monthly thermal demand. It is obtained from the following expression:

$$D_1 = \frac{(Ac \cdot F'_R \cdot (\tau\alpha) \cdot E \cdot N_{month})}{Q_{DHW}} \quad (25)$$

Where,

$F'_R \cdot (\tau\alpha)$ = non-dimensional parameter. F'_R is the heat transfer efficiency coefficient of the collector and $\tau\alpha$ is the transmittance-absorptance product.

N_{month} = number of days of each month.

$$F'_R \cdot (\tau\alpha) = F_R \cdot (\tau\alpha)_n \cdot \tau\alpha/(\tau\alpha)_n \cdot F'_R/F_R \quad (26)$$

Where,

$F_R \cdot (\tau\alpha)_n$ = correction factor that corresponds to the optical efficiency of the solar collector (η_0) and is the ordinate-intercept of the characteristic curve of the collector.

$\tau\alpha/(\tau\alpha)_n$ = correction factor that represents the modification of the incidence angle. It can be taken as constant and it depends on the type of frontal cover of the flat plate collector, with a value of 0.96 for simple cover and 0.94 for double transparent cover.

F'_R/F_R = correction factor for the thermal losses collector-heat exchanger. It depends, among other factors, on the efficiency of the heat exchanger. When the characteristics of the heat exchanger are unknown, a value of 0.95 is recommended.

Coefficient D_2 represents the relationship between the energetic losses in the collector and the monthly thermal demand. It is calculated as follows:

$$D_2 = \frac{(A_c \cdot F_R \cdot U_L \cdot F'_R/F_R \cdot (100 - T_{amb}) \cdot \Delta T \cdot K_1 \cdot K_2)}{Q_{DHW}} \quad (27)$$

Where,

ΔT = total number of seconds of the month [s].

$F_R \cdot U_L$ = global thermal losses coefficient of the solar collector (a_1). It is the slope of the collector characteristic curve.

The ambient temperature is expressed in Kelvin [K].

K_1 and K_2 are also parameters defined in the F-Chart method. K_1 is a correction factor for the storage capacity (volume of storage tank). The F-Chart method has been designed considering a storage capacity of 75 L/m² of collector surface but the application range may be increased by introducing this correction coefficient. K_2 is a correction coefficient for the DHW, taking into account the cold water and ambient temperatures. Once the monthly solar fraction f is obtained from the first formula presented above (having calculated D_1 and D_2 as explained), the useful heat can be easily calculated from this expression:

$$Q_u = f \cdot Q_{DHW} \quad (28)$$

Thus, the annual solar fraction is obtained from this formula:

$$F = \frac{\sum_{i=1}^{i=12} Q_{u,i}}{\sum_{i=1}^{i=12} Q_{DHW,i}} \quad (29)$$

Further details can be checked and better analysed by looking at Annex 1, where the EES codes are presented. Among all the simulations, only the first one of thermal calculations of PVT panels has been attached with the complete solution, including the arrays, to illustrate the reader. In the others, only the general solution is presented, for the sake of simplicity.

- **The cooling system:**

Reversible heat pump:

The ideal vapour compression cycle

As it was explained in the theory of section 2.2 Cooling technologies, a typical ideal vapour compression cycle can be easily characterised with a few data. The calculations are firstly shown for an ideal cycle to give an idea of the maximum performance.

Operational assumptions:

- Each component of the cycle is analysed as a control volume in steady state.
- No pressure drop, the refrigerant flows at constant pressure in both heat exchangers since irreversibilities inside the evaporator and condenser are not taken into account.
- Except for the expansion, which is isenthalpic, all the processes are internally reversible.
- Adiabatic operation in both the compressor and the expansion valve.
- The effects of kinetic and potential energy are neglected (insignificant).
- Saturated vapour enters the compressor and saturated liquid exits the condenser.

In order to simulate the ideal cycle, it is necessary to initialise some thermodynamic variables [70]:

- Evaporator temperature: $T_{\text{evap}} = 2^{\circ}\text{C}$
- Condenser temperature: $T_{\text{cond}} = 45^{\circ}\text{C}$

An ideal vapour compression cycle is described by means of a pressure-enthalpy diagram in Figure 25.

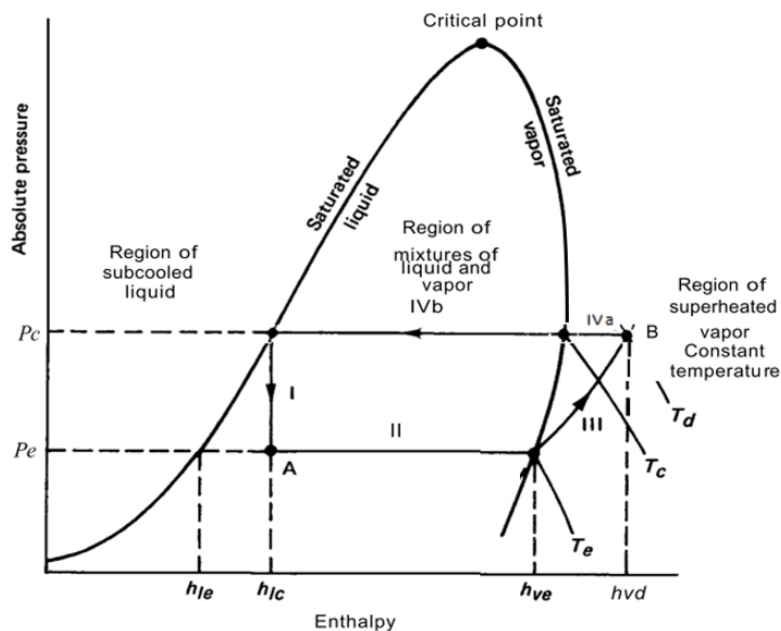


Figure 25. Generic pressure-enthalpy diagram of a vapour-compression cycle [33].

Process I, in which the hot liquid refrigerant expands reducing its pressure to the evaporator pressure, is isenthalpic (enthalpy is constant). As pressure is reduced, so does the temperature, and some vapour is produced [33].

Process II represents the vaporisation of the liquid refrigerant. In this process heat is removed from the space or room that needs to be cooled. The mass flow rate of refrigerant, \dot{m}_r , necessary for a heat-transfer rate of \dot{Q}_r is defined as follows:

$$\dot{m}_r = \dot{Q}_r / (h_{ve} - h_{lc}) \quad (30)$$

Where h is the specific enthalpy and subscripts v and l refer to vapour and liquid states, respectively; c and e refer to condenser and evaporator pressures, respectively.

Process III in the P-h diagram corresponds to the compression of the refrigerant from pressure P_e (evaporation pressure) to P_c (condensing pressure). It requires work input from an external source. In general, the work of compression \dot{W}_c is obtained from the expression [33]:

$$\dot{W}_c = \dot{m}_r (h_{vd} - h_{ve}) \quad (31)$$

Where h_{vd} is the specific enthalpy of superheated vapour. The compressor is usually assumed to be isentropic, considering an idealised cycle.

Process IV represents the condensation of refrigerant. First, in the subprocess IVa, the vapour is cooled removing the sensible heat, at constant pressure from T_d to T_c .

At T_c , the vapour is condensed at the saturation pressure and latent heat is removed:

$$\dot{Q}_c = \dot{m}_r (h_{vd} - h_{lc}) \quad (32)$$

This heat must be rejected into the environment, either to cooling water or to the atmosphere.

The overall performance of a cooling/refrigeration machine is usually expressed by means of the Energy Efficiency Ratio (*EER*): the ratio of the heat transferred in the evaporator \dot{Q}_r (cooling or refrigeration effect) to the shaft work of the compressor [33].

$$EER = \dot{Q}_r / \dot{W}_c = (h_{ve} - h_{lc}) / (h_{vd} - h_{ve}) \quad (33)$$

The maximum value of the *EER* for any given evaporator and condenser temperatures corresponds to that of the reversible Carnot cycle for the same system.

$$EER_{Carnot} = \frac{T_e}{T_d - T_e} \quad (34)$$

In real systems, frictional effects and irreversible heat losses reduce the performance much below this value [33].

Vapour compression cycle of a real system

As previously explained in section 2.2, for real vapour compression cycles, the pressure drop in both heat exchangers and the connecting piping needs to be considered. Therefore, the process lines that correspond to the evaporation and condensation steps are no longer isobars, as in Figure 25. Furthermore, the refrigerant leaving the evaporator is superheated [35].

The degree of subcooling is primarily determined by the amount of refrigerant charged to a heat pump, whereas the degree of superheat at the evaporator outlet is primarily determined by the setting of the expansion valve [35].

These parameters are intrinsic and specific of the particular system or installation subject to study in a real case and different from other real systems or configurations. Therefore, since this master thesis focuses in a preliminary study for a real case of a 4-star hotel but the cooling installations do not exist yet, they are just suggested at this step, those parameters needed to know the degree of subcooling and superheating as well as the pressure drop are unknown. The approach for the simulation of a real system has been to apply a coefficient of 0.8 (correction factor) to the COP or EER of the ideal system obtained with EES, since it is normally used as correction coefficient in thermodynamic cycles.

In order to suggest a real example of an air-water reversible heat pump that would be suitable for the studied system, a commercial model has been considered for the economic analysis in Chapter 4.

Most of the commercially available reversible heat pumps that have been checked for the required capacity use conventional refrigerants such as R134a or R410A, which are commonly used in air-conditioning systems. The ones that have been recently investigated (for being more environmentally friendly) for these kind of applications are not available yet for an installation of this size.

The selected heat pump, the model ROOFTOP KRB-W 075 from Kosner, uses the refrigerant R410A. Its P-h graph is presented in Figure 26:

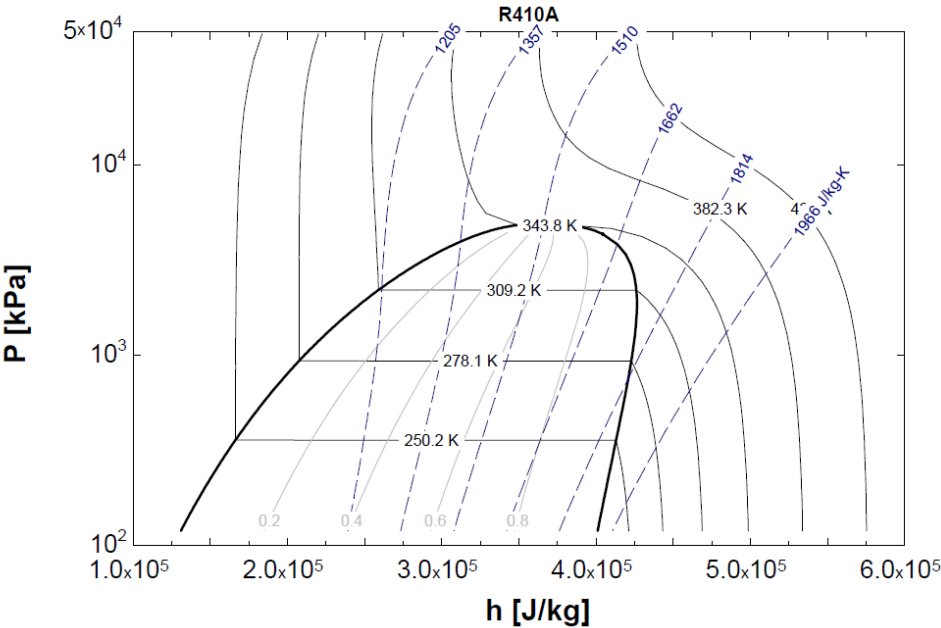


Figure 26. P-h diagram of R410A

It is important to note that the code developed for this cycle is organized in thermodynamic states defined by the main thermodynamic variables: temperature, pressure, quality and specific enthalpy or entropy. For further details on the calculations and characterisation of the cycle, all the variables and equations can be revised in Annex 1, where the full codes are attached.

Absorption cycle:

In this case, as well as in the vapour compression cycle, the approach for a real system is based on the correction of an ideal cycle with a factor of 0.8.

The ideal absorption cycle considered in the simulation implies some operational simplifying assumptions:

- The refrigerant and absorbent phases are in equilibrium in the generator, evaporator, condenser and absorber.
- Pressure reductions in the pipes and heat exchangers are neglected.
- Pressures at the evaporator and condenser are equal to the vapour pressure of refrigerant.
- The pump work can be neglected to ease the estimation of temperatures.

For the simulation of the ideal cycle, it is necessary to initialise the following thermodynamic variables, as well as the approach at the low-temperature end of the liquid heat exchanger [33]:

- Evaporator temperature: $T_{\text{evap}} = 3^{\circ}\text{C}$
- Absorber temperature: $T_{\text{ab}} = 34^{\circ}\text{C}$
- Condenser temperature: $T_{\text{cond}} = 36^{\circ}\text{C}$
- Generator temperature: $T_{\text{gen}} = 88^{\circ}\text{C}$

Figure 27 presents the ideal LiBr-H₂O absorption cycle subject to analysis. In the following, the main steps of the simulation of the system are explained.

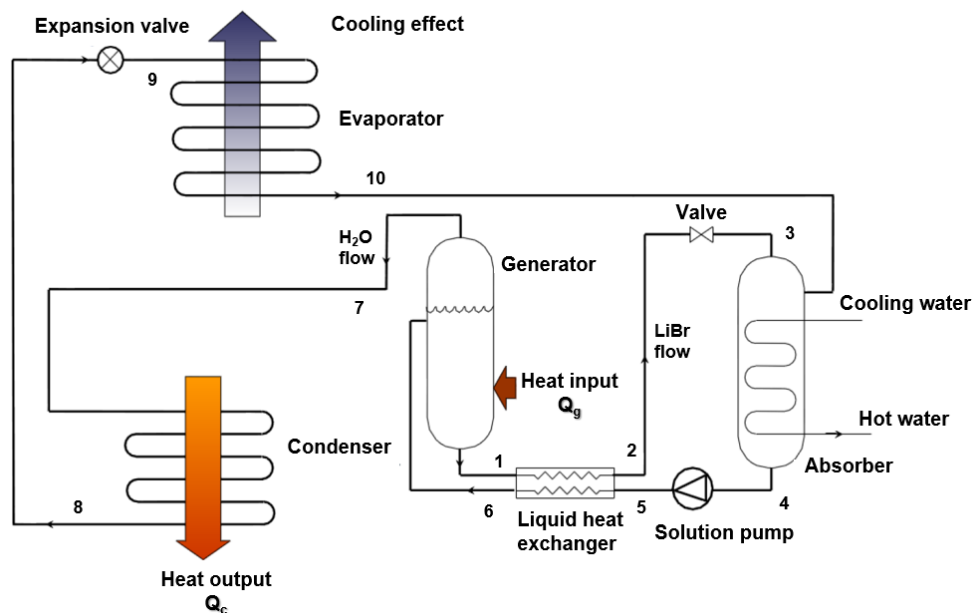


Figure 27. LiBr-H₂O absorption cooling cycle.

EES has a specific library for LiBr-H₂O solutions that allows to obtain thermodynamic properties of the mixture by using the suitable functions. At conditions 7, 8, 9 and 10 of the cycle shown in Figure 27 the fluid is pure water and the saturation pressure can be easily found since the temperatures at the evaporator and condenser are known.

Therefore, the first step is to obtain the high pressure and low pressure levels of the system. Then the corresponding temperatures, enthalpies and mass compositions can be sequentially calculated in EES. As in the previous cooling cycle, the calculations are structured in thermodynamic states numbered according to the steps in Figure 27.

The mass flow rate of refrigerant (water) is calculated from the equation:

$$\dot{Q}_r = \dot{m}_r \cdot (h_{10} - h_9) \quad (35)$$

And since $\dot{m}_r = \dot{m}_7$, the following mass balances can be easily solved:

$$\dot{m}_6 = \dot{m}_1 + \dot{m}_7 \quad (36)$$

$$\dot{m}_6 \cdot x_s = \dot{m}_1 \cdot x_{ab} \quad (37)$$

Being x_s the concentration (in mass) of LiBr in the refrigerant-absorbent solution and x_{ab} the mass fraction of LiBr in the absorbent solution, previously obtained.

The enthalpy of the solution at point 6 can be obtained from an energy balance in the heat exchanger:

$$\dot{m}_5 \cdot h_5 + \dot{m}_1 \cdot h_1 = \dot{m}_2 \cdot h_2 + \dot{m}_6 \cdot h_6 \quad (38)$$

Knowing that $\dot{m}_5 = \dot{m}_6$ and $\dot{m}_1 = \dot{m}_2$.

The heat rate that must be provided at the generator is calculated from the following heat balance:

$$\dot{Q}_g = \dot{m}_7 \cdot h_7 + \dot{m}_1 \cdot h_1 - \dot{m}_6 \cdot h_6 \quad (39)$$

The heat transfer rate at the condenser, which represents the heat rejected to the environment is:

$$\dot{Q}_c = \dot{m}_7 (h_7 - h_8) \quad (40)$$

And last but not least, the energy efficiency ratio of this absorption cycle is:

$$EER = \dot{Q}_r / \dot{Q}_g \quad (41)$$

The values of the EER and COP for the real cycles calculated with a correction factor applied to the ideal values, as already explained, are presented in Table 5 for the reversible heat pump (two modes) and the absorption unit:

Table 5. EER and COP values of the real cycles subject to analysis.

Thermodynamic cycle	EER or COP
Heat pump, winter mode	4.48
Heat pump, summer mode	3.68
Absorption unit	0.63

The real model of the heat pump selected in this study has already been introduced when presenting the P-h diagram for R410A in the explanation of the vapour compression cycle. Likewise, the commercial model of absorption chiller, Yazaki WFC SC20, is also chosen according to the requirements of the installation and the technical specifications of these machines available in the market.

Chapter 4. Results

In this chapter, the results from the calculations of the analysis parameters and other relevant variables are presented, as well as those for the case studies comparison, in economic and environmental terms.

The results of this study are presented for the different configurations of solar cooling installations in the four case studies that are being compared:

1. Hotel fully provided with gas and the common electrical grid
2. Hotel with Ecomesh hybrid solar panels
3. Hotel with Ecomesh hybrid solar panels and a reversible heat pump
4. Hotel with Ecomesh hybrid solar panels and absorption cooling

4.1. Hotel fully provided with gas and the common electrical grid

This is the initial case, the hotel as it is now, without the installation of solar panels. In order to study if it is profitable and worth it for the hotel to make the investment and install Ecomesh solar panels on the rooftop, this “base” case must be considered as well for the comparison. The total consumption of electricity and heat in the 4-star hotel along the year is represented in Figure 28.

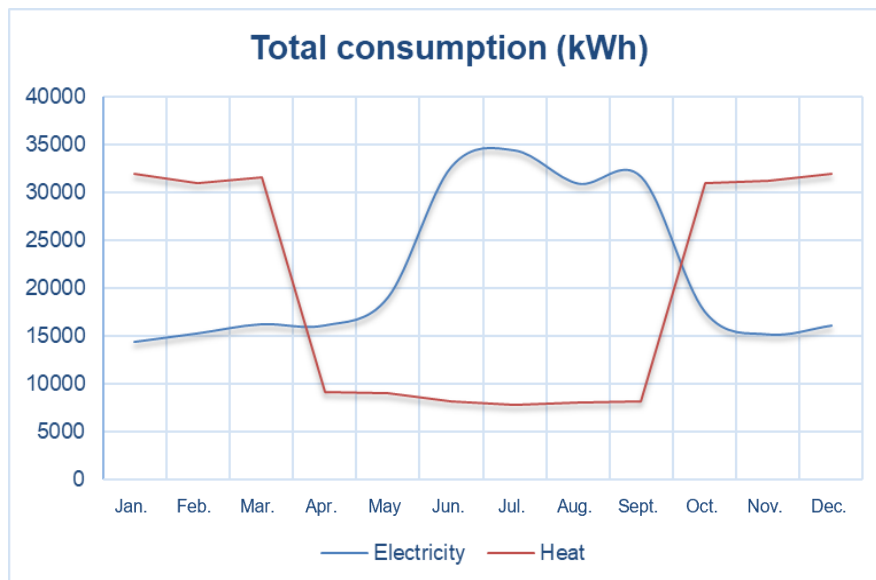


Figure 28. Total energy consumption of electricity and heat in the hotel.

As already introduced in Chapter 1, the motivation of this master thesis was, among other aspects, the high electricity consumption in these type of hotels, especially during the summer months, and the coincidence (in time) of this increase with the decrease in the DHW consumption. This may be observed in Figure 29 and 30, which present the electricity consumption and hot water demand along the year, in a monthly basis, for the 4-star hotel.

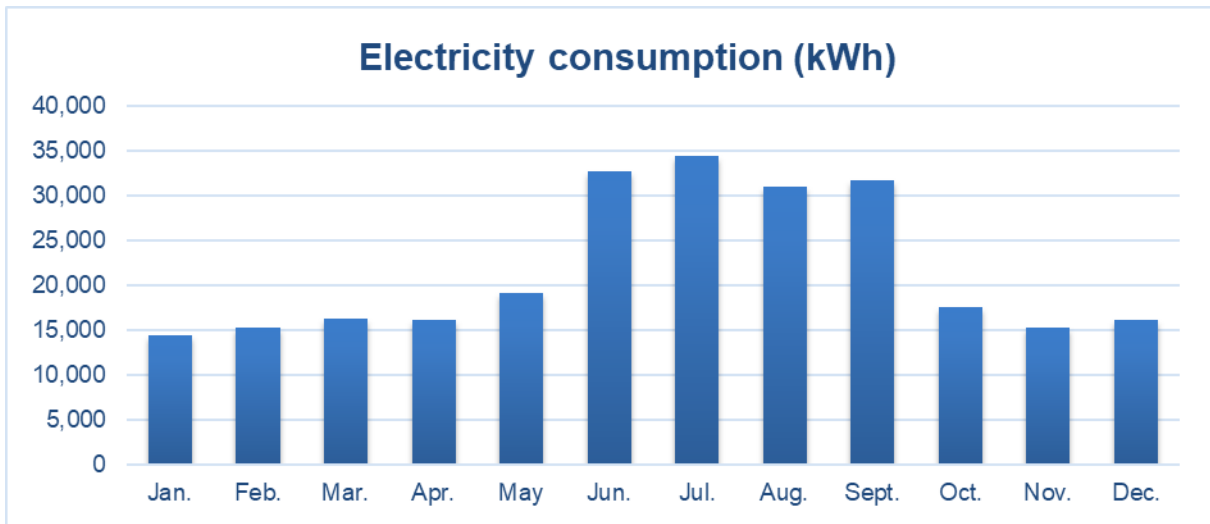


Figure 29. Electricity consumption [kWh] in the hotel along the year.

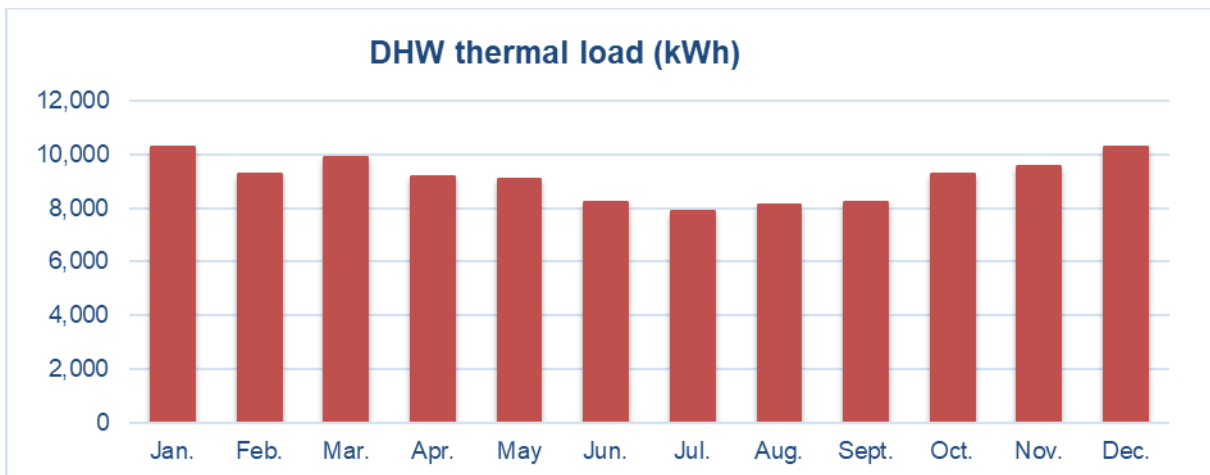


Figure 30. Domestic hot water thermal demand [kWh] along the year.

From the previous graphs, it seems clear that electrical air conditioning systems consume a lot of electricity. As already mentioned, the DHW thermal load reaches the minimum value during the summer, specifically in July, whereas the solar energy production is maximum during this season.

The energy consumption in the hotel divided into electricity, hot water and space heating as well as the current annual costs of energy in the hotel are summarized in Figure 31.

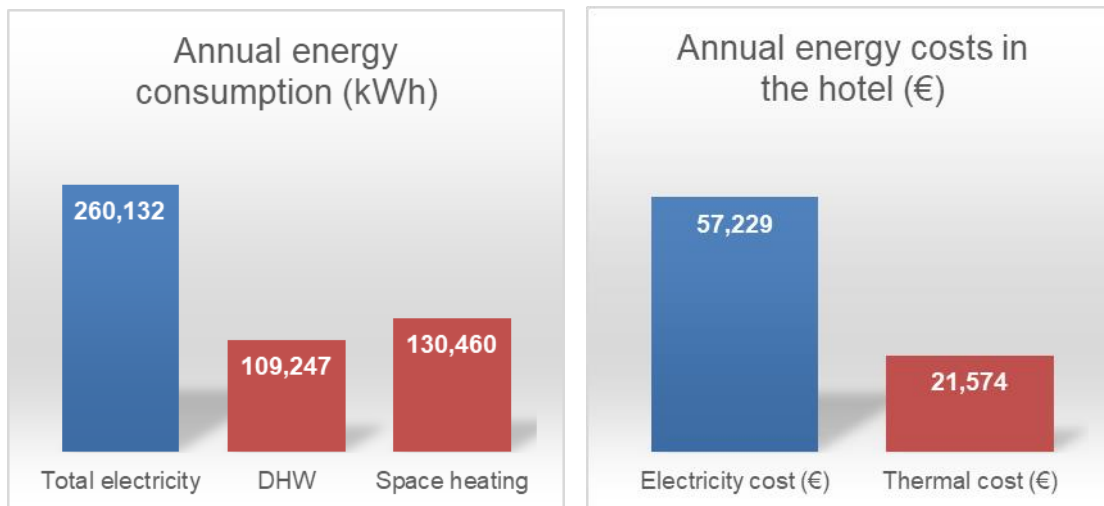


Figure 31. Annual energy consumption [MWh] (left) and costs [€] (right) in the hotel.

4.2. Hotel with Ecomesh hybrid solar panels

This second case study consists on the installation of hybrid solar panels on the rooftop of the building to provide electricity for the general use in the hotel (saving from the amount needed from the common grid) and heat for DHW consumption.

The thermal and electrical contributions from the Ecomesh hybrid solar panels are obtained with EES and Excel, respectively. Figure 32 presents both the electrical and thermal energy productions from the panels for every month of the year:

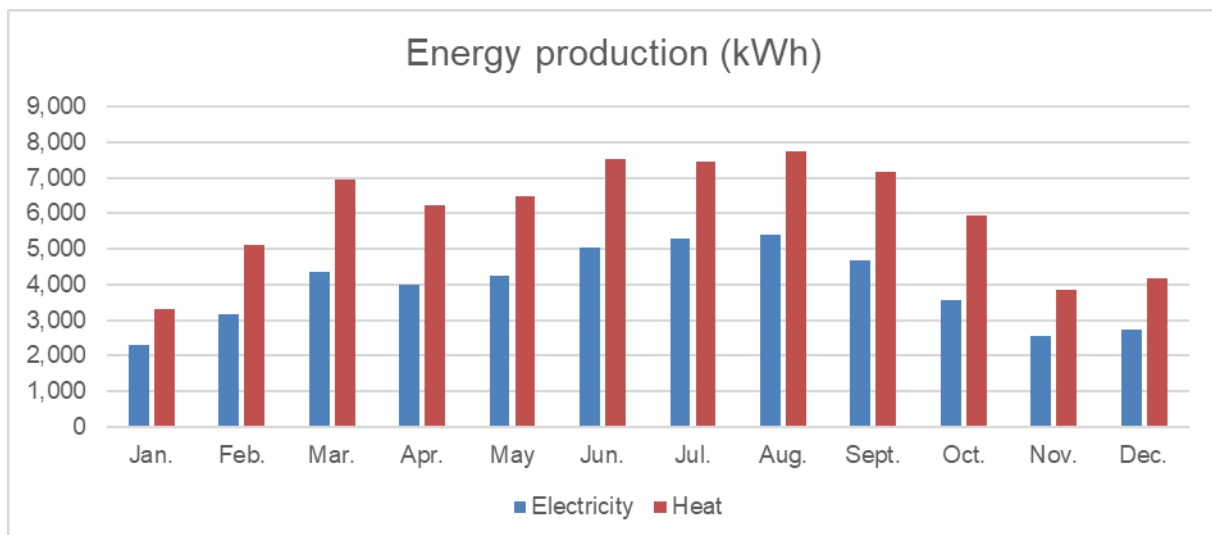


Figure 32. Energy production [kWh] from the Ecomesh hybrid solar panels.

The energy production is higher during the summer months than in the winter, as it is expected for an installation in the northern hemisphere. As it may be observed in Figure 32, there is a difference of 57% in the production between January and August (in both thermal and electrical energy generation).

Table 6 shows the energy produced in a year by the hybrid panels, presenting each contribution separately, and the corresponding economic savings in the costs of energy.

The prices per kWh for both electricity and heat in Spain have been obtained from the Eurostat database (second half of 2017) [101], [102].

Table 6. Annual energy production and energy savings from the Ecomesh hybrid panels.

	Price (€/kWh)	Energy production (kWh)	Energy savings (€)
Thermal	0.09	71,988	6,479
Electrical	0.22	47,355	10,418

For a more detailed analysis, Figure 33 shows the electrical and thermal energy savings for every month of the year.

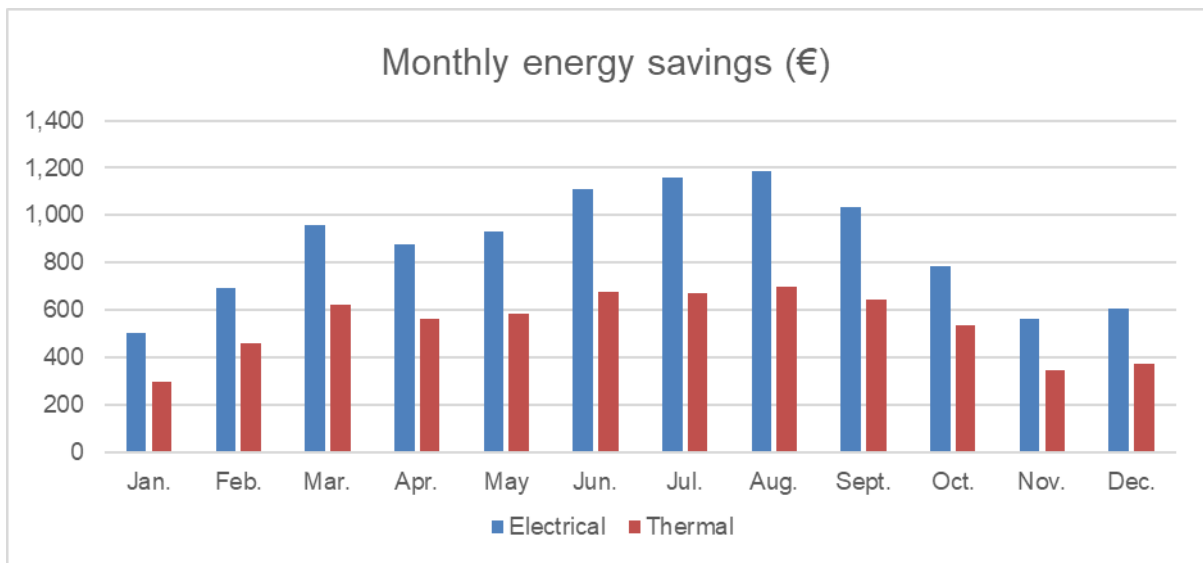


Figure 33. Monthly energy savings [€] from the installation of Ecomesh hybrid solar panels.

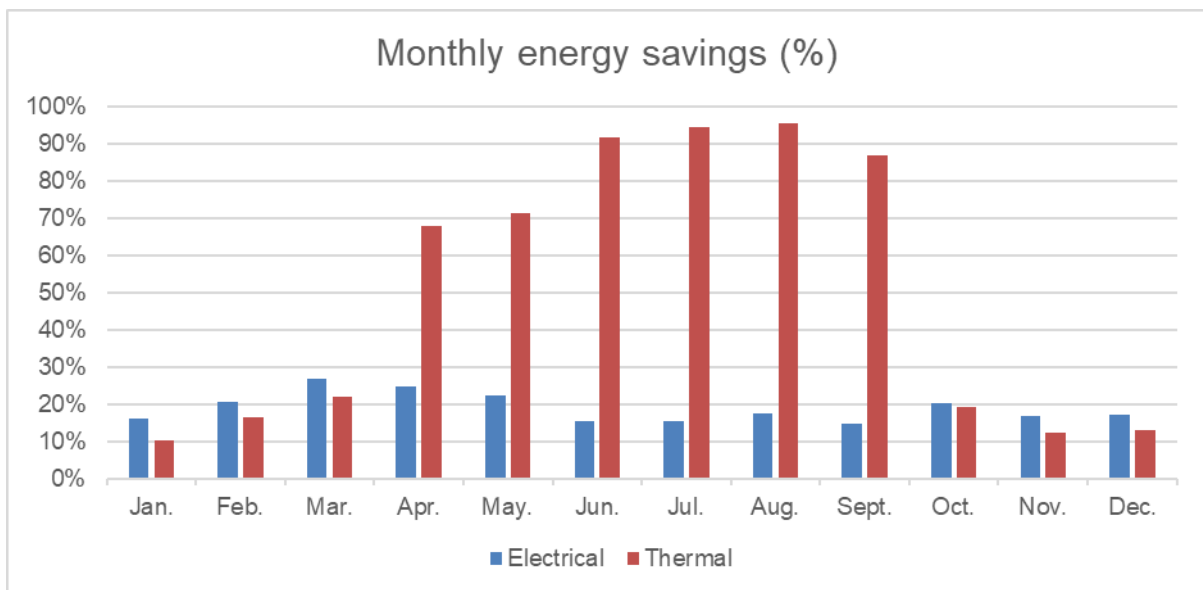


Figure 34. Monthly energy savings [%] from the installation of Ecomesh hybrid solar panels.

Another important aspect is the environmental impact and the effect of renewable energy sources, solar energy in this case, on the reduction of harmful gases emissions. Table 7 shows the annual CO₂ emissions cut, often expressed as the tons of CO₂ avoided, by the implementation of the hybrid solar panels on the rooftop of the hotel building. The data of CO₂ emissions per kWh have been acquired from the emissions factors and carbon footprint document titled: “Factores de emisión. Registro de huella de carbono, compensación y proyectos de absorción de dióxido de carbono”, from the Spanish Ministry of Agriculture and Environment [103].

Table 7. Carbon dioxide emissions cut achieved by the installation of Ecomesh hybrid panels.

	CO₂ emissions factor (kg CO₂/kWh)	Energy production (kWh)	Initial energy consumption (kWh)	Mass of CO₂ avoided (tons)	Amount of CO₂ avoided (%)
Thermal	0.203	71,988	239,707	14.61	30.03
Electrical	0.390	47,355	260,132	18.47	18.20

The efficiency indicators explained in section 3.3 are calculated and presented in Table 8 and 9.

Table 8. Energy yield and efficiency indicators for the installation of Ecomesh hybrid panels.

	Annual energy production (kWh)	Efficiency (%)	Solar fraction (%)
Thermal	71,988	23.14	65.70
Electrical	47,355	16.00	18.20

As it is expected, the thermal efficiency is lower than that of flat plate collectors whereas the electrical is higher than that of PV panels. The results obtained are consistent with the literature review of solar cooling technologies (see section 2.3) and there is a compromise between electricity and heat generation regarding the optical efficiency and the higher thermal insulation provided by the TIC [27].

Table 9. Primary Energy Consumption and Primary Energy Ratio for the 2nd case study.

W_{aux} (kWh)	Q_{aux} (kWh)	PEC_{elect} (kWh)	PEC_{thermal} (kWh)	PER
212,778	167,719	531,944	186,355	0.745

The primary energy consumption is much higher for electricity than heat because the thermal production from the panels is higher as well as the thermal efficiency and the total electricity consumption in the hotel is also higher than the heat consumption (see Figure 31), as observed in the first case study.

4.3. Hotel with Ecomesh hybrid solar panels and a reversible HP

The third case study consists on a solar electric cooling installation by means of the Ecomesh hybrid panels and a reversible heat pump, so that it allows to provide space heating during the winter and air conditioning or cooling during the summer. Apart from electricity, the hybrid panels also provide heat for DHW consumption in the hotel.

For this case study, the efficiency indicators regarding the solar part of the installation are calculated and shown in Table 10 with the solar fraction divided into winter and summer modes where applicable.

Table 10. Efficiency indicators for the solar part of the cooling installation, 3rd case study.

			Solar fraction (%)	
	Annual energy production (kWh)	Efficiency (%)	Winter mode	Summer mode
Thermal	71,988	23.14	65.70	
Electrical	47,355	16.00	17.36	18.85

The annual energy production from the solar panels, both electrical and thermal, is the same as in the second case study (see Table 6). However, the energy savings are different: the real thermal savings are higher in this case because of the additional saving from the space heating, which is now covered by the heat pump, electrically. Nevertheless, the annual net electrical savings are lower than in case 2 since there is an increase in the electricity consumption. This is mainly due to the electrical space heating (installation of a reversible heat pump), because the heat pump has a higher EER than any other conventional AC equipment and consumes less electricity than those during the summer (cooling mode). All the relevant figures related to the annual energy savings will be provided in the economic comparison of the four case studies (section 4.5.1.).

The indicators related to the heat pump parameters and the overall system as well as the use of primary energy are presented in Table 11, for each of the modes (winter, summer).

Table 11. Efficiency indicators related to the overall solar cooling system (HP) and the use of primary energy.

		PEC (kWh)		
	OSE	Electrical	Thermal	PER
Winter mode	1.096	320,558	38,597	0.888
Summer mode	0.784	219,671	2,802	0.888

The overall system efficiency is high, especially during the winter when it is more than the unit, which is a positive aspect of this case since the space heating system changed to be electrical. The lower OSE in summer is due to the higher irradiance during this time and the lower energy demand (64 kW) compared to the winter. As in case 2, the electrical PEC is higher than the thermal due to the higher thermal yield but also, in this case, because the space heating is electrical.

The value is higher in winter due to the higher energy demand than in summer and the longer period (six months of winter).

Table 12 shows the global values of primary energy for the whole year, with a unique PEC and PER.

Table 12. Primary Energy Consumption and Primary Energy Ratio for the 3rd case study.

W _{aux} (kWh)	Q _{aux} (kWh)	PEC _{elect} (kWh)	PEC _{thermal} (kWh)	PER
216,091	37,259	540,228	41,399	0.888

Apart from these parameters, the SPF may be obtained by using the nominal value of the COP from the technical sheet of the selected commercial model and applying the correction factors in order to figure out if the installation can be considered renewable according to the Spanish and European regulations:

$$SPF = COP_{nominal} \cdot FP \cdot FC = 4.41 \cdot 0.86 \cdot 0.77 = 2.92$$

Since the obtained value, 2.92, is higher than 2.5, this heat pump can be considered renewable according to Directive 2009/28/EC and the decision of the European Commission of 2013/114/EU [93].

4.4. Hotel with Ecomesh hybrid panels and absorption cooling

The fourth case study consists on a solar thermal cooling installation by means of the Ecomesh hybrid panels and an absorption unit. The hybrid panels provide heat to the generator of refrigerant vapour (the desorber), but it is not enough to cover its thermal demand. This means that a boiler is needed between the solar installation and the absorption unit, in order to achieve the temperature of 88°C required at the generator. Therefore, in this case the annual energy production from the solar panels is not the same as in the second case study (see Table 6), because the thermal demand is higher. Apart from the thermal contribution, the Ecomesh hybrid solar panels provide electricity for the general use in the hotel (saving from the amount needed from the common grid).

The absorption chiller works only during the summer season; thus, during the winter, the solar panels would provide both electricity and heat for DHW consumption in the hotel. Therefore, in this case study, the electrical and thermal savings during the winter would be identical to the ones obtained in case 2.

The space heating would be provided by the conventional gas boiler currently used in the hotel. During the summer, the thermal savings are clearly different from case 2 since the thermal demand for the absorption chiller is much higher, as previously stated. All of these savings are further discussed and presented in monetary units in the economic comparison (section 4.5.1.).

For this case study, the efficiency indicators regarding the solar part of the installation are calculated and shown in Table 13 with the thermal contribution divided into winter and summer.

Table 13. Efficiency indicators related to the solar part of the absorption cooling installation for the 4th case study.

	Annual energy production (kWh)		Efficiency (%)		Solar fraction (%)	
	Winter	Summer	Winter	Summer	Winter	Summer
Thermal	42,068	42,913	23.96	31.66	54.54	34.49
Electrical	47,355		16.00		21.80	

The thermal efficiency is quite higher during the summer because in the F-Chart method the energy production is very influenced by the energy demand. The electrical solar fraction is the highest among all the studied cases because the demand for electricity is the lowest since there is no electrical AC equipment, but an absorption chiller thermally run.

The indicators related to the overall system and the primary energy consumption are presented in Table 14, divided into winter and summer. Table 15 shows the overall values of PEC and PER along the year.

Table 14. Efficiency indicators related to the use of primary energy for the 4th case study.

	PEC (kWh)		
	Electrical	Thermal	PER
Winter	258,082	183,553	0.764
Summer	166,650	126,632	0.674

Table 15. Primary Energy Consumption and Primary Energy Ratio for the 4th case study.

W_{aux} (kWh)	Q_{aux} (kWh)	PEC_{elect} (kWh)	$PEC_{thermal}$ (kWh)	PER
169,893	279,166	424,732	310,185	0.728

In this case, even if the annual electrical consumption has decreased, the primary energy consumption continues to be higher for the electrical contribution, probably influenced by the thermal yield of the PVT panels. Unfortunately, the PER for the absorption installation is the lowest among all the case studies.

4.5. Comparison of the case studies

4.5.1. Economics

Investment cost:

The investment cost of each of the installations considered refers to the equipment cost or the sum of the different equipment costs and is presented in Table 16.

For the heat pump, the absorption unit and the required boiler, suitable commercial models have been selected according to the energy demands and the technical specifications. They are suggested, together with the Ecomesh solar panels, as real examples of installations.

In order to be consistent with the nature of this master thesis, the first approach was to install a biomass boiler (zero emissions) preceding the absorption unit since the importance of renewable energy sources, clean and beneficial, has been clearly remarked at the introduction of this document. However, it is important to note that the fourth case study already includes the most expensive technology with only the absorption unit and the cost of a biomass boiler is significantly higher than that of a conventional natural gas boiler.

Table 16. Investment cost of each of the solar installations considered.

	EQUIPMENT COST (€)			
	CASE 2	CASE 3	CASE 4	
100-Ecomesh PVT panels installation	125,000	125,000	125,000	
Reversible Heat pump, <i>Kosner</i>		16,875		
Absorption unit, <i>Yazaki</i>			51,289	
Biomass boiler, <i>KWB</i>			21,806	
Gas boiler, <i>De Dietrich</i>				8,313
TOTAL (€)	125,000	141,875	198,095	184,602

Since the biomass boiler is more than two times more expensive than the gas boiler, the latter has been selected for this comparative analysis.

Apart from the second case which refers only to the installation of Ecomesh hybrid panels on the rooftop of the hotel, the lowest investment out of the solar cooling installations is represented by case 3, the one with a reversible heat pump. Moreover, the difference in cost between this option and the one in case 4 is significant: 42,727 € (with the natural gas boiler).

Operational costs:

These costs are the total consumption costs when the solar cooling installations are operating. Therefore, they are calculated by subtracting the total energy savings (both electrical and thermal) in a year from the initial operational cost in the hotel (case 1), for each of the case studies, as presented in Table 17.

Table 17. Operational costs for each of the case studies.

	CASE 1	CASE 2	CASE 3	CASE 4
Annual energy savings (€/year)	-	16,897	27,909	20,164
Operational cost (€/year)	78,803	61,906	50,893	58,639

Regarding this indicator, the preferred option upon all of the case studies would be the solar electric cooling installation (case 3), which has the lowest operational cost of the four (50,893€), followed by the solar absorption cooling installation (case 4), and finally the solar installation considered in the second case, with the lowest annual energy saving.

The annual energy savings, divided in electrical and thermal contributions, for the three case studies (2 to 4) suggested are further described in Figure 35 to illustrate and ease the comparison.

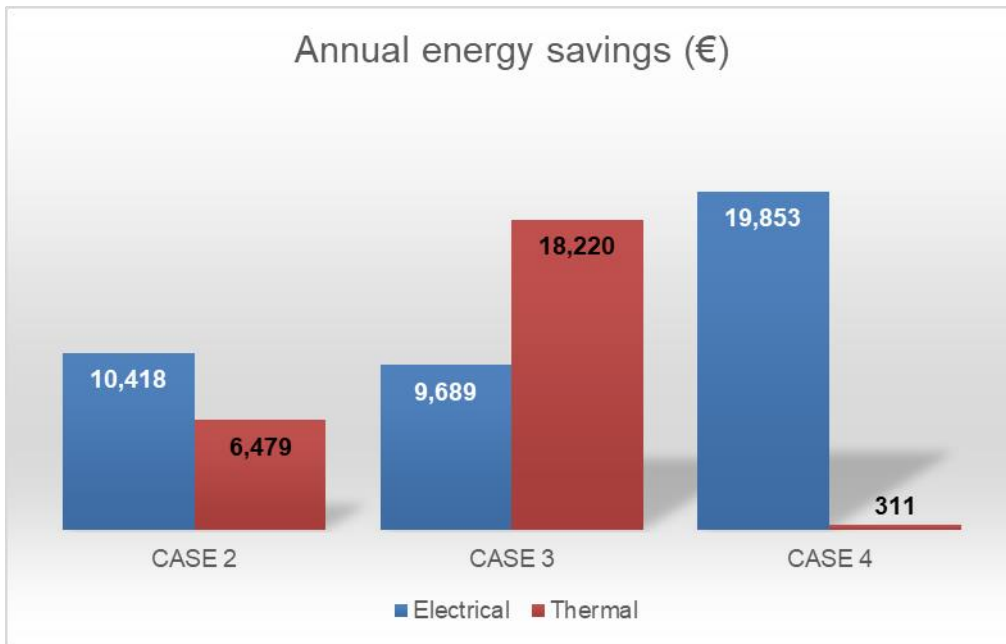


Figure 35. Comparison of the electrical and thermal annual energy savings [€].

Since this master thesis focuses on solar cooling technologies, applicable during the summer, the energy savings for this period are presented in Figure 36.

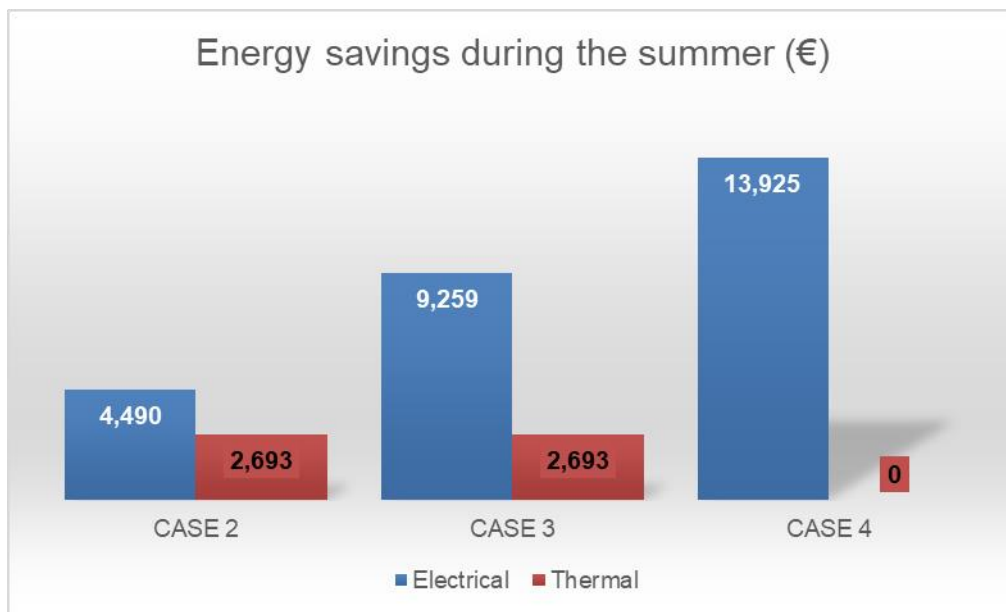


Figure 36. Comparison of the electrical and thermal energy savings [€] during the summer.

For case 3, one can observe that the majority of the electrical savings corresponds to the summer, whereas the thermal savings are much higher during the winter since the heat consumption from the gas boiler for space heating is saved.

In case 4, the electrical savings during the summer are quite higher than in the second case because the electricity used for the conventional AC system in case 2 is saved. The air conditioning is now thermally provided by the absorption unit. It is important to note that there is not thermal saving during the summer but during the winter.

This means that the thermal savings during the summer are lower than the exceeding expense (the extra cost) in these months due to the high thermal consumption of the absorption unit, which requires an extra preceding boiler that feeds most of the thermal energy needed at the generator.

In order to summarise the economic comparison in terms of costs, both the investment and the operational costs are represented in Figure 37 for each of the case studies, now including the first case (current situation of the hotel), which has zero investment cost.

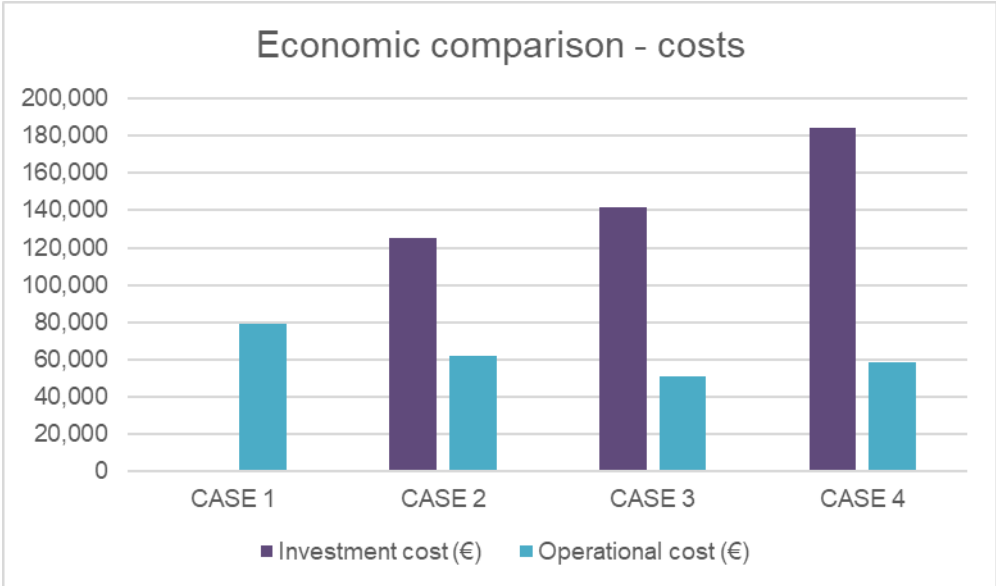


Figure 37. Investment and operational costs of each of the case studies analysed.

It is observed that in case 4, the investment cost is the highest with a large difference (59,602€) compared to case 2, whereas its annual operational cost is slightly lower, with a difference of 3,267€. However, in the third case study, one can observe a bigger decrease in the annual operational cost (11,013€), more than triple of the previously explained scenario, for a much lower increase (16,875€) in the initial investment compared to the second case study.

Simple Payback Period (SPP):

The simple payback period is chosen to easily compare the investigated options. It refers to the time (years) required for the amortization of the solar cooling installation and is calculated as the ratio of the investment cost to the annual energy savings.

The results for each of the case studies are shown in Table 18.

Table 18. Simple Payback Period for each of the case studies.

	CASE 2	CASE 3	CASE 4
Investment cost (€)	125,000	141,875	184,602
Annual energy savings (€/year)	16,897	27,909	20,163
SPP (years)	7.4	5.1	9.2

It can be observed that the lowest payback period corresponds to the third case study. It means that in five years and a half the investment would be recovered. Thus, even if the investment cost is higher for case 3 than case 2, it can be returned sooner due to the larger energy savings per year in case 3. However, case 4, absorption cooling system, results on both the highest investment and payback time, with more than 9 years.

Cost of primary energy saved:

This parameter is defined as the ratio of the extra costs for the solar installation per year to the amount of primary energy saved in kWh also in a year. In order to calculate the primary energy saved, the total primary energy consumption is previously obtained for each of the case studies:

Table 19. Total primary energy consumption in a year for each of the case studies.

	CASE 1	CASE 2	CASE 3	CASE 4
PEC_{elect} (kWh)	650,331	531,944	540,228	424,732
PEC_{thermal} (kWh)	266,341	186,355	41,399	310,185
TOTAL (kWh)	916,672	718,298	581,627	734,917

In order to comparatively analyse the PEC for each of the four case studies, the results are also illustrated in Figure 38.

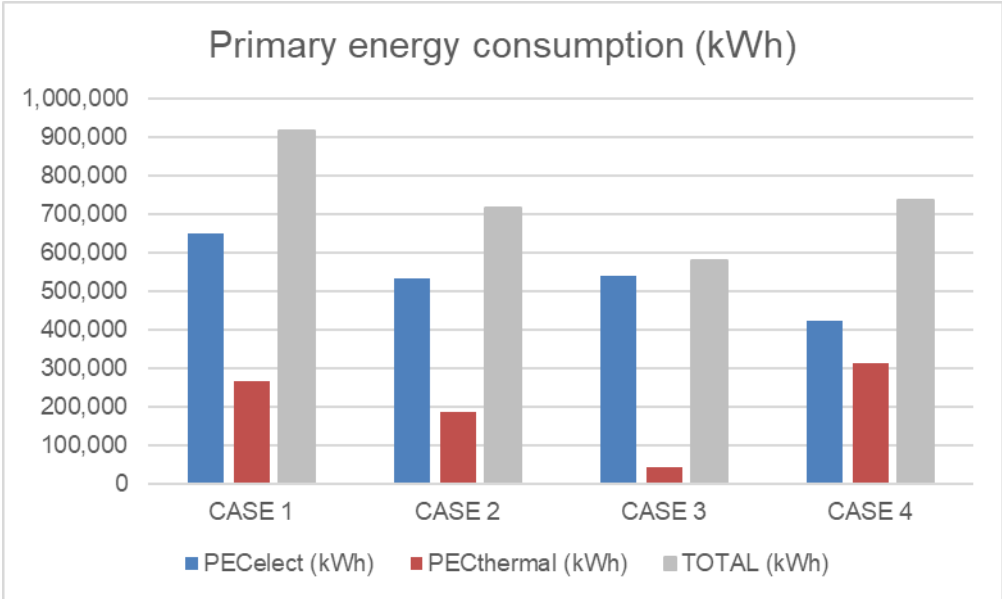


Figure 38. Comparison of the Primary Energy Consumption [kWh] for the 4 case studies.

Now the primary energy saved can be easily obtained by subtracting the corresponding total PEC (see Table 19) from the one in the initial case 1. Assuming a plant life time of 20 years, the costs per kWh of primary energy saved are calculated and presented in Table 20:

Table 20. Cost of primary energy saved for each of the case studies.

	CASE 2	CASE 3	CASE 4
$\Delta C_{a,s}$ (€/year)	6,250	7,094	9,230
PE_{saved} (kWh)	198,374	335,045	181,755
CPE_{saved} (€/kWh_{PE})	0.03	0.02	0.05

Regarding the cost of primary energy saved, case 3 represents again the best option, the cheapest, with the lowest cost per kWh of primary energy saved, 2 cents of €.

Net Present Value (NPV) and Internal Rate of Return (IRR):

Considering that the lifetime of the installations is 20 years and the annual increase of the electricity and gas prices are 3% and 4% respectively, the NPV and the IRR are calculated for every case and presented in Table 21:

Table 21. NPV (€) and IRR (%) results.

	CASE 2	CASE 3	CASE 4
NPV (€)	226,409	471,187	219,603
IRR (%)	12	20	9

Since in all of them the NPV is positive and the IRR higher than 2%, every case is economically feasible. However, the project suggested in case 3 would be much more profitable than the other two since the NPV is quite higher (more than two times than case 2), as well as the IRR.

4.5.2. Environmental impact

CO₂ emissions cut:

The amount of CO₂ avoided, expressed in tons of CO₂/year is presented in Table 22.

Table 22. CO₂ emissions cut in tons of CO₂ avoided for each of the case studies.

	CASE 2	CASE 3	CASE 4
Tons of CO₂ avoided/year	33.1	58.3	35.9

It can be observed that the preferred option, now environmentally speaking, is again case 3, the solar cooling installation based on the combination of 100 Ecomesh hybrid panels and a reversible heat pump. It seems that the extra investment cost of installing a solar absorption cooling system in the hotel does not have an environmental advantage compared to the simple hybrid solar panels installation (case 2). It is true that case 4 leads to higher annual energy savings and CO₂ emissions cut, but there is not such a large difference when comparing to the second case; however, there is a big difference in the initial investment cost.

Global Warming Potential (GWP):

Despite the advantages of installing the reversible heat pump of case 3, it is important to take into account that the vapour compression cycle includes the use of a hydrofluorocarbon gas, the refrigerant R410A, which has a GWP of 1,924. In the case of using an absorption unit (case 4) for solar cooling, the refrigerant is just water, which is a harmless substance with a GWP of zero.

As already introduced in Chapter 3, there are many refrigerants being developed nowadays and some more beneficial options such as the R32, but they have not been used yet in large-capacity heat pumps that require high values of power as it is the case of the 4-star hotel considered in this master thesis. Thus, less harmful refrigerants may be used for the residential sector (smaller residential buildings, family houses) heat pumps with a lower value of GWP.

Ozone Depletion Potential (ODP):

Another important environmental indicator is the ozone depletion potential, which was already explained in Chapter 3. The refrigerant R410A (used in case 3) has a zero ozone depletion potential as well as the water, used as refrigerant in the fourth case study.

4.6. Discussion

All the analysed solar cooling technologies allow significant energy savings ranging from 27.3% for the second case study, 54.8% for the third (heat pump) and 34.4% for the fourth case (absorption). The decrease of the initial cost of PVT collectors seems a key factor to reduce the cost of solar cooling systems, since the panels represent 88.1% of the total investment cost of the system in the third case study and 67.7% of this cost in the fourth case study (absorption). Developing the design of PVT panels in order to improve its efficiency might be another way to reduce the initial investment cost.

After the previous techno-economic and environmental analysis of the different case studies, the pros and cons of each alternative option to the initial case 1 are summarised and explained as follows:

Case 2: Installation of 100 PVT panels on the hotel rooftop

Pros

- This installation of the panels coupled with the electrical grid in the hotel, in general, and the conventional AC system, in particular for solar cooling, is more eco-friendly than the initial case, with a reduction of 33.1 tons of CO₂ per year.
- The investment cost is the lowest among the three installations suggested here for solar cooling.

Cons

- This installation does not change the AC system that is already working in the hotel, only adds the panels and conventional AC systems are generally much less efficient than heat pumps, with a lower EER (usually around 2). Therefore, the total electricity consumption is higher and the CO₂ emissions cut is lower than in cases 3 and 4.
- The annual energy savings are the lowest among the three cases and the SPP is higher than in case 3, which includes the reversible heat pump.

Case 3: Installation of 100 PVT panels coupled with an air-water reversible heat pump

Pros

- This case presents the highest annual saving and the lowest SPP, making the investment worth.
- The CO₂ emissions cut is also the largest among the three cases.
- The PEC is the lowest of the three and the PER the highest. Therefore, the primary energy saved is higher than in cases 2 and 4 and the cost of primary energy saved is the lowest.
- Regarding the project economic viability, the NPV and the IRR are the highest among the three case studies.

Cons

- The initial investment is significant, even though it is not the largest since the absorption chiller is more expensive than the heat pump and it also requires the boiler. However, it is important to note that the PVT panels represent about 88% of the total investment cost in case 3.
- The suggested heat pump uses refrigerant R410A, which is a greenhouse gas with quite a high GWP value. This may affect the environment in the event of a leakage.

Case 4: Installation of 100 PVT panels coupled with an absorption chiller

Pros

- In principle, one could think that this installation has an advantage that is intrinsic to the nature of the system since it is a thermal cooling system. The thermal kWh is more economic and has a lower CO₂ emissions factor, which could affect the profitability and environmental viability of the system regarding the consumption of its auxiliary sources. Moreover, all the electricity produced by the PVT panels can be utilised in the internal grid of the hotel, being the price of the electrical kWh higher than the thermal. Actually, this case presents the highest electrical solar fraction since the electricity demand decreases because the cooling is thermally achieved.
- The refrigerant used in the thermodynamic cycle of a LiBr-H₂O absorption chiller is water, which is an environmentally friendly substance with zero ODP and GWP.

Cons

- This installation has a very high investment cost, actually the highest among the three suggested installations (184,602€). The PVT panels account for 68% of the investment cost.
- The SPP is the highest, with more than 9 years to recoup the investment.
- The CO₂ emissions cut is lower than in case 3, although it is higher than in case 2, but the difference is quite small compared to the investment.
- Moreover, this installation consumes a higher amount of primary energy than the others since the savings in primary energy are the lowest. The PEC is the highest and the PER the lowest among the three cases. The cost of primary energy saved is higher than in cases 2 and 3.
- Accordingly, the NPV and the IRR are the lowest among the three cases.

Since the investment cost seems to be a bottle neck in these installations, and in order to generalise a bit more this study for different situations or hotels, the case of a hotel that already has PVT panels and plans to install a cooling system coupled with them is also considered. For this, only cases 3 and 4 could be compared. Now the investment cost corresponds to the cost of the reversible heat pump and the total cost of the absorption installation (including the natural gas boiler), respectively. But it is clear that the latter is much higher and it is not profitable, as previously explained.

Therefore, this analysis aims to observe the impact on adding a reversible heat pump to an already existing PVT installation in a hotel for solar cooling.

The annual energy savings and all the operational parameters already studied (including the environmental) would remain the same, but the key indicator now is the SPP, with a new value of 0.60. This means that for those hotels that already have PVT panels, it is profitable to install such a heat pump since the investment would be recovered in less than a year.

4.6.1. Additional consideration

Moreover, one can observe that the hybrid panels investment cost is the highest (see Table 16). There may be some hotels that are more interested in a cheaper solar installation, for example with photovoltaic panels, which prices have dropped dramatically along the last years, as explained in Chapter 2. This may be considered either for the first (only solar panels) or the second (solar panels coupled with a reversible heat pump) case study of the ones previously analysed. There would be only electrical savings and the difference is whether the electricity produced is used in the internal grid of the hotel, in general, or fed to the heat pump to reduce its electrical consumption from the common grid.

However, it is important to note that although the investment cost is lower, the electricity production of the same installation with solar PV panels is lower than the obtained from the hybrid panels, mostly due to the losses from the temperature increase. Another important factor is the lack of thermal savings in this case, in comparison with the dual contribution of hybrid solar panels. Thus, it is interesting to analyse this alternative case and compare it with the use of Ecomesh hybrid panels in order to state some conclusions. For such purpose, Ecomesh PV panels are considered, which actually have the same photovoltaic laminate as the already studied hybrid panels.

A calculation of the economic and environmental impact of replacing the PVT panels with the PV ones in the two cases explained above is presented in Table 23 and the following figures.

Table 23. Economic and environmental key indicators for a PV-based alternative system.

Installation	Investment cost (€)	Annual energy savings (€)	CO₂ emissions cut (tons of CO₂ avoided)
100 Solar PV panels	30,000	10,031	17.8
100 Solar PV panels + Reversible heat pump	46,875	21,043	43.0

The comparison of the investment cost for the initial solar system based on Ecomesh hybrid solar panels and the one proposed above with PV panels is shown in Figure 39.

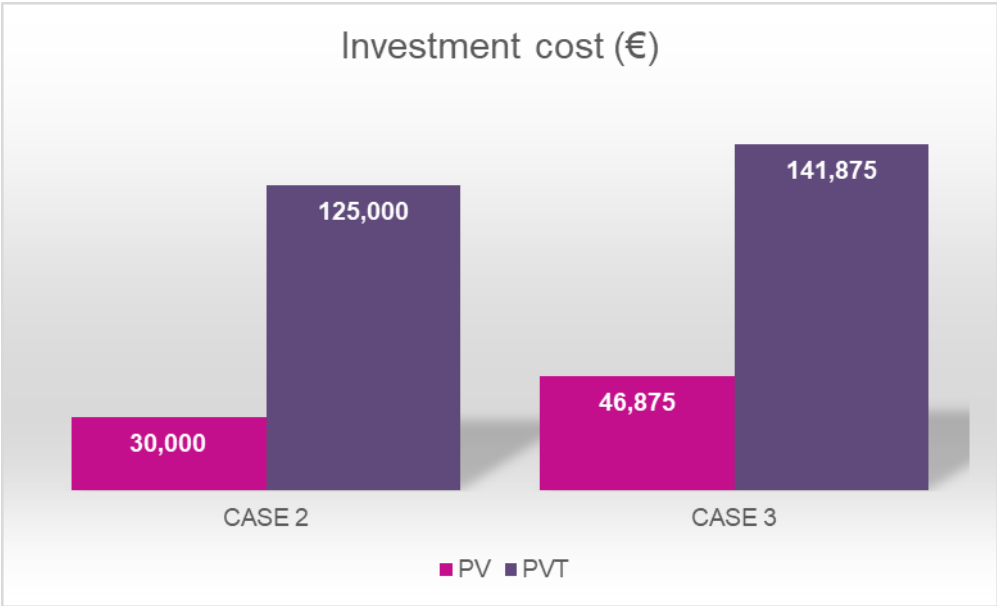


Figure 39. Comparison of the investment costs for PV and PVT panels.

In case 2, the installation of PV panels would lead to a decrease of 76% in the investment cost, whereas in case 3 the investment decreases by 67%. Therefore, according only to the change in the investment cost, the installation of only PV panels on the rooftop of the hotel (case 2) would be preferred.

Figure 40 presents the annual energy savings (initial and alternative case with PV) for both case studies considered here, the installation with only solar panels on the rooftop of the hotel and the solar electric cooling installation of the third case study (solar panels coupled with a reversible heat pump).

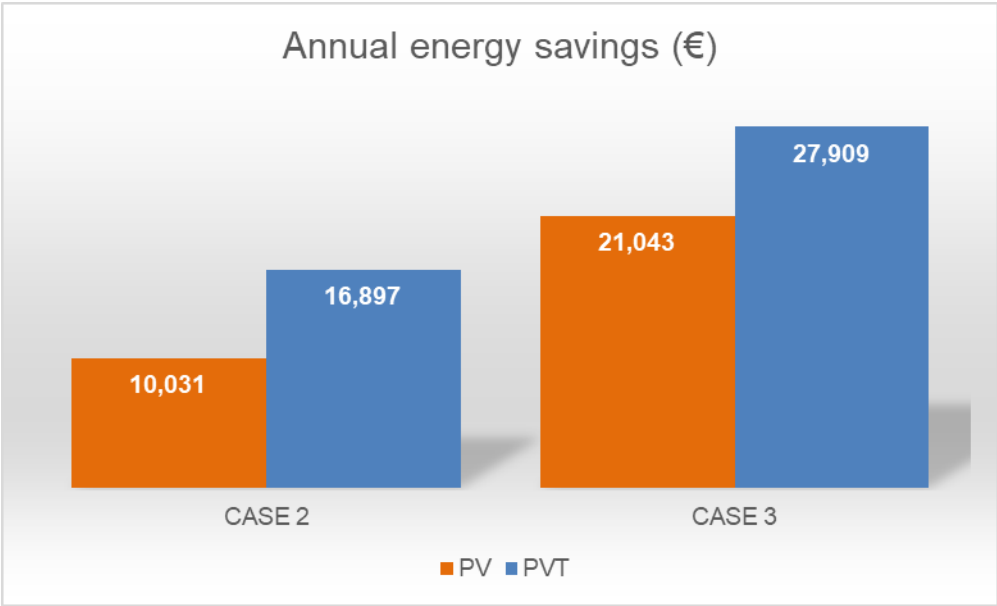


Figure 40. Comparison of the annual energy savings for PV and PVT panels.

The annual energy savings are generally lower when PV panels are used because unlike the hybrid ones, they do not provide heat. Moreover, the efficiency of PV panels is lower than the electrical efficiency of PVT ones, due to the higher temperature in the module, as already explained.

Actually, the efficiency obtained for this installation of PV panels is 15.4%, whereas the value for PVT panels was 16%, as presented in Table 8.

In case 2, the installation of PV panels instead of hybrid ones would lead to a decrease of 40.6% in the annual energy savings. However, in case 3, it may be observed a decrease on the annual energy savings of 24.6% when solar PV panels are used instead of hybrid ones, which is almost half of the decrease observed in case 2. Thus, according only to the change in the annual energy savings, this option (case 3) seems quite favourable in case of deciding to install PV panels. It is preferable compared to the installation of only the panels, without the heat pump for solar cooling/heating.

With regard to the economic analysis, the ratio of the decreases in the savings between case 2 and case 3 is higher than that of the decreases in the investment costs. Therefore, it is generally more economical to install a solar electric system with a reversible heat pump coupled with 100 PV panels than just 100 PV panels on the rooftop for the general use of electricity since the annual savings will be higher in the former case, unless the bottle neck is on the initial investment.

The comparison of the CO₂ emissions cut for the two systems, with PV and PVT panels, for each of the case studies considered in this section is presented in Figure 41.

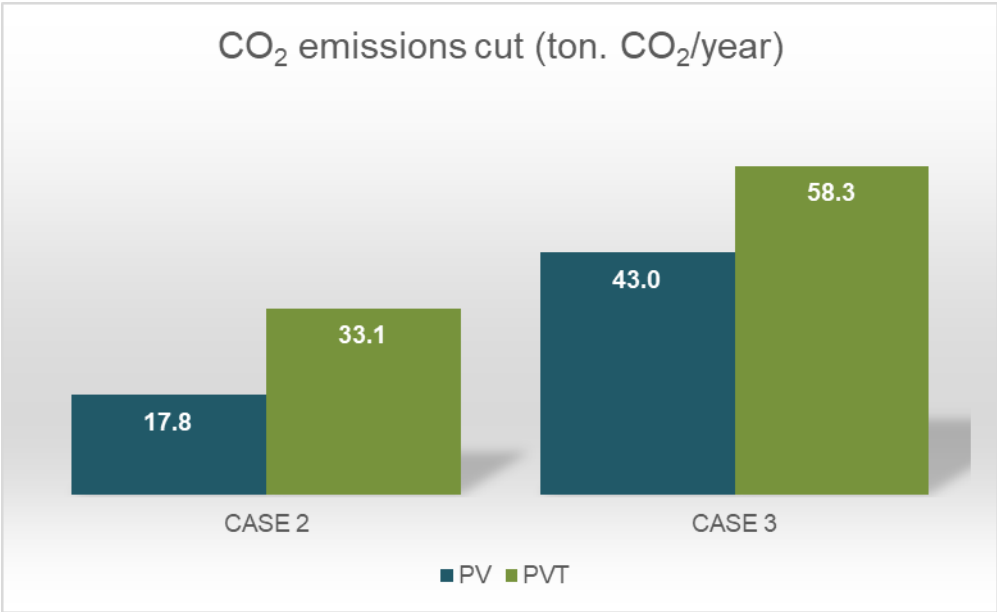


Figure 41. Comparison of the CO₂ emissions cut for PV and PVT panels.

With the installation of PV panels instead of PVT, the tons of CO₂ avoided decrease in 46.2% for case 2 and 26.2% for case 3. Therefore, once again the relative value (percentage) shows that the decrease is lower, proportionally, for the third case study, becoming the preferred option for an installation of PV panels instead of PVT.

The NPV, the IRR and the SPP of these other two alternatives are presented in Table 24.

Table 24. NPV, IRR and SPP for a PV-based alternative system.

Installation	NPV (€)	IRR (%)	SPP (years)
100 Solar PV panels	167,749	32	3.0
100 Solar PV panels + Reversible heat pump	412,006	44	2.2

One can observe that the NPV is again higher in case of installing the PV panels together with the reversible heat pump. The IRR value is also larger in this case. Actually, both IRR values are larger than in the previous cases with the use of PVT panels whereas the NPV ones are lower. This is due to the high value of investment cost in a PVT installation and proves that it is worth it to invest the money in such a project rather than another financial product. Moreover, the SPP is lower in case of installing the PV panels together with the reversible heat pump, as it could be expected from the values of the other economic parameters.

Consequently, in case of rejecting the installation of hybrid solar panels initially suggested due to the high investment cost, it is recommended to select the solar electric cooling installation with the set of PV panels. This constitutes a first approach and a comparative study since the master thesis is based on the calculations and design for a PVT-based installation. But it is clear that the client may not consider the option of installing hybrid panels from the beginning and therefore, the comparison with this reference may not be useful in that case. It is important to note that each situation must be analysed according to its bottle necks and that there may be cases where the initial investment already limits the possibilities of the client to the installation of just a system of PV panels. However, this thesis aims to discuss those cases in which there is an interest on a new cooling system, more sustainable and aided by renewable energy sources.

Chapter 5. Conclusion and outlook

This chapter highlights the most important findings of this research and presents the conclusions of the master thesis regarding the most favourable cooling technologies to be installed in a 4-star hotel by using solar energy. Furthermore, some possible improvements and recommendations are suggested giving a future prospective on solar cooling technologies and applications.

In this master thesis, the main solar cooling technologies have been investigated to write a proper state of the art and the focus has been the coupling of PVT panels with cooling systems since there are not enough data and results of calculations in the literature with the use of this type of panels. The company EndeF Engineering S.L. has patented a special type of hybrid panel with a transparent insulating cover called Ecomesh and is interested in exploring the available solar cooling technologies in which the panels could be coupled with as well as analysing the profitability and environmental benefits of these integrated installations. After the previous research, two different cooling technologies have been selected to study for the case of a 4-star hotel with 100 guests located in Madrid, as an example. The performance, economic and environmental feasibility of the installations are analysed by means of a comparative study of four different cases for the hotel.

According to the results obtained, the preferred option regarding most of the indicators used in the analysis is a solar electric cooling system with 100 Ecomesh PVT panels and a reversible heat pump. The annual saving is 27,909€ and the CO₂ emissions cut is about 58 tons of CO₂/year. However, the investment cost is higher for this option than the installation with only the PVT panels. Therefore, some recommendations are presented below, depending on the different situations of a 4-star hotel:

- For those 4-star hotels (or similar-size commercial buildings) that already have installed the Ecomesh hybrid panels on the rooftop, the installation of a cooling cycle coupled with them is considered: either by absorption or with the use of a heat pump. From this study, it is demonstrated that the only profitable option in this case is a solar electric cooling system with a reversible heat pump. It has 71.7% lower investment cost than the absorption installation and 38.4% higher annual savings during operation. An alternative option could be to continue only with the hybrid solar panels installation, but it is important to note that the payback time in this case would be longer (more than 7 years) than in case of installing the heat pump for cooling/heating in the building. Actually, the SPP has been calculated taking into account the whole installation as new, but in a real case like this part of the total investment may be already paid (panels) so it would be less.

- For a new 4-star hotel or a 4-star hotel without any renewable energy source installation, there may be an interest in installing solar panels on the rooftop or a whole solar cooling installation at once. In this case, the investment cost gains more importance since it would be high in any case and all at once. According to the results, the option of solar thermal cooling system by absorption is not so profitable among the solar cooling options, especially due to quite a higher investment cost. Therefore, two options are recommended: installing only Ecomesh hybrid panels on the rooftop or installing the panels plus a reversible heat pump for solar cooling and heating. The second of these options seems more beneficial from a long-term perspective. It implies higher savings (lower operating costs) and shorter payback period.

Later on, two alternative options have been suggested with PV panels since they are much cheaper than the PVT. The first one consists on a solar installation with these PV panels and the other on the PV panels and a reversible heat pump for solar electric cooling.

In both, the investment cost is lower than in case of using hybrid panels, but also the annual energy savings. The decrease on these savings is lower for the installation of the reversible heat pump; therefore this second option has been also recommended in case of deciding for Ecomesh PV panels instead of the PVT ones. In all of the systems (cases) suggested and analysed in this master thesis, the NPV is positive and the IRR higher than 2%; therefore, every case is economically feasible. However, the project suggested in the solar electric cooling system operated by a reversible heat pump would be much more profitable than the rest since the NPV is quite higher as well as the IRR. This occurs both for the systems with PVT panels and the ones with PV panels previously discussed. Actually, the IRR is larger in those systems coupled with PV panels due to the decrease in the investment cost. Nevertheless, the NPV are lower in those cases, therefore it is difficult to directly compare the profitability in these terms. What is clear is that all the options are economically feasible.

Finally, it is important to note that this is a preliminary study performed in a simplified way with the example of a hotel in order to compare the possibilities and announce some conclusions. There was a lack of real data of the cooling part of the installation since this will still be part of a research project. Thus, it was necessary to make several assumptions for certain parameters. Moreover, the F-Chart method has several limitations. It is highly used for small and medium-sized installations; but for a future more detailed study for a real application, it is recommended to use more accurate calculation methods based on dynamic simulations.

The analysis was based on real thermodynamic cycles estimated from the correction of ideal ones by means of a coefficient since otherwise, a lot of unknown data would have to be assumed and some were not possible to. But in order to give an outlook on future steps of this work, which seems very interesting nowadays when solar energy is gaining popularity and profitability, it would be interesting to acquire more data to be able to simulate the proper real thermodynamic cycles (vapour compression and absorption cycles). This would provide more reliable results as well as accuracy to the variations among the different months. One could also think of analysing other types of absorption cycles that typically have a higher performance than the single-effect cycle, as explained in Chapter 2.

However, this study shows that it may not be worth it, since double or triple-effect absorption cycle installations are more complex and therefore expensive than the analysed in this master thesis, whereas this one is not profitable, as concluded here.

Another interesting aspect to take into account for future works related to this one is the Life Cycle Assessment (LCA). In this master thesis it had no sense to do it since there is not a real specific case with all the known values for the inputs and outputs of every step of the whole installation. Once that the real problem is defined for a particular hotel, for instance a solar electric cooling installation with PVT panels, this analysis can be done including all the steps. Actually, there is a LCA software specially developed by IEA SHC programme for solar cooling applications. It is called Elisa and is available online since the end of 2018.

Annex 1. EES codes

In this annex, the codes from the software EES are presented and briefly described. They include the solar thermal calculations of the hybrid solar panels, the simulation of a basic vapour compression cycle and the simulation of an absorption LiBr-H₂O cycle.

A.1 Calculations for the solar system

Important equivalences:

F-Chart coefficient	Equivalence in the code (used nomenclature)
$\tau\alpha/(\tau\alpha)_n$	coef1
F'_R/F_R	coef2
$F'_R \cdot (\tau\alpha)$	coef3

Solar installation in a 4 hotel by using Ecomesh hybrid panels. Calculation of the thermal efficiency and the energy yield of the PVT panels system.*

General data:

$N_{\text{guests}} = 100$ *Capacity (n° of guests) of the hotel.*

$N_p = 100$ *Number of solar panels installed on the rooftop.*

$T_{\text{DHW,C}} = 60$ [C] *Reference temperature of Domestic Hot Water (DHW).*

$T_{\text{DHW}} = T_{\text{DHW,C}} + 273$ [K] *Reference temperature of DHW in K.*

$V_{\text{tank}} = 20000$ [L] *Storage tank volume.*

$q = 50 \text{ [L/(h}\cdot\text{m}^2\text{)]}$ *Nominal flow rate per unit of area of the solar collector.*

Thermal data of Ecomesh solar panel:

$A_c = 1.56 \text{ [m}^2\text{]}$ *Collector area of the Ecomesh hybrid panel.*

$n_o = 0.51$ *Optical efficiency.*

$a_1 = 4.93 \text{ [W/m}^2\cdot\text{K]}$ *Thermal losses coefficient, a1.*

$a_2 = 0.021 \text{ [W/m}^2\cdot\text{K}^2\text{]}$ *Thermal losses coefficient, a2.*

$\text{coef1} = 0.94$ *Coefficient for a double glass cover (TIC).*

$\text{Capacity} = 1.2 \text{ [L]}$

$\text{coef2} = 0.95$ *Correction factor collector-heat exchanger (typical value).*

Data for Madrid (4 Hotel):*

$T_{\text{amb_C}}[1..12] = [7.7, 7, 8.3, 11.3, 15.9, 24.3, 28.9, 27.8, 23.1, 16.5, 8.9, 6.6]$

$T_{\text{red_C}}[1..12] = [8, 8, 10, 12, 14, 17, 20, 19, 17, 13, 10, 8]$

$E[1..12] = [340.2, 471.6, 658.8, 601.2, 630, 774, 802.8, 824.4, 727.2, 558, 385.2, 406.8]$

$\text{Cons}_{\text{day,L}} = 55 \cdot N_{\text{guests}}$ *Total daily consumption of DHW in L for the 4* hotel.*

$\text{Cons}_{\text{day}} = \text{Cons}_{\text{day,L}} \cdot \left| 0.001 \cdot \frac{\text{m}^3}{\text{L}} \right|$ *Total daily consumption of DHW in m³.*

----- *Thermal calculations: F-Chart Method* -----

$N = 12$

$T_{\text{amb},i} = T_{\text{amb,C},i} + 273$ for $i = 1$ to N *Ambient temperature array in K.*

$T_{\text{red},i} = T_{\text{red,C},i} + 273$ for $i = 1$ to N *Cold water temperature array in K.*

$N_{\text{month}}[1..12] = [31, 29, 31, 30, 31, 30, 31, 31, 30, 31, 30, 31]$

$\text{Cons}_{\text{month},i} = \text{Cons}_{\text{day}} \cdot N_{\text{month},i}$ for $i = 1$ to N *Monthly DHW consumption for the hotel in m³.*

$T = 298 \text{ [K]}$

$P = 101.325 \text{ [kPa]}$

$\rho = \rho[\text{water}, T = T, P = P]$

$\text{cp} = \text{Cp}[\text{water}, T = T, P = P]$

$Q_{\text{DHW},i} = \frac{\rho \cdot \text{Cons}_{\text{month},i} \cdot \text{cp} \cdot [T_{\text{DHW}} - T_{\text{red},i}]}{10^3}$ for $i = 1$ to N *Monthly thermal energy demand of DHW in MJ.*

$\text{coef3} = n_o \cdot \text{coef1} \cdot \text{coef2}$

$$D1_i = \frac{Np \cdot Ac \cdot \text{coef3} \cdot E_i}{Q_{DHW,i}} \quad \text{for } i = 1 \text{ to } N$$

$$\delta_{t,i} = N\text{month}_i \cdot 24 \cdot 3600 \quad \text{for } i = 1 \text{ to } N \quad \textit{Total amount of seconds in each month.}$$

$$K1 = \left[\frac{V_{\text{tank}}}{75 \cdot Np \cdot Ac} \right]^{-0.25}$$

$$K2_i = \frac{11.6 + 1.18 \cdot T_{DHW,C} + 3.86 \cdot T_{\text{red},C,i} - 2.32 \cdot T_{\text{amb},C,i}}{100 - T_{\text{amb},C,i}} \quad \text{for } i = 1 \text{ to } N$$

$$D2_i = \frac{Np \cdot Ac \cdot a_1 \cdot \text{coef2} \cdot [100 - T_{\text{amb},C,i}] \cdot \delta_{t,i} \cdot K1 \cdot K2_i}{Q_{DHW,i} \cdot 10^6} \quad \text{for } i = 1 \text{ to } N$$

$$f_i = 1.029 \cdot D1_i - 0.065 \cdot D2_i - 0.245 \cdot D1_i^2 + 0.0018 \cdot D2_i^2 + 0.0215 \cdot D1_i^3 \quad \text{for } i = 1 \text{ to } N$$

$$Qu_i = f_i \cdot Q_{DHW,i} \quad \text{for } i = 1 \text{ to } N \quad \textit{Useful heat produced in a month in MJ.}$$

$$Qu_{A,i} = \frac{Qu_i}{Np \cdot Ac} \quad \text{for } i = 1 \text{ to } N \quad \textit{Useful heat per m}^2 \textit{ produced in a month in MJ.}$$

$$Qu_{kWh,i} = \frac{Qu_i}{3.6} \quad \text{for } i = 1 \text{ to } N \quad \textit{Useful heat produced in a month in kWh.}$$

$$Qu_{kWh,A,i} = \frac{Qu_i}{3.6 \cdot Np \cdot Ac} \quad \text{for } i = 1 \text{ to } N \quad \textit{Useful heat per m}^2 \textit{ produced in a month in kWh.}$$

Thermal efficiency and energy yield:

$$Qu_{\text{total}} = \sum_{i=1}^N [Qu_i]$$

$$QDHW_{\text{total}} = \sum_{i=1}^N [Q_{DHW,i}]$$

$$F = \frac{Qu_{\text{total}}}{QDHW_{\text{total}}} \quad \textit{Annual solar fraction: fraction of energy covered by the hybrid collectors every year.}$$

$$\eta_{t,i} = \frac{Qu_i}{E_i \cdot Np \cdot Ac} \quad \text{for } i = 1 \text{ to } N \quad \textit{Monthly thermal yield.}$$

$$E_{\text{total}} = \sum_{i=1}^N [E_i]$$

$$\eta_{t,\text{annual}} = \frac{Qu_{\text{total}}}{E_{\text{total}} \cdot Np \cdot Ac} \quad \textit{Thermal efficiency.}$$

SOLUTION

Unit Settings: SI K kPa kJ mass deg

Ac = 1.56 [m²]

Capacity = 1.2 [L]

coef3 = 0.4554 [W/K-MJ]

cp = 4.183 [kJ/kg-K]

F = 0.657 [-]

Np = 100

P = 101.3 [kPa]

QUtotal = 259161 [MJ]

T_{DHW} = 333 [K]

a₁ = 4.93 [W/m²*K]

coef1 = 0.94

Cons_{day} = 5.5 [m³/day]

η_{t,annual} = 0.2314

K1 = 0.8746

N_{guests} = 100

q = 50 [L/(h*m²)]

ρ = 997.1 [kg/m³]

T_{DHW,C} = 60 [C]

a₂ = 0.021 [W/m²*K²]

coef2 = 0.95

Cons_{day,L} = 5500 [L/day]

E_{total} = 7180 [MJ/m²]

N = 12

n_o = 0.51

QDHW_{total} = 394480 [MJ]

T = 298 [K]

V_{tank} = 20000 [L]

Arrays Table: Main

	Cons _{month,i} [m ³]	D1 _i	D2 _i	δ _{t,i} [s]	η _{t,i}	f _i	K2 _i	Nmonth _i [day]	Qu _i [MJ]
1	170.5	0.6536	4.416	2.678E+06	0.2243	0.322	1.034	31	11906
2	159.5	0.9685	4.491	2.506E+06	0.2496	0.5307	1.043	29	18360
3	170.5	1.316	4.897	2.678E+06	0.2435	0.7039	1.11	31	25028
4	165	1.293	5.139	2.592E+06	0.2398	0.6809	1.156	30	22492
5	170.5	1.368	5.208	2.678E+06	0.2379	0.7146	1.184	31	23378
6	165	1.858	5.129	2.592E+06	0.225	0.918	1.211	30	27168
7	170.5	2.005	5.568	2.678E+06	0.2147	0.9454	1.302	31	26894
8	170.5	2.009	5.356	2.678E+06	0.2168	0.9562	1.264	31	27880
9	165	1.746	5.285	2.592E+06	0.2272	0.8709	1.228	30	25772
10	170.5	1.186	4.829	2.678E+06	0.2457	0.6398	1.129	31	21385
11	165	0.7953	4.83	2.592E+06	0.2304	0.4023	1.102	30	13842
12	170.5	0.7816	4.534	2.678E+06	0.2372	0.4071	1.049	31	15056

Arrays Table: Main

	QU _{kWh,i} [kWh]	QU _{kWh,A,i} [kWh/m ²]	T _{amb,i} [K]	T _{amb,C,i} [C]	T _{red,i} [K]	T _{red,C,i} [C]	QU _{A,i} [MJ/m ²]	Q _{DHW,i} [MJ]	E _i [MJ/m ²]
1	3307	21.2	280.7	7.7	281	8	76.32	36980	340.2
2	5100	32.69	280	7	281	8	117.7	34594	471.6
3	6952	44.57	281.3	8.3	283	10	160.4	35557	658.8
4	6248	40.05	284.3	11.3	285	12	144.2	33034	601.2
5	6494	41.63	288.9	15.9	287	14	149.9	32713	630
6	7547	48.38	297.3	24.3	290	17	174.2	29593	774
7	7470	47.89	301.9	28.9	293	20	172.4	28446	802.8
8	7744	49.64	300.8	27.8	292	19	178.7	29157	824.4
9	7159	45.89	296.1	23.1	290	17	165.2	29593	727.2
10	5940	38.08	289.5	16.5	286	13	137.1	33424	558
11	3845	24.65	281.9	8.9	283	10	88.73	34410	385.2
12	4182	26.81	279.6	6.6	281	8	96.51	36980	406.8

Calculation of the thermal efficiency, solar fraction and monthly production during the summer for a solar cooling installation with PVT panels and an absorption unit.

General data:

$N_{\text{guests}} = 100$ Capacity (n° of guests) of the hotel.

$N_p = 100$ Number of solar panels installed on the rooftop.

$T_{w,C} = 80$ [C] Temperature required for the water coming from the hybrid panels.

$T_w = T_{w,C} + 273$ [K] Temperature required for the water coming from the hybrid panels in K.

$V_{\text{tank}} = 20000$ [L] Storage tank volume.

$q = 50$ [L/(h*m²)] Nominal flow rate per unit of area of the solar collector.

Thermal data of Ecomesh solar panel:

$A_c = 1.56$ [m²] Collector area of the Ecomesh hybrid panel.

$n_o = 0.51$ Optical efficiency.

$a_1 = 4.93$ [W/m²*K] Thermal losses coefficient, a1.

$a_2 = 0.021$ [W/m²*K²] Thermal losses coefficient, a2.

$\text{coef1} = 0.94$ Coefficient for a double glass cover (TIC).

Capacity = 1.2 [L]

$\text{coef2} = 0.95$ Correction factor collector-heat exchanger (typical value).

Data for Madrid (4* Hotel):

$T_{\text{amb}_C}[1..4] = [24.3, 28.9, 27.8, 23.1]$

$T_{\text{red}_C}[1..4] = [17, 20, 19, 17]$

$E[1..4] = [774, 802.8, 824.4, 727.2]$

$\dot{Q}_g = 102$ [kW] Heat power demand at the generator of the absorption unit.

----- Thermal calculations: F-Chart Method -----

$N = 4$

$T_{\text{amb},i} = T_{\text{amb},C,i} + 273$ for $i = 1$ to N Ambient temperature array in K.

$T_{\text{red},i} = T_{\text{red},C,i} + 273$ for $i = 1$ to N Cold water temperature array in K.

$N_{\text{month}}[1..4] = [30, 31, 31, 30]$

$Q_{g,i} = \dot{Q}_g \cdot 10 \cdot N_{\text{month}_i} \cdot 3.6$ for $i = 1$ to N Monthly thermal energy demand at the generator of the absorption unit, in MJ.

$$\text{coef3} = n_o \cdot \text{coef1} \cdot \text{coef2}$$

$$D1_i = \frac{Np \cdot Ac \cdot \text{coef3} \cdot E_i}{Q_{g,i}} \quad \text{for } i = 1 \text{ to } N$$

$$\delta_{t,i} = N\text{month}_i \cdot 24 \cdot 3600 \quad \text{for } i = 1 \text{ to } N \quad \textit{Total amount of seconds in each month.}$$

$$K1 = \left[\frac{V_{\text{tank}}}{75 \cdot Np \cdot Ac} \right]^{-0.25}$$

$$K2_i = \frac{11.6 + 1.18 \cdot T_{w,C} + 3.86 \cdot T_{\text{red},C,i} - 2.32 \cdot T_{\text{amb},C,i}}{100 - T_{\text{amb},C,i}} \quad \text{for } i = 1 \text{ to } N$$

$$D2_i = \frac{Np \cdot Ac \cdot a_1 \cdot \text{coef2} \cdot [100 - T_{\text{amb},C,i}] \cdot \delta_{t,i} \cdot K1 \cdot K2_i}{Q_{g,i} \cdot 10^6} \quad \text{for } i = 1 \text{ to } N$$

$$f_i = 1.029 \cdot D1_i - 0.065 \cdot D2_i - 0.245 \cdot D1_i^2 + 0.0018 \cdot D2_i^2 + 0.0215 \cdot D1_i^3 \quad \text{for } i = 1 \text{ to } N$$

$$Qu_i = f_i \cdot Q_{g,i} \quad \text{for } i = 1 \text{ to } N \quad \textit{Useful heat produced in a month in MJ.}$$

$$Qu_{A,i} = \frac{Qu_i}{Np \cdot Ac} \quad \text{for } i = 1 \text{ to } N \quad \textit{Useful heat per m}^2 \textit{ produced in a month in MJ.}$$

$$Qu_{kWh,i} = \frac{Qu_i}{3.6} \quad \text{for } i = 1 \text{ to } N \quad \textit{Useful heat produced in a month in kWh.}$$

$$Qu_{kWh,A,i} = \frac{Qu_i}{3.6 \cdot Np \cdot Ac} \quad \text{for } i = 1 \text{ to } N \quad \textit{Useful heat per m}^2 \textit{ produced in a month in kWh.}$$

Thermal efficiency and energy yield:

$$Qu_{\text{total}} = \sum_{i=1}^N [Qu_i]$$

$$Qg_{\text{total}} = \sum_{i=1}^N [Q_{g,i}]$$

$$F = \frac{Qu_{\text{total}}}{Qg_{\text{total}}} \quad \textit{Solar fraction for the summer: fraction of energy covered by the hybrid collectors during this season.}$$

$$\eta_{t,i} = \frac{Qu_i}{E_i \cdot Np \cdot Ac} \quad \text{for } i = 1 \text{ to } N$$

$$E_{\text{total}} = \sum_{i=1}^N [E_i]$$

$$\eta_{t,\text{summer}} = \frac{Qu_{\text{total}}}{E_{\text{total}} \cdot Np \cdot Ac} \quad \textit{Thermal efficiency of the hybrid panels during the summer.}$$

SOLUTION

Unit Settings: SI K kPa kJ mass deg

$$A_c = 1.56 \text{ [m}^2\text{]}$$

$$\text{Capacity} = 1.2 \text{ [L]}$$

$$\text{coef3} = 0.4554 \text{ [W/K-MJ]}$$

$$F = 0.3449 \text{ [:]}$$

$$N_p = 100$$

$$q = 50 \text{ [L/(h}\cdot\text{m}^2\text{)]}$$

$$\dot{Q}_g = 102 \text{ [kW]}$$

$$V_{\text{tank}} = 20000 \text{ [L]}$$

$$a_1 = 4.93 \text{ [W/m}^2\cdot\text{K]}$$

$$\text{coef1} = 0.94$$

$$\eta_{t,\text{summer}} = 0.3166$$

$$K_1 = 0.8746$$

$$N_{\text{guests}} = 100$$

$$Q_{g,\text{total}} = 447984 \text{ [MJ]}$$

$$T_w = 353 \text{ [K]}$$

$$a_2 = 0.021 \text{ [W/m}^2\cdot\text{K}^2\text{]}$$

$$\text{coef2} = 0.95$$

$$E_{\text{total}} = 3128 \text{ [MJ/m}^2\text{]}$$

$$N = 4$$

$$n_o = 0.51$$

$$Q_{u,\text{total}} = 154488 \text{ [MJ]}$$

$$T_{w,C} = 80 \text{ [C]}$$

Calculation of the thermal efficiency, solar fraction and monthly production during the winter for a solar cooling installation with PVT panels and an absorption unit.

General data:

$$N_{\text{guests}} = 100 \text{ Capacity (n}^\circ\text{ of guests) of the hotel.}$$

$$N_p = 100 \text{ Number of solar panels installed on the rooftop.}$$

$$T_{\text{DHW,C}} = 60 \text{ [C] Reference temperature of Domestic Hot Water (DHW).}$$

$$T_{\text{DHW}} = T_{\text{DHW,C}} + 273 \text{ [K] Reference temperature of DHW temperature in K.}$$

$$V_{\text{tank}} = 20000 \text{ [L] Storage tank volume.}$$

$$q = 50 \text{ [L/(h}\cdot\text{m}^2\text{)] Nominal flow rate per unit of area of the solar collector.}$$

Thermal data of Ecomesh solar panel:

$$A_c = 1.56 \text{ [m}^2\text{] Collector area of the Ecomesh hybrid panel.}$$

$$n_o = 0.51 \text{ Optical efficiency.}$$

$$a_1 = 4.93 \text{ [W/m}^2\cdot\text{K] Thermal losses coefficient, a1.}$$

$$a_2 = 0.021 \text{ [W/m}^2\cdot\text{K}^2\text{] Thermal losses coefficient, a2.}$$

$$\text{coef1} = 0.94 \text{ Coefficient for a double glass cover (TIC).}$$

$$\text{Capacity} = 1.2 \text{ [L]}$$

$$\text{coef2} = 0.95 \text{ Correction factor collector-heat exchanger (typical value).}$$

Data for Madrid (4* Hotel):

$$T_{\text{amb_C}}[1..8] = [7.7, 7, 8.3, 11.3, 15.9, 16.5, 8.9, 6.6]$$

$$T_{red_C}[1..8] = [8, 8, 10, 12, 14, 13, 10, 8]$$

$$E[1..8] = [340.2, 471.6, 658.8, 601.2, 630, 558, 385.2, 406.8]$$

$$Cons_{day,L} = 55 \cdot N_{guests} \quad \text{Total daily consumption of DHW in L for the 4* hotel.}$$

$$Cons_{day} = Cons_{day,L} \cdot \left| 0.001 \cdot \frac{m^3}{L} \right| \quad \text{Total daily consumption of DHW in m}^3.$$

----- Thermal calculations: F-Chart Method -----

$$N = 8$$

$$T_{amb,i} = T_{amb,C,i} + 273 \quad \text{for } i = 1 \text{ to } N \quad \text{Ambient temperature array in K.}$$

$$T_{red,i} = T_{red,C,i} + 273 \quad \text{for } i = 1 \text{ to } N \quad \text{Cold water temperature array in K.}$$

$$N_{month}[1..8] = [31, 29, 31, 30, 31, 31, 30, 31]$$

$$Cons_{month,i} = Cons_{day} \cdot N_{month,i} \quad \text{for } i = 1 \text{ to } N \quad \text{Monthly DHW consumption for the hotel in m}^3.$$

$$T = 298 \quad [K]$$

$$P = 101.325 \quad [kPa]$$

$$\rho = \rho[\text{water}, T = T, P = P]$$

$$cp = Cp[\text{water}, T = T, P = P]$$

$$Q_{DHW,i} = \frac{\rho \cdot Cons_{month,i} \cdot cp \cdot [T_{DHW} - T_{red,i}]}{10^3} \quad \text{for } i = 1 \text{ to } N \quad \text{Monthly thermal energy demand of DHW in MJ.}$$

$$coef3 = n_o \cdot coef1 \cdot coef2$$

$$D1_i = \frac{Np \cdot Ac \cdot coef3 \cdot E_i}{Q_{DHW,i}} \quad \text{for } i = 1 \text{ to } N$$

$$\delta_{t,i} = N_{month,i} \cdot 24 \cdot 3600 \quad \text{for } i = 1 \text{ to } N \quad \text{Total amount of seconds in each month.}$$

$$K1 = \left[\frac{V_{tank}}{75 \cdot Np \cdot Ac} \right]^{-0.25}$$

$$K2_i = \frac{11.6 + 1.18 \cdot T_{DHW,C} + 3.86 \cdot T_{red,C,i} - 2.32 \cdot T_{amb,C,i}}{100 - T_{amb,C,i}} \quad \text{for } i = 1 \text{ to } N$$

$$D2_i = \frac{Np \cdot Ac \cdot a_1 \cdot coef2 \cdot [100 - T_{amb,C,i}] \cdot \delta_{t,i} \cdot K1 \cdot K2_i}{Q_{DHW,i} \cdot 10^6} \quad \text{for } i = 1 \text{ to } N$$

$$f_i = 1.029 \cdot D1_i - 0.065 \cdot D2_i - 0.245 \cdot D1_i^2 + 0.0018 \cdot D2_i^2 + 0.0215 \cdot D1_i^3 \quad \text{for } i = 1 \text{ to } N$$

$$Qu_i = f_i \cdot Q_{DHW,i} \quad \text{for } i = 1 \text{ to } N \quad \text{Useful heat produced in a month in MJ.}$$

$$Qu_{A,i} = \frac{Qu_i}{Np \cdot Ac} \quad \text{for } i = 1 \text{ to } N \quad \text{Useful heat per m}^2 \text{ produced in a month in MJ.}$$

$$Qu_{kWh,i} = \frac{Qu_i}{3.6} \quad \text{for } i = 1 \text{ to } N \quad \text{Useful heat produced in a month in kWh.}$$

$$Qu_{kWh,A,i} = \frac{Qu_i}{3.6 \cdot Np \cdot Ac} \quad \text{for } i = 1 \text{ to } N \quad \text{Useful heat per } m^2 \text{ produced in a month in kWh.}$$

Thermal efficiency and energy yield:

$$Qu_{total} = \sum_{i=1}^N [Qu_i]$$

$$QDHW_{total} = \sum_{i=1}^N [Q_{DHW,i}]$$

$$F = \frac{Qu_{total}}{QDHW_{total}} \quad \text{Solar fraction for the winter: fraction of energy covered by the hybrid collectors during this season.}$$

$$\eta_{t,i} = \frac{Qu_i}{E_i \cdot Np \cdot Ac} \quad \text{for } i = 1 \text{ to } N$$

$$E_{total} = \sum_{i=1}^N [E_i]$$

$$\eta_{t,winter} = \frac{Qu_{total}}{E_{total} \cdot Np \cdot Ac} \quad \text{Thermal efficiency of the hybrid panels during the winter.}$$

SOLUTION

Unit Settings: SI K kPa kJ mass deg

Ac = 1.56 [m²]

Capacity = 1.2 [L]

coef3 = 0.4554 [W/K-MJ]

cp = 4.183 [kJ/kg-K]

a1 = 4.93 [W/m²*K]

coef1 = 0.94

Consday = 5.5 [m³/day]

$\eta_{t,winter}$ = 0.2396

a2 = 0.021 [W/m²*K²]

coef2 = 0.95

Consday,L = 5500 [L/day]

Etotal = 4052 [MJ/m²]

F = 0.5454 [-]

Np = 100

P = 101.3 [kPa]

Qu_{total} = 151447 [MJ]

T_{DHW} = 333 [K]

K1 = 0.8746

N_{guests} = 100

q = 50 [L/(h*m²)]

ρ = 997.1 [kg/m³]

T_{DHW,c} = 60 [C]

N = 8

n_o = 0.51

QDHW_{total} = 277691 [MJ]

T = 298 [K]

V_{tank} = 20000 [L]

A.2 The vapour compression cycle

- Summer mode:

-----Cooling cycle by conventional vapour compression using refrigerant R410A-----

Data:

$$Q_r = 64 \text{ [kW]}$$

$$T_3 = 275 \text{ [K]}$$

$$T_1 = 318 \text{ [K]}$$

$$x_3 = 1 \text{ Saturated vapor}$$

$$x_1 = 0 \text{ Saturated liquid}$$

Equations:

State 1:

$$P_1 = P \text{ [R410A , } T = T_1, x = x_1 \text{] High pressure}$$

$$h_1 = h \text{ [R410A , } P = P_1, x = x_1 \text{]}$$

$$s_1 = s \text{ [R410A , } P = P_1, x = x_1 \text{]}$$

State 3:

$$P_3 = P \text{ [R410A , } T = T_3, x = x_3 \text{] Low pressure}$$

$$h_3 = h \text{ [R410A , } P = P_3, x = x_3 \text{]}$$

$$s_3 = s \text{ [R410A , } P = P_3, x = x_3 \text{]}$$

State 2:

$$P_2 = P_3$$

$$h_2 = h_1$$

$$s_2 = s \text{ [R410A , } P = P_2, h = h_2 \text{]}$$

$$T_2 = T \text{ [R410A , } P = P_2, h = h_2 \text{]}$$

State 4:

$$P_4 = P_1$$

$$h_4 = h \text{ [R410A , } P = P_4, s = s_4 \text{]}$$

$$s_4 = s_3$$

$$T_4 = T \text{ [R410A , } P = P_4, h = h_4 \text{] Output temperature of the compressor}$$

$$Q_r = \dot{m}_r \cdot \left[\frac{h_3 - h_2}{1000} \right] \quad \text{Calculation of mass flow rate of refrigerant, in kg/s.}$$

$$W_c = \dot{m}_r \cdot \left[\frac{h_4 - h_3}{1000} \right] \quad \text{Power of the compressor, in kW.}$$

$$EER = \frac{Q_r}{W_c} \quad \text{Energy Efficiency Ratio}$$

$$Q_c = \dot{m}_r \cdot \left[\frac{h_4 - h_1}{1000} \right] \quad \text{Heat released in the condenser, to the sink or cooling water.}$$

$$r = \frac{P_1}{P_3} \quad \text{Compression ratio}$$

$$EER_{\text{Carnot}} = \frac{T_3}{T_1 - T_3} \quad \text{EER of the equivalent Carnot cycle, with the same evaporation and condensation temperatures.}$$

SOLUTION

Unit Settings: SI K kPa J mass deg

$$EER = 4.602$$

$$EER_{\text{Carnot}} = 6.395$$

$$\dot{m}_r = 0.437 \text{ [kg/s]}$$

$$Q_c = 77.91 \text{ [kW]}$$

$$Q_r = 64 \text{ [kW]}$$

$$r = 3.219$$

$$W_c = 13.91 \text{ [kW]}$$

- Winter mode:

-----Heating cycle by conventional vapour compression using refrigerant R410A-----

Data:

$$Q_h = 72 \text{ [kW]}$$

$$T_3 = 275 \text{ [K]}$$

$$T_1 = 318 \text{ [K]}$$

$$x_3 = 1 \quad \text{Saturated vapor}$$

$$x_1 = 0 \quad \text{Saturated liquid}$$

Equations:

State 1:

$$P_1 = P \text{ [R410A, } T = T_1, x = x_1 \text{]} \quad \text{High pressure}$$

$$h_1 = h \text{ [R410A, } P = P_1, x = x_1 \text{]}$$

$$s_1 = s [R410A, P = P_1, x = x_1]$$

State 3:

$$P_3 = P [R410A, T = T_3, x = x_3] \text{ Low pressure}$$

$$h_3 = h [R410A, P = P_3, x = x_3]$$

$$s_3 = s [R410A, P = P_3, x = x_3]$$

State 2:

$$P_2 = P_3$$

$$h_2 = h_1$$

$$s_2 = s [R410A, P = P_2, h = h_2]$$

$$T_2 = T [R410A, P = P_2, h = h_2]$$

State 4:

$$P_4 = P_1$$

$$h_4 = h [R410A, P = P_4, s = s_4]$$

$$s_4 = s_3$$

$$T_4 = T [R410A, P = P_4, h = h_4] \text{ Output temperature of the compressor}$$

$$Q_h = m_r \cdot \left[\frac{h_4 - h_1}{1000} \right] \text{ Calculation of mass flow rate of refrigerant, in kg/s.}$$

$$W_c = m_r \cdot \left[\frac{h_4 - h_3}{1000} \right] \text{ Power of the compressor, in kW.}$$

$$COP = \frac{Q_h}{W_c} \text{ Coefficient of performance}$$

$$Q_e = m_r \cdot \left[\frac{h_3 - h_2}{1000} \right] \text{ Heat absorbed by the evaporator from the cold source, in kW.}$$

$$r = \frac{P_1}{P_3} \text{ Compression ratio}$$

$$COP_{Carnot} = \frac{T_3}{T_1 - T_3} \text{ COP of the equivalent Carnot cycle, with the same evaporation and condensation temperatures.}$$

SOLUTION

Unit Settings: SI K kPa J mass deg

$$COP = 5.602$$

$$Q_e = 59.15 \text{ [kW]}$$

$$W_c = 12.85 \text{ [kW]}$$

$$COP_{Carnot} = 6.395$$

$$Q_h = 72 \text{ [kW]}$$

$$m_r = 0.4038 \text{ [kg/s]}$$

$$r = 3.219$$

A.3 Absorption cooling cycle

----- ABSORPTION COOLING CYCLE -----

Water-LiBr absorption refrigeration system to provide 64 kW of refrigeration. The generator is heated by flat-plate solar collectors:

Determination of the EER, absorbent and refrigerant flow rates and heat input required at the generator.

DATA:

$$Q_r = 64 \text{ [kW]}$$

$$T_{\text{evap}} = 3 \text{ [C]} \text{ Evaporator temperature.}$$

$$T_{\text{ab}} = 34 \text{ [C]} \text{ Absorber outlet temperature.}$$

$$T_{\text{cond}} = 36 \text{ [C]} \text{ Condenser temperature.}$$

$$T_{\text{gen}} = 88 \text{ [C]} \text{ Temperature level at the generator.}$$

$$\delta T_{\text{HX}} = 6 \text{ [C]} \text{ Approach at the low-temperature end of the liquid heat exchanger.}$$

Definition of thermodynamic variables:

State 8:

$$x_8 = 0 \text{ Saturated liquid in the condenser}$$

$$T_8 = T_{\text{cond}}$$

$$P_8 = P_{\text{sat}} [\text{water}, T = T_8]$$

$$h_8 = h [\text{water}, P = P_8, x = x_8]$$

State 7:

$$T_7 = T_{\text{gen}}$$

$$P_7 = P_8 \text{ High pressure side.}$$

$$h_7 = h [\text{water}, P = P_7, T = T_7]$$

State 10:

$$x_{10} = 1 \quad \text{Saturated vapour in the evaporator}$$

$$T_{10} = T_{\text{evap}}$$

$$P_{10} = P_{\text{sat}} [\text{water}, T = T_{10}]$$

$$h_{10} = h [\text{water}, P = P_{10}, x = x_{10}]$$

State 9:

$$P_9 = P_{10} \quad \text{Low pressure side.}$$

$$h_9 = h_8 \quad \text{Isoenthalpic expansion valve}$$

$$T_9 = T [\text{water}, P = P_9, h = h_9]$$

State 4:

$$T_4 = T_{\text{ab}}$$

$$P_4 = P_{10} \quad \text{Low pressure side.}$$

$$x_s = x_{\text{LiBrH}_2\text{O}} [T_4, P_4] \quad \text{Concentration of LiBr in refrigerant-absorbent solution, at } T_4 \text{ and } P_4.$$

$$h_4 = h_{\text{LiBrH}_2\text{O}} [T_4, x_s] \quad \text{Specific enthalpy for LiBr-water solution at } T_4 \text{ (per kg of solution).}$$

State 5:

$$T_5 = T_4 \quad \text{Neglecting the pump work.}$$

$$P_5 = P_8 \quad \text{High pressure side.}$$

$$h_5 = h_4 \quad \text{Neglecting the pump work.}$$

State 1:

$$T_1 = T_{\text{gen}}$$

$$P_1 = P_8 \quad \text{High pressure side.}$$

$$x_{\text{ab}} = x_{\text{LiBrH}_2\text{O}} [T_1, P_1] \quad \text{Concentration of LiBr in absorbent solution, at } T_1 \text{ and } P_1.$$

$$h_1 = h_{\text{LiBrH}_2\text{O}} [T_1, x_{\text{ab}}] \quad \text{Specific enthalpy for the absorbent solution at } T_1 \text{ (per kg of solution).}$$

State 2:

$$T_2 = T_5 + \delta T_{\text{HX}}$$

$$P_2 = P_1 \quad \text{High pressure side.}$$

$$h_2 = h_{\text{LiBrH}_2\text{O}} [T_2, x_{\text{ab}}] \quad \text{Specific enthalpy for the absorbent solution at } T_2 \text{ (per kg of solution).}$$

State 3:

$$T_3 = T_2$$

$$P_3 = P_{10} \quad \text{Low pressure side.}$$

$$h_3 = h_2$$

State 6:

$$P_6 = P_8 \quad \text{High pressure side.}$$

$$T_6 = T_{\text{LiBrH}_2\text{O}} [P_6, x_s] \quad \text{Temperature of the LiBr-water solution at } P_6 \text{ and } x_s \text{ (LiBr mass fraction).}$$

Flow rate of refrigerant:

$$Q_r = m_r \cdot [h_{10} - h_9]$$

$$m_7 = m_r$$

Mass balance equations:

$$m_6 = m_1 + m_7 \quad \text{Total material balance on the generator.}$$

$$m_6 \cdot x_s = m_1 \cdot x_{ab} \quad \text{Partial mass balance on LiBr.}$$

h_6 may be found from an energy balance at the heat exchanger:

$$m_5 = m_6$$

$$m_2 = m_1$$

$$m_5 \cdot h_5 + m_1 \cdot h_1 = m_2 \cdot h_2 + m_6 \cdot h_6$$

Heat supplied to the generator for the cycle to start working:

$$Q_g = m_7 \cdot h_7 + m_1 \cdot h_1 - m_6 \cdot h_6$$

$$\text{EER} = \frac{Q_r}{Q_g} \quad \text{Coefficient of Performance.}$$

Heat transfer in the other 3 heat exchangers:

$$Q_{12} = m_1 \cdot [h_1 - h_2] \quad \text{Rate of heat transferred from the absorbent stream to the refrigerant-absorbent stream.}$$

$$Q_{78} = m_7 \cdot [h_7 - h_8] \quad \text{Rate of heat transfer rejected to the environment at the condenser.}$$

$$Q_a = Q_{78} - Q_g - Q_r \quad \text{Overall heat balance on the system to obtain the rate of heat removal from the absorber.}$$

SOLUTION

Unit Settings: SI C kPa kJ mass deg

$$\delta T_{\text{HX}} = 6 \text{ [C]}$$

$$m_2 = 0.2052 \text{ [kg/s]}$$

$$m_7 = 0.02717 \text{ [kg/s]}$$

$$Q_g = 81.23 \text{ [kW]}$$

$$Q_{78} = 68.31 \text{ [kW]}$$

$$T_{\text{evap}} = 3 \text{ [C]}$$

$$x_s = 0.5595$$

$$\text{EER} = 0.7879$$

$$m_5 = 0.2324 \text{ [kg/s]}$$

$$m_r = 0.02717 \text{ [kg/s]}$$

$$Q_r = 64 \text{ [kW]}$$

$$T_{\text{ab}} = 34 \text{ [C]}$$

$$T_{\text{gen}} = 88 \text{ [C]}$$

$$m_1 = 0.2052 \text{ [kg/s]}$$

$$m_6 = 0.2324 \text{ [kg/s]}$$

$$Q_a = -76.92 \text{ [kW]}$$

$$Q_{12} = 17.88 \text{ [kW]}$$

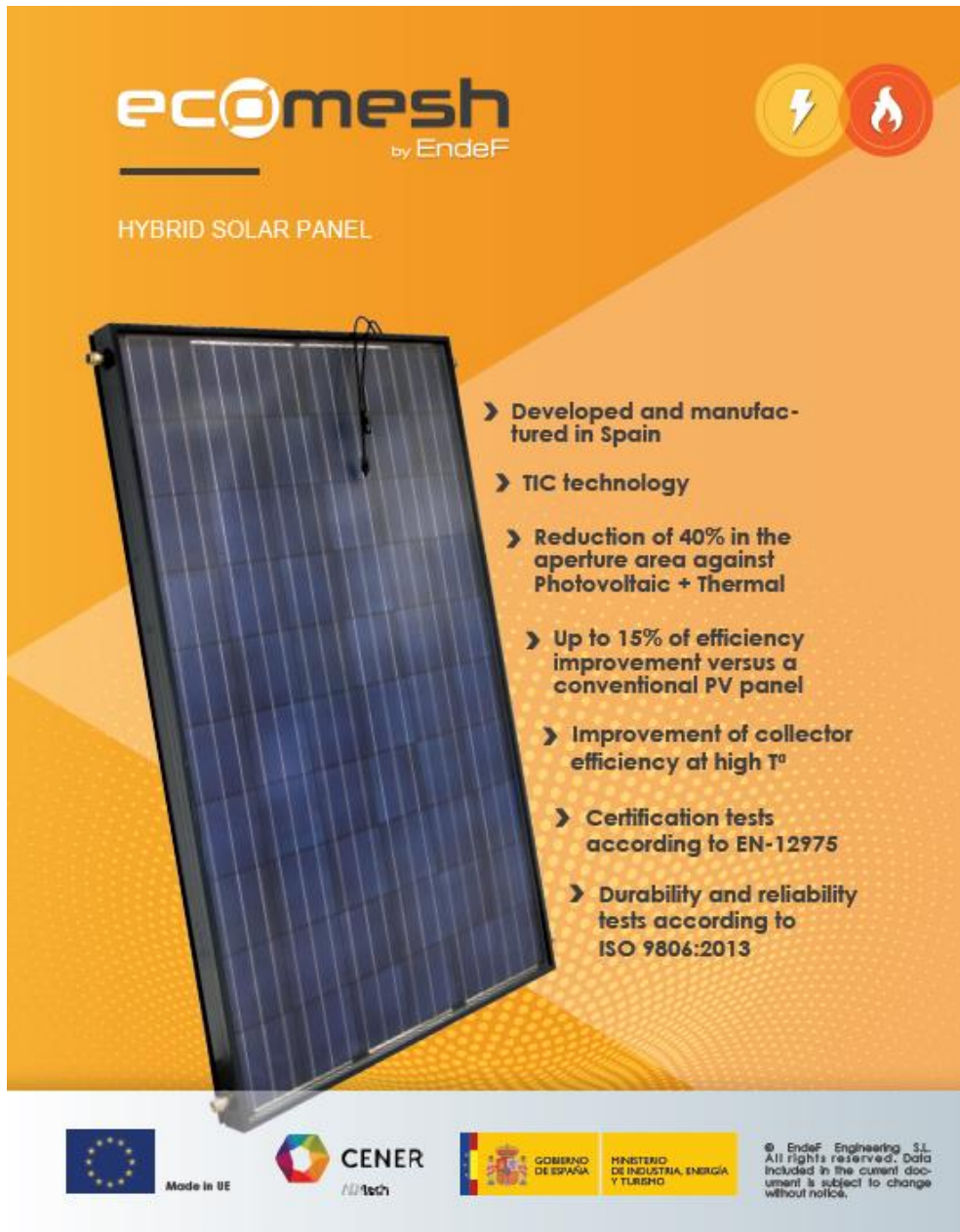
$$T_{\text{cond}} = 36 \text{ [C]}$$

$$x_{\text{ab}} = 0.6335$$

Annex 2. Technical sheets

This annex provides the technical sheets of the equipment considered in the analysis and comparison of the four case studies. It shows the characteristics and technical parameters of the solar panels from the company EndeF, both the hybrid and the PV.

Ecomesh hybrid solar panel:



The technical sheet for the Ecomesh Hybrid Solar Panel features a blue and black panel image on the left. The background is orange with a grid pattern. The logo 'ecomesh by EndeF' is at the top left, and two circular icons (lightning bolt and flame) are at the top right. The text 'HYBRID SOLAR PANEL' is centered below the logo. A list of seven bullet points describes the panel's features. At the bottom, there are logos for the European Union, CENER, the Spanish Government, and the Ministry of Industry, Energy, and Tourism, along with a copyright notice for EndeF Engineering S.L.

ecomesh
by EndeF

HYBRID SOLAR PANEL

- › Developed and manufactured in Spain
- › TIC technology
- › Reduction of 40% in the aperture area against Photovoltaic + Thermal
- › Up to 15% of efficiency improvement versus a conventional PV panel
- › Improvement of collector efficiency at high T°
- › Certification tests according to EN-12975
- › Durability and reliability tests according to ISO 9806:2013

Made in UE

CENER

GOBIERNO DE ESPAÑA

MINISTERIO DE INDUSTRIA, ENERGÍA Y TURISMO

© EndeF Engineering S.L. All rights reserved. Data included in the current document is subject to change without notice.

(+34) 976 365 811
www.ecomesh.es
info@endef.com

ecomesh
by EndeF

General features

Cell size	156x156mm
Cell number	60
Front glass	3.2mm tempered glass
Weight (empty)	45.8 kg
Dimensions (LxWxT)	1645 x 978 x 93(+25)mm
Junction box	IP65 / IP67 available
Cable length	1000mm
Cable section	4mm ²
Diodes number	3
Connectors	MC4 compatible
Frame	Aluminium

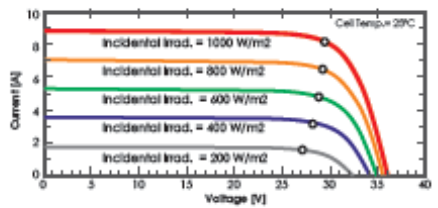
Electric specifications

Values tested under Standard Conditions STC (AM 1.5, irradiance 1000 W/m², Cell temperature 25°C)

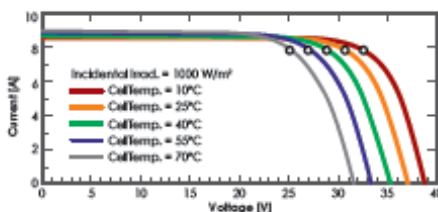
Nominal Power (P _{max})	270 Wp
Nominal Voltage (V _{mp})	31.65 V
Nominal Current (I _{mp})	8.06 A
Open circuit voltage (V _{oc})	38.58 V
Short circuit current (I _{sc})	9.06 A
Output Tolerance	0 + 4.99 Wp
Module Efficiency	16.4%
Voltage temp. coefficient	-0.37%/K
Current temp. coefficient	+0.06%/K
Power temp. coefficient	-0.47%/K
Maximum system voltage	DC 1000V (TU V)
Working temperature	-40°C / +85°C
Maximum reverse current	1.5A
Protection degree IP	IP65
Safety class	II

Ecomesh panels are distinguished by the incorporation of the TIC technology, which improves the global efficiency of the panel by recovering the heat lost through the frontal face. This technology has been validated, patented, tested and installed by EndeF Engineering.

I-V Curve according to incidental irradiance



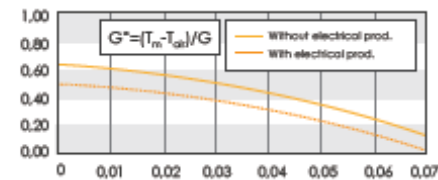
I-V Curve according to temperature



Thermal specifications

Maximum pressure	10 bar
Absorber	Copper
Fluid Volume	1,2 L
Optical performance (η _o)	0.51
Heat loss coefficient, a1	4.93 W/m ² K
Heat loss coefficient, a2	0.021 W/m ² K ²
Pressure loss	0.04 bar

Thermal efficiency



Made in UE



CENER
AD Tech



GOBIERNO DE ESPAÑA

MINISTERIO DE INDUSTRIA, ENERGIA Y TURISMO

© EndeF Engineering S.L. All rights reserved. Data included in the current document is subject to change without notice.

(+34) 976 345 811
www.ecomesh.es
info@endef.com

ecomesh
by EndeF

Ecomesh photovoltaic solar panel:

The advertisement features three solar panels with different backsheet colors: transparent, white, and black. The background is orange with a lightning bolt icon in the top right. The text includes the brand name 'ecomesh by EndeF', the product name 'PHOTOVOLTAIC PANEL 270W', and various certification logos at the bottom.

ecomesh
by EndeF

PHOTOVOLTAIC PANEL 270W

TRANSPARENT BACKSHEET
WHITE BACKSHEET
BLACK BACKSHEET

©EndeF Engineering S.L.R. All rights reserved.
Data included in the current document is subject to change without notice.

(+34) 976 365 811
www.ecomesh.es
info@endef.com

ecomesh
by EndeF

General features

Cell size	156x156mm
Cell number	60
Front glass	3.2mm tempered glass
Weight	19kg
Dimensions (LxWxT)	1640x992x40mm
Junction box	IP65 / IP67 disponibles
Cable length	1000mm
Cable section	4mm ²
Diodes number	3
Connectors	MC4 compatible
Frame	Anodised aluminium

Electric specifications

Values tested under Standard Conditions STC (AM 1.5, Irradiance 1000 W/m², Cell temperature 25°C)

Nominal Power (P _{max})	270 Wp
Nominal Voltage (V _{mp})	31.65 V
Nominal Current (I _{mp})	8.40 A
Open circuit voltage(V _{oc})	38.58 V
Short circuit current	9.06 A
Output Tolerance	0 + 4.99 Wp
Module efficiency	16.4%

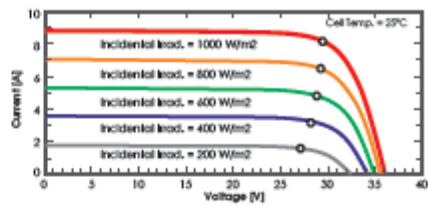
Maximum system voltage	DC 1000V [TUV]
Operating cell temperature	-40°C / +85°C
Maximum reverse current	1.5A
Máximum wind/snow load	2400Pa/5400Pa
Protection degree IP	IP65
Safety class	II

Voltage temp. coefficient	-0.37%/K
Current temp. coefficient	+0.06%/K
Power temp. coefficient	-0.47%/K

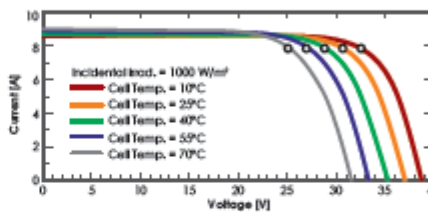
Packing information

Container	20' GP	40' GP	40' HQ
Pallets per container	12	28	28
Units per container	300	700	770

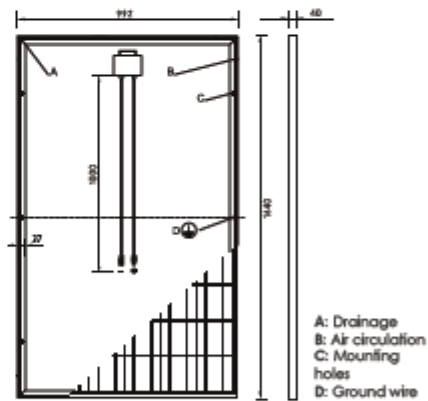
I-V Curve according to incidental irradiance



I-V Curve according to temperature



Dimensions



©EndeF Engineering S.L. All rights reserved.
Data included in the current document is
subject to change without notice

(+34) 976 365 811
www.ecomesh.es
info@endef.com

ecomesh
by EndeF

Annex 3. The company, EndeF Engineering S.L.

This annex provides a more extensive description of the Spanish company, EndeF Engineering S.L., with which this master thesis has been developed. It gives a general overview of the main focus and business approach of the company to continue with its development and expansion throughout the years and finally, highlights the achieved prizes, awards and international recognition as an innovative solar energy company.

EndeF Engineering S.L. is a technological and engineering company that provides innovative solutions in the renewable energy sector. Founded in June 2012, it is the first Spanish company specialised in hybrid solar panels. It is one of the founder companies of the cluster “Aragón Energética-Smart Solutions”.

EndeF Engineering has developed along three main lines: engineering, manufacturing and installation. The first consists on the development of new products such as the Ecomesh hybrid solar panels, installation projects development, Research and Development (R&D), patents and trainings. The manufacturing division is focused on the Ecomesh solar panels although new equipment prototypes are also produced to be tested before entering the market. The installations division carries out renewable energies-integration projects in buildings: biomass, solar energy, heating systems, etc.

The three main lines of the company were enlarged and two more areas or departments were developed: R&D and monitorization. The R&D department coordinates the innovation activities aimed to develop and improve the technical process. This has led the company to take part in national and European research projects, publish scientific papers, patents, etc. Although the innovative approach of the company is quite recent, during the six years of R&D, all its activity has been focused on the development of new products and innovative solutions within the solar energy sector. Some examples are the new manufacturing line of Ecomesh hybrid solar panels, the development of solar passive heating system prototypes or the building integrated photovoltaics technology, among others. The monitorization line, recently incorporated to the company, complements the rest of departments developing electronic devices for the hybrid solar installations and improving the monitoring and control of energy consumption and production in these installations.

EndeF Engineering is a solar technology company with a strong innovation approach and a large capacity to develop new products in Spain such as the hybrid solar panels. With this product, the company took part in *Galería de Innovación de Genera 2014* and it has been working since then to successfully introduce it in the market, controlling the quality of every production stage, from its design to the installation. The company has received several prizes for its innovative work, such as the *Entrepreneurs Fund Repsol 2013*, *Concurso IDEA 2014* or the *KIC Innoenergy Iberia Award 2014*.

References

- [1] A. Ghafoor and A. Munir, "Worldwide overview of solar thermal cooling technologies," *Renew. Sustain. Energy Rev.*, pp. 763–774, 2015.
- [2] J. P. Praene, O. Marc, F. Lucas, and F. Miranville, "Simulation and experimental investigation of solar absorption cooling system in Reunion Island," *Appl. Energy*, vol. 88, no. 3, pp. 831–839, 2011.
- [3] International Energy Agency (IEA) and M. Beerepoot (lead author), "Technology Roadmap: Solar Heating and Cooling," *Int. Energy Agency*, p. 50, 2012.
- [4] M. Alobaid, B. Hughes, J. K. Calautit, D. O'Connor, and A. Heyes, "A review of solar driven absorption cooling with photovoltaic thermal systems," *Renew. Sustain. Energy Rev.*, vol. 76, no. May 2016, pp. 728–742, 2017.
- [5] A. Zervos and C. Lins, "Renewables 2016, Global status report," Paris, 2016.
- [6] N. Fumo, V. Bortone, and J. C. Zambrano, "Comparative Analysis of Solar Thermal Cooling and Solar Photovoltaic Cooling Systems," *J. Sol. Energy Eng.*, vol. 135, no. 2, p. 6, 2012.
- [7] I. Sarbu and C. Sebarchievici, "Review of solar refrigeration and cooling systems," *Energy Build.*, pp. 286–297, 2013.
- [8] European Commission, "Green Paper. A European strategy for sustainable, competitive and secure energy," *COM(2006) 105 Final*, pp. 1–20, 2006.
- [9] H. Z. Hassan and A. A. Mohamad, "A review on solar cold production through absorption technology," *Renew. Sustain. Energy Rev.*, vol. 16, no. 7, pp. 5331–5348, Sep. 2012.
- [10] A. I. Zamfir, "Management of renewable energy and regional development: European experiences and steps forward," *Theor. Empir. Res. Urban Manag.*, vol. 6, no. 3, pp. 35–42, 2011.
- [11] A. Rossetti, E. Paci, and G. Alimonti, "Analyse expérimentale de la performance d'une installation frigorifique solaire à moyenne température," *Int. J. Refrig.*, pp. 264–273, 2017.
- [12] B. Choudhury, P. K. Chatterjee, and J. P. Sarkar, "Review paper on solar-powered air-conditioning through adsorption route," *Renew. Sustain. Energy Rev.*, vol. 14, no. 8, pp. 2189–2195, Oct. 2010.
- [13] M. Soussi, M. Balghouthi, A. Guizani, and C. Bouden, "Model performance assessment and experimental analysis of a solar assisted cooling system," *Sol. Energy*, pp. 43–62, 2017.
- [14] G. K. Singh, "Solar power generation by PV (photovoltaic) technology: A review," *Energy*, vol. 53, pp. 1–13, 2013.
- [15] M. M. Islam, A. K. Pandey, M. Hasanuzzaman, and N. A. Rahim, "Recent progresses and achievements in photovoltaic-phase change material technology: A review with special treatment on photovoltaic thermal-phase change material systems," *Energy Convers. Manag.*, vol. 126, pp. 177–204, 2016.
- [16] J. Loureiro, "Solar Cell Fundamentals," Lisboa, 2017.

- [17] The German Energy Society, Ed., *Planning and installing Photovoltaic Systems. A guide for installers, architects and engineers.*, 2nd Ed. London: Earthscan, 2008.
- [18] A. Luque and S. Hegedus, *Handbook of Photovoltaic Science and Engineering*. Wiley, 2003.
- [19] "Earth Policy Institute." [Online]. Available: www.earth-policy.org.
- [20] K. Saha, *Planning and installing Solar Thermal Systems: a guide for installers, architects and engineers*, 2nd Ed. London: Earthscan, 2010.
- [21] J. M. García de María and M. Camarasa Rius, "Apuntes de Energía Solar Térmica.," Madrid, España: Universidad Politécnica de Madrid (UPM), Escuela Técnica Superior de Ingenieros Industriales (ETSII), pp. 1–21.
- [22] J. A. Duffie and W. A. Beckman, *Solar Engineering of Thermal Processes.*, 4th Ed. University of Wisconsin, Madison: Wiley, 2013.
- [23] Instituto para la Diversificación y Ahorro de la Energía (IDAE), "Pliego de Condiciones Técnicas de Instalaciones de Baja Temperatura.," Madrid, España, 2009.
- [24] R. Simón Allué, "Hybrid Solar technologies. Sustainable Energy Management.," 2017.
- [25] W. Weiss and M. Spork-Dur, "Solar Heat worldwide. Global Market Development and Trends in 2017. Detailed Market Figures 2016," Gleisdorf, Austria., 2018.
- [26] J.-C. Hadorn, *Solar and Heat Pump Systems for Residential Buildings*. Wiley, 2015.
- [27] M. Lämmle, A. Oliva, M. Hermann, K. Kramer, and W. Kramer, "PVT collector technologies in solar thermal systems: A systematic assessment of electrical and thermal yields with the novel characteristic temperature approach," *Sol. Energy*, vol. 155, pp. 867–879, 2017.
- [28] M. Bakker, H. A. Zondag, M. J. Elswijk, K. J. Strootman, and M. J. M. Jong, "Performance and costs of a roof-sized PV/thermal array combined with a ground coupled heat pump," *Sol. Energy*, vol. 78, no. 2, pp. 331–339, 2005.
- [29] P. A. Domínguez, "Proyecto Fin de Carrera. 'Software de cálculo para el diseño de instalaciones solares con captadores híbridos'.," Universidad de Zaragoza, 2015.
- [30] EndeF Engineering S.L., "Panel solar híbrido Ecomesh." [Online]. Available: www.ecomesh.es.
- [31] "EndeF Engineering S.L." [Online]. Available: www.endef.com.
- [32] Ministerio de Fomento (Gobierno de España), *Documento Básico HE. Ahorro de energía (Código Técnico de la Edificación)*. España: Secretaría de Estado de Infraestructuras, Transporte y Vivienda. Dirección general de Arquitectura, Vivienda y Suelo., 2017, pp. 1–77.
- [33] D. Y. Goswami, F. Kreith, and J. F. Kreider, *Principles of Solar Engineering*, 2nd Ed. Taylor & Francis, 2000.
- [34] M. Zogg, "History of Heat Pumps," Oberburg, Switzerland, 2008.
- [35] R. Radermacher and Y. Hwang, *Vapor compression heat pumps with refrigerant mixtures*. Boca Raton: Taylor & Francis, 2005.
- [36] Soliclíma, "Aeroterminia-Bomba de calor." [Online]. Available: <https://www.soliclíma.es/bomba-de-calor>.
- [37] K. Janani Gamage, "Numerical Methodology for Feasibility Analysis of Ground Source Heat Pumps," Middle East Technical University Northern Cyprus Campus, 2014.
- [38] "General Training Air conditioning II-Module 7: Heat pumps," New York, U.S.A., 1991.

- [39] C. Wemhoener, R. Dott, and T. Afjei, "Heating and Cooling in Low Energy Houses - Results of the International Research Project IEA HPP Annex 32," no. October, pp. 1–12, 2010.
- [40] M. Miara, D. Gunther, T. Kramer, T. Oltersdorf, and J. Wapler, "Wärmepumpen Effizienz – Messtechnische Untersuchung von Wärmepumpenanlagen zur Analyse und Bewertung der Effizienz im realen Betrieb," 2011.
- [41] I. Wyssen, L. Gasser, and B. Wellig, "Effiziente Niederhub-Wärmepumpen und -Klimakälteanlagen. News aus der Wärmepumpen-Forschung – 19. Tagung des BFE-Forschungsprogramms 'Wärmepumpen und Kälte,'" pp. 22–35, 2013.
- [42] P. Srihirin, S. Aphornratana, and S. Chungpaibulpatana, "A review of absorption refrigeration technologies," *Renew. Sustain. Energy Rev.*, vol. 5, no. 4, pp. 343–372, 2000.
- [43] A. Allouhi, T. Kousksou, A. Jamil, P. Bruel, Y. Mourad, and Y. Zeraouli, "Solar driven cooling systems: An updated review," *Renewable and Sustainable Energy Reviews*. pp. 159–181, 2015.
- [44] Robert A. Parsons (ASHRAE Handbook Editor), *ASHRAE Fundamental Handbook*. Frank M. Coda, 1999.
- [45] F. de' Rossi, R. Mastrullo, and P. Mazzei, "Working fluids thermodynamic behavior for vapor compression cycles," *Appl. Energy*, vol. 38, no. 3, pp. 163–180, Jan. 1991.
- [46] K. R. Ullah, R. Saidur, H. W. Ping, R. K. Akikur, and N. H. Shuvo, "A review of solar thermal refrigeration and cooling methods," *Renew. Sustain. Energy Rev.*, vol. 24, pp. 499–513, 2013.
- [47] A. Aliane, S. Abboudi, C. Seladji, and B. Guendouz, "An illustrated review on solar absorption cooling experimental studies," *Renewable and Sustainable Energy Reviews*. pp. 443–458, 2016.
- [48] "HVAC Systems and equipment," in *ASHRAE Handbook*, Atlanta: American Society of Heating, Refrigerating and Air Conditioning Engineers, 2012.
- [49] H. Moser, E. Podesser, D. Mugnier, and L. Reinholdt, "Task 38 Solar Air-Conditioning and Refrigeration. Market Available Components for Systems for Solar Heating and Cooling with a Cooling Capacity < 20kW," *Sol. Heat. Cool. Program. (SHC)*, IEA., no. November, pp. 1–44, 2009.
- [50] R. E. Critoph, "Rapid cycling solar/biomass powered adsorption refrigeration system," *Renew. Energy*, vol. 16, no. 1–4, pp. 673–678, Jan. 1999.
- [51] C. Infante Ferreira and D. S. Kim, "Techno-economic review of solar cooling technologies based on location-specific data," *International Journal of Refrigeration*. pp. 23–37, 2014.
- [52] A. Sapienza, S. Santamaria, A. Frazzica, and A. Freni, "Influence of the management strategy and operating conditions on the performance of an adsorption chiller," *Energy*, vol. 36, no. 9, pp. 5532–5538, 2011.
- [53] D. C. Wang, Y. H. Li, D. Li, Y. Z. Xia, and J. P. Zhang, "A review on adsorption refrigeration technology and adsorption deterioration in physical adsorption systems," *Renew. Sustain. Energy Rev.*, vol. 14, no. 1, pp. 344–353, Jan. 2010.
- [54] "SOLAIR.," *Market report for small and medium-sized solar air-conditioning appliances. Analysis of market potential.*, 2009. [Online]. Available: www.solair-project.eu.
- [55] T. S. Ge *et al.*, "Solar heating and cooling: Present and future development," *Renew. Energy*, pp. 1–15, 2017.

- [56] E. G. Papoutsis, I. P. Koronaki, and V. D. Papaefthimiou, "Numerical simulation and parametric study of different types of solar cooling systems under Mediterranean climatic conditions," *Energy Build.*, pp. 601–611, 2017.
- [57] N. Nakahara, Y. Miyakawa, and M. Yamamoto, "Experimental study on house cooling and heating with solar energy using flat plate collector," *Sol. Energy*, vol. 19, no. 6, pp. 657–662, Jan. 1977.
- [58] D. S. Ward, "Solar absorption cooling feasibility," *Sol. Energy*, vol. 22, no. 3, pp. 259–268, Jan. 1979.
- [59] R. M. Lazzarin, "Solar cooling: PV or thermal? A thermodynamic and economical analysis," *Int. J. Refrig.*, pp. 38–47, 2014.
- [60] C. Baldwin and C. A. Cruickshank, "A review of solar cooling technologies for residential applications in Canada," *Energy Procedia*, vol. 30, pp. 495–504, 2012.
- [61] "Solair project.," 2016. [Online]. Available: <http://www.solair-project.eu/>.
- [62] C. A. Balaras *et al.*, "Solar air conditioning in Europe-an overview," *Renew. Sustain. Energy Rev.*, vol. 11, no. 2, pp. 299–314, 2007.
- [63] D. S. Kim and C. A. Infante Ferreira, "Solar refrigeration options - a state-of-the-art review," *Int. J. Refrig.*, vol. 31, no. 1, pp. 3–15, 2008.
- [64] R. Porumb, B. Porumb, and M. BĂlan, "Baseline Evaluation of Potential to Use Solar Radiation in Air Conditioning Applications," *Energy Procedia*, vol. 85, no. November 2015, pp. 442–451, 2016.
- [65] N. Hartmann, C. Glueck, and F. P. Schmidt, "Solar cooling for small office buildings: Comparison of solar thermal and photovoltaic options for two different European climates," *Renew. Energy*, vol. 36, no. 5, pp. 1329–1338, 2011.
- [66] T. Otanicar, R. A. Taylor, and P. E. Phelan, "Prospects for solar cooling - An economic and environmental assessment," *Sol. Energy*, vol. 86, no. 5, pp. 1287–1299, 2012.
- [67] P. Navarro-Rivero and B. Ehrismann, "Durability issues, maintenance and costs of solar cooling systems. Task Report 5.3.2," *Qual. Assur. Sol. Heat. Cool. Technol.*, pp. 1–52, 2012.
- [68] Y. Li, G. Zhang, G. Z. Lv, A. N. Zhang, and R. Z. Wang, "Performance study of a solar photovoltaic air conditioner in the hot summer and cold winter zone," *Sol. Energy*, vol. 117, pp. 167–179, 2015.
- [69] F. J. Aguilar, P. V. Quiles, and S. Aledo, "Operation and energy efficiency of a hybrid air conditioner simultaneously connected to the grid and to photovoltaic panels," *Energy Procedia*, vol. 48, pp. 768–777, 2014.
- [70] M. J. Morán and H. N. Shapiro, "Sistemas de refrigeración y bomba de calor," in *Fundamentos de Termodinámica técnica*, 2nd Ed., Editorial Reverté, 2004, pp. 515–545.
- [71] DAIKIN, "R32 Product information," Dusseldorf, Germany.
- [72] X. Q. Zhai, M. Qu, Y. Li, and R. Z. Wang, "A review for research and new design options of solar absorption cooling systems," *Renew. Sustain. Energy Rev.*, vol. 15, no. 9, pp. 4416–4423, 2011.
- [73] A. Syed *et al.*, "A novel experimental investigation of a solar cooling system in Madrid," *Int. J. Refrig.*, vol. 28, no. 6, pp. 859–871, 2005.

- [74] D. Kim and C. Machielsen, "Evaluation of air-cooled solar absorption cooling systems.," in *Proceedings of International Sorption Heat Pump Conference (ISHPC)*, 2002.
- [75] M. J. Tierney, "Options for solar-assisted refrigeration-Trough collectors and double-effect chillers," *Renew. Energy*, vol. 32, no. 2, pp. 183–199, 2007.
- [76] G. Grossman, "Solar-powered systems for cooling, dehumidification and air-conditioning," *Sol. Energy*, vol. 72, no. 1, pp. 53–62, 2002.
- [77] M. Balghouthi, M. H. Chahbani, and A. Guizani, "Feasibility of solar absorption air conditioning in Tunisia," *Build. Environ.*, vol. 43, no. 9, pp. 1459–1470, 2008.
- [78] J. Castro, A. Oliva, C. D. Perez-Segarra, and C. Oliet, "Modelling of the heat exchangers of a small capacity, hot water driven, air-cooled H₂O-LiBr absorption cooling machine," *Int. J. Refrig.*, vol. 31, no. 1, pp. 75–86, 2008.
- [79] G. A. Florides, S. A. Kalogirou, S. A. Tassou, and L. C. Wrobel, "Modelling, simulation and warming impact assessment of a domestic-size absorption solar cooling system," *Appl. Therm. Eng.*, vol. 22, no. 12, pp. 1313–1325, 2002.
- [80] L. A. Chidambaram, A. S. Ramana, G. Kamaraj, and R. Velraj, "Review of solar cooling methods and thermal storage options," *Renew. Sustain. Energy Rev.*, vol. 15, no. 6, pp. 3220–3228, 2011.
- [81] R. Sekret and M. Turski, "Research on an adsorption cooling system supplied by solar energy," *Energy Build.*, vol. 51, pp. 15–20, 2012.
- [82] R. Z. Wang, M. Li, Y. X. Xu, and J. Y. Wu, "An energy efficient hybrid system of solar powered water heater and adsorption ice maker," *Sol. Energy*, vol. 68, no. 2, pp. 189–195, 2000.
- [83] H. M. Henning and H. Glaser, "Solar assisted adsorption system for a laboratory of the University Freiburg.," *Bine information service*. [Online]. Available: <http://www.bine.info/en/topics/>.
- [84] A. Fasfous *et al.*, "Potential of utilizing solar cooling in The University of Jordan," *Energy Convers. Manag.*, vol. 65, pp. 729–735, Jan. 2013.
- [85] I. P. Koronaki, E. G. Papoutsis, and V. D. Papaefthimiou, "Thermodynamic modeling and exergy analysis of a solar adsorption cooling system with cooling tower in Mediterranean conditions," *Appl. Therm. Eng.*, vol. 99, pp. 1027–1038, 2016.
- [86] G. Santori, S. Santamaria, A. Sapienza, S. Brandani, and A. Freni, "A stand-alone solar adsorption refrigerator for humanitarian aid," *Sol. Energy*, vol. 100, pp. 172–178, 2014.
- [87] A. El Fadar, A. Mimet, and M. Pérez-García, "Modelling and performance study of a continuous adsorption refrigeration system driven by parabolic trough solar collector," *Sol. Energy*, vol. 83, no. 6, pp. 850–861, 2009.
- [88] K. Bataineh and Y. Taamneh, "Review and recent improvements of solar sorption cooling systems," *Energy Build.*, vol. 128, pp. 22–37, 2016.
- [89] Krause *et al.*, "Task 38: Solar Air-Conditioning and Refrigeration.," *Int. Energy Agency*, no. October, pp. 1–77, 2010.
- [90] European Council, *Directive 2009/125/EC of the European Parliament and of the Council of 21 October 2009 establishing a framework for the setting of ecodesign requirements for energy-related products*. 2009, pp. 10–35.

- [91] European Parliament and the Council of the European Union, *Directive 2010/30/EU of the European Parliament and of the Council; on the indication by labelling and standard product information of the consumption of energy and other resources by energy-related products.*, no. 4. 2010, pp. 1–12.
- [92] European Parliament, *Directive 2010/31/EU of the European Parliament and of the Council of 19 May 2010 on the energy performance of buildings.* 2010, pp. 13–35.
- [93] European Parliament, *Directive 2013/114/EU on Renewable energy from different heat pump technologies.*, no. December. 2013, pp. 27–35.
- [94] European Parliament, *Directive 2012/27/EU of the European Parliament and of the Council of 25 October 2012 on energy efficiency.*, no. October. 2012, pp. 1–56.
- [95] K. F. Fong, T. T. Chow, C. K. Lee, Z. Lin, and L. S. Chan, “Comparative study of different solar cooling systems for buildings in subtropical city,” *Sol. Energy*, vol. 84, no. 2, pp. 227–244, 2010.
- [96] “Prestaciones medias estacionales de las bombas de calor para producción de calor en edificios.,” Madrid, España, 2014.
- [97] D. Neyer and D. Mugnier, “Task 53-Technical and Economic Assessment. Best practice examples of new generation solar thermal and PV driven heating and cooling systems,” 2018.
- [98] D. Neyer, M. Ostheimer, C. Dipasquale, and R. Köll, “Technical and economic assessment of solar heating and cooling – Methodology and examples of IEA SHC Task 53,” *Sol. Energy*, no. October 2017, pp. 1–12, 2018.
- [99] M. Beccali, P. Finocchiaro, and B. Nocke, “Energy and economic assessment of desiccant cooling systems coupled with single glazed air and hybrid PV/thermal solar collectors for applications in hot and humid climate,” *Sol. Energy*, vol. 83, no. 10, pp. 1828–1846, 2009.
- [100] L. F-Chart Software, “EES. F-Chart software.” [Online]. Available: <http://www.fchart.com/ees/>.
- [101] European Union, “eurostat. Statistics Explained. Electricity price statistics.” [Online]. Available: https://ec.europa.eu/eurostat/statistics-explained/index.php/Electricity_price_statistics.
- [102] European Union, “eurostat. Statistics Explained. Natural gas price statistics.” [Online]. Available: https://ec.europa.eu/eurostat/statistics-explained/index.php/Natural_gas_price_statistics.
- [103] Ministerio de Agricultura y Pesca Alimentación y Medio Ambiente., *Factores de Emisión. Registro de huella de carbono, compensación y proyectos de absorción de dióxido de carbono.* 2017, pp. 1–12.